CHARACTERIZATION OF IMMUNE RESPONSES CORRELATING WITH PROTECTION AND THE DEVELOPMENT OF AN EFFICACIOUS TREATMENT AGAINST EBOLA VIRUS INFECTIONS

BY

GARY CHUNG KEI WONG

A THESIS SUBMITTED TO THE FACULTY OF GRADUATE STUDIES OF THE UNIVERSITY OF MANITOBA
IN PARTIAL FULFILLMENT OF THE REQUIREMENTS FOR THE DEGREE OF

DOCTOR OF PHILOSOPHY

DEPARTMENT OF MEDICAL MICROBIOLOGY

UNIVERSITY OF MANITOBA

WINNIPEG

THIS THESIS HAS BEEN EXAMINED AND APPROVED

Thesis supervisor, Dr. Gary P. Kobinger, Ph.D.
Adjunct Professor, Department of Medical Microbiology
University of Manitoba
Chief, Special Pathogens Program
National Microbiology Laboratory, Canadian Science Center for Human and Animal Health, Public Health Agency of Canada

---

Dr. Kevin M. Coombs, Ph.D.
Professor, Department of Medical Microbiology
Assistant Dean (Research), Faculty of Medicine
University of Manitoba

Dr. Sam K. P. Kung, Ph.D.
Assistant Professor, Department of Immunology
University of Manitoba

External examiner, Dr. Peter A. Bretscher, Ph.D.
Professor and Head, Department of Microbiology and Immunology
College of Medicine
University of Saskatchewan

August 8th, 2014

DEDICATION

This thesis is dedicated to my loving family, who may not have always fully understood exactly what I was doing during my graduate degree, but nevertheless has always been unconditionally supportive while I pursue my dreams.

ACKNOWLEDGMENTS

As I sit here reflecting on my experiences in graduate school (how time flies!), I realized that this doctorate degree, and research in general, is truly a collaborative effort. This endeavour would definitely not have been as smooth, enjoyable or even possible without all the help I have received over the years. I would like to thank the following from the bottom of my heart:

First I would like to thank my thesis supervisor, Dr. Gary Kobinger, for all his help and support over the years. You are truly an inspirational researcher, and the ideal boss any student would be lucky to have. Throughout my graduate career you have always encouraged and supported me in the form of grants, trips to present at national and international conferences, and of course the unforgettable opportunity in Johannesburg to gain overseas research experience. It was a blast. You have given me the best experience possible in preparation for a future research career and I could never repay you enough for the faith you showed in me.

I would like to thank Dr. Xiangguo Qiu for graciously taking me under her wing for the monoclonal antibody studies. I learned a lot from you and the experience will serve me well for the next phase in my career. It is exciting to see this field grow exponentially over the past few years, and I feel humbled and privileged to be part of something so impactful and meaningful. I look forward to seeing you and Gary K. taking this to the next level. Exciting times ahead!

I would like to thank the Canadian Institutes of Health Research (CIHR), who funded me during both my Master's and Doctoral degree through the Canadian Graduate Scholarships Program. I am also thankful that they were willing to fund me once again through the Michael Smith Foreign Supplement Study Award, as I continued my training in South Africa.

I would like to thank the University of Manitoba and the National Microbiology Laboratory for providing the space, reagents and/or support needed to perform this research. I

would also like to thank my committee members, Dr. Kevin Coombs and Dr. Sam Kung, for their invaluable advice, which has greatly contributed to my development as a scientist.

To everyone in the Kobinger lab (past and present), thank you for keeping my sanity (for the most part), driving me crazy on other occasions, but always entertaining me over the last several years. It was definitely good times. We all had our share of unforgettable stories (some of the more embarrassing ones should never ever be mentioned again though), and our lab ultimate frisbee team will always be one of my favorite and most cherished memories. To everyone in the Special Pathogens Program, I would like to thank you for having me around ever since I started as a co-op student here, and even though I am not from Winnipeg (a fact that I have pointed out on more than a couple of occasions because I'm a snobby Vancouverite – ahem– fine…Coquitlam…), scientifically speaking I am made in Winnipeg. I learned everything I know about microbiology from this place, and I will always remain proud to be a part-Winnipegger. The winters here may be bitterly cold (I still wonder how people can live here sometimes), but the people are warm and friendly, and in the end that is what truly matters.

To Karen, Ben and Ann (KBAG), I (finally) made it! It seemed like it was only yesterday when we met as nerdy undergrad students. Now that we've transitioned from nerdy grad students to nerdy "doctors", this is only the start of our dreams! Hopefully we can make an impact in the world soon in our own unique ways, but not in the supervillain-created-from-a-lab-accident kind of way though…seriously, why do so many evil comic book characters have advanced degrees? Dr. Octopus, Dr. Evil, Dr. Doom, Prof. Zoom…etc etc… ☺☺☺

Last but not least, I would like to thank May. Thank you for being my best friend in all this and allowing me to selfishly pursue my dreams. You mean the world to me and I love you forever.

TABLE OF CONTENTS

LIST OF TABLES

LIST OF FIGURES

LIST OF ABBREVIATIONS

A_{405}	absorbance at 405 nanometers
Ad5	human adenovirus serotype 5
Ad5-GP	Ad5 expressing Ebola virus glycoprotein
Ad5-lacZ	Ad5 expressing β-galactosidase
Ad5-optGP	Ad5 expressing the human codon-optimized Ebola virus glycoprotein
Ad5-IFN-α	Ad5 expressing interferon-alpha
adjuvanted ZMAb	Ad5-IFN-α and ZMAb combination treatment
aPTT	activated partial thromboplastin time
BDBV	Bundibugyo virus
CAG	chicken-β-actin
CD	cluster of differentiation
CFR	case fatality rate
CO_2	carbon dioxide
CoP	correlate of protection
CPE	cytopathic effects
DC	dendritic cells
DMEM	Dulbecco's modified eagle medium
DNA	deoxyribonucleic acid
DNA-GP	DNA vector expressing Ebola virus glycoprotein
dpi	days post-infection
dpv	days post-vaccination
EBOV	Ebola virus
EBOV-eGFP	Ebola virus expressing the enhanced green fluorescent protein
EBOVΔG/RESTVGP	Ebola virus lacking its wild-type glycoprotein, replaced with the Reston virus glycoprotein
eGFP	enhanced green fluorescent protein
ELISA	enzyme-linked immunosorbent assay
ELISpot	enzyme-linked immunosorbent spot assay
EVD	Ebola virus disease
FACS	fluorescence-activated cell sorting
FBS	fetal bovine serum
FFU	focus forming units
g	gram
GA-EBOV	Guinea pig adapted Ebola virus
GP	glycoprotein
GP_0	full length Ebola virus glycoprotein precursor
GP_1	amino acid 1 to 501 of Ebola virus glycoprotein
$GP_{1,2}$	full length transmembrane Ebola virus glycoprotein
$GP_{1,2\Delta TM}$	full length Ebola virus glycoprotein lacking the transmembrane domain
GP_2	amino acid 501 to 676 of Ebola virus glycoprotein
HEK	human embryonic kidney
His-$GP_{1,2\Delta TM}$	Histidine-tagged Ebola virus glycoprotein lacking the transmembrane domain

HPIV3	human parainfluenza virus type 3
ID	intradermal
IFN	interferon
Ig	immunoglobulin
IL	interleukin
IM	intramuscular
IN	intranasal
IRF	interferon regulatory factor
ISG	interferon stimulated genes
IT	intratracheal
IV	intravenous
JAK	janus kinase
kb	kilobases
kDa	kilodalton (10^3 daltons)
kg	kilogram (10^3 grams)
L	RNA-dependent RNA polymerase
L-15	Leibovitz's medium
LD_{50}	lethal dose of virus resulting in 50% survival
LLOV	Lloviu virus
mAb	monoclonal antibody
MA-EBOV	Mouse adapted Ebola virus
MARV	Marburg virus
mg	milligram (10^{-3} grams)
MHC	major histocompatibility complex
MIP	macrophage inflammatory protein
mL	milliliter (10^{-3} liter)
mM	millimolar (10^{-3} molar)
NAb	neutralizing antibody
NC	nucleocapsid
ng	nanogram (10^{-9} grams)
NHP	nonhuman primates
nm	nanometer (10^{-9} meter)
nM	nanomolar (10^{-9} molar)
NP	nucleoprotein
NPC1	Niemann-Pick C1
OR	oral
PBMC	peripheral blood mononuclear cells
PBS	phosphate buffered saline
PEI	pre-existing immunity
PFU	plaque forming units
pg	picogram (10^{-12} grams)
PMOplus	positively charged phosphorodiamidate morpholino oligomers
pre-sGP	precursor of the secreted Ebola virus glycoprotein
PT	prothrombin time
RABV	rabies virus

RANTES	regulated on activation, normal T cell expressed and secreted
RBC	Red blood cells
RESTV	Reston virus
RESTVΔG/EBOVGP	Reston virus lacking its wild-type glycoprotein, replaced with the Ebola virus glycoprotein
rhAPC	recombinant human activated protein C
RIG	retinoic acid-inducible gene
RNA	ribonucleic acid
rNAPc2	recombinant nematode anticoagulant protein c2
RNP	ribonucleoprotein
rpm	revolutions per minute
RPMI	Roswell Park Memorial Institute medium
RT-PCR	reverse transcription polymerase chain reaction
RT-qPCR	quantitative reverse transcriptase polymerase chain reaction
SC	subcutaneous
SFC	spot forming cells
sGP	secreted Ebola virus glycoprotein
siRNA	small, interfering RNA
ssGP	small, soluble Ebola virus glycoprotein
STAT	signal transducers of activation and transcription
SUDV	Sudan virus
TAFV	Tai Forest virus
$TCID_{50}$	infectious dose in 50% of tissue culture cells
TLR	Toll-like receptor
TM	transmembrane domain
TNF	tumour necrosis factor
TP	total protein
unvacc	unvaccinated
vacc	vaccinated
VEEV	Venezuelan equine encephalitis virus
VLP	virus-like particles
VP	viral protein
VSV	vesicular stomatitis virus
VSVΔG/EBOVGP	vesicular stomatitis virus lacking the wild-type glycoprotein, expressing Ebola virus glycoprotein
WBC	white blood cells
WT	wild type
xg	times gravity
ZMAb	Ebola virus glycoprotein-specific monoclonal antibody cocktail comprising the antibodies 1H3, 2G4 and 4G7
^{o}C	degrees Celsius
µg	microgram (10^{-6} grams)
µL	microliter (10^{-6} liter)
µM	micromolar (10^{-6} molar)

ABSTRACT

CHARACTERIZATION OF IMMUNE RESPONSES CORRELATING WITH PROTECTION AND THE DEVELOPMENT OF AN EFFICACIOUS TREATMENT AGAINST EBOLA VIRUS INFECTIONS

Gary Chung Kei Wong, B. Sc.

University of Manitoba, 2014

Ebola virus (EBOV) is a zoonotic pathogen which causes a fulminant hemorrhagic fever and results in up to 90% fatality. Despite efforts over the past 38 years, a licensed prophylactic or post-exposure option remains unavailable. Several experimental vaccines have already demonstrated protection from lethal EBOV disease in nonhuman primates (NHPs). However, attempts to translate this research from bench to bedside have been hampered, since the immune responses that correlate with protection against EBOV are not well-defined. Without this information, it is not possible to reliably predict the efficacy of vaccines or treatments in humans without lethal challenge.

The goal of this thesis is to determine the immune parameters that are predictive of protection against EBOV. Due to the rapid speed of EBOV pathogenesis, it was originally hypothesized that a rapid and robust $CD8^+$ T-cell response must be crucial for survival. Using a previously-characterized adenovirus-vectored Ebola vaccine (Ad5-optGP), transgenic/knockout C57BL/6J mice with ablation for selected immune responses were vaccinated and challenged 28 days later. Surprisingly, while $CD8^+$ T-cell knockout mice survived infection, B-cell knockout mice did not, indicating that the antibody response played a critical role in protection. Humoral and cell-mediated responses were compared between survivor and moribund guinea pigs and NHPs from previous vaccination and post-exposure therapy experiments, either with Ad5-optGP

or a vesicular stomatitis virus (VSV)-vectored vaccine (VSVΔG/EBOVGP). Circulating EBOV glycoprotein (GP)-specific IgG antibody levels were the best correlation for protection independent of vaccine platform or timing of exposure ($p<0.0001$), strongly supporting the role of antibody responses in the control of EBOV infection.

To demonstrate that antibodies are also responsible for protection, three previously-characterized monoclonal antibodies recognizing different GP epitopes were combined into a cocktail (ZMAb). Initiation of ZMAb treatment 1 and 2 days post infection (dpi) with EBOV protected 100% and 50% of NHPs, respectively. These results provide a reliable measure for predicting protection from EBOV in three commonly used animal models, and present a strong case for the use of antibodies as an effective post-exposure treatment. This knowledge will ultimately help in the development and validation of a clinical product against EBOV infection.

CHAPTER I: INTRODUCTION

1.1 Taxonomy and nomenclature

Ebola virus belongs to the order *Mononegavirales* (non-segmented, negative-sense, single-stranded RNA viruses), family *Filoviridae* (filamentous viruses), and the genus *Ebolavirus*. Filoviruses contain three genera, *Ebolavirus*, *Marburgvirus*, and *Cuevavirus* (Figure 1.1). *Marburgvirus* contains one species, *Marburg marburgvirus*, which contain two member viruses, Marburg virus (MARV) and Ravn virus (RAVV). *Cuevavirus* contains *Lloviu cuevavirus*, which contains one member virus, Lloviu virus (LLOV). The genus *Ebolavirus* is more diverse by comparison and contains five distinct species, which are named based on their geographic origin: *Zaire ebolavirus*, *Bundibugyo ebolavirus*, *Sudan ebolavirus*, *Taï Forest ebolavirus*, and *Reston ebolavirus*. Each *Ebolavirus* species contain one member virus: Ebola virus (EBOV), Bundibugyo virus (BDBV), Sudan virus (SUDV), Tai Forest virus (TAFV) and Reston virus (RESTV). EBOV is the pathogen that has historically caused the most deaths stemming from past outbreaks, and of all the Ebola species, EBOV is viewed as the largest threat to public health. Past research on Ebola has centered on utilizing EBOV as a model virus; therefore, the work presented in this thesis will also use EBOV in order to maximize relevance to the research field and practicality of results, unless otherwise stated.

The *Ebolavirus* and *Marburgvirus* species are distinguishable from each other by their lack of serological cross-reactivity and significant divisions in the phylogenetic tree (Figure 1.2). Genome organization also differs between *Ebolavirus* and *Marburgvirus* with respect to the number and position of gene overlaps, in addition to the absence of an RNA editing side in the glycoprotein (GP) gene in *Marburgvirus* (Groseth, Stroher et al. 2002). By definition, a filovirus belongs to the genus *Ebolavirus* if: 1) the viral genome has more than one gene overlap, 2) the

GP gene encodes four gene products by RNA editing, 3) the viral genome differs from *Marburgvirus* by greater than 50% and less than 50% from *Ebolavirus* at the nucleotide level, and 4) if the viral antigens do not show cross-reactivity with *Marburgvirus* antigens (Kuhn, Becker et al. 2010). A number of different viruses have been identified for *Marburgvirus* as well as several species of *Ebolavirus*, and the nucleotide sequence of the glycoprotein gene are compared for selected viruses (Figure 1.2). Since the live, infectious virion has not yet been successfully isolated for LLOV, current knowledge and research into LLOV is substantially restricted beyond the availability of a full-length virus genome sequence.

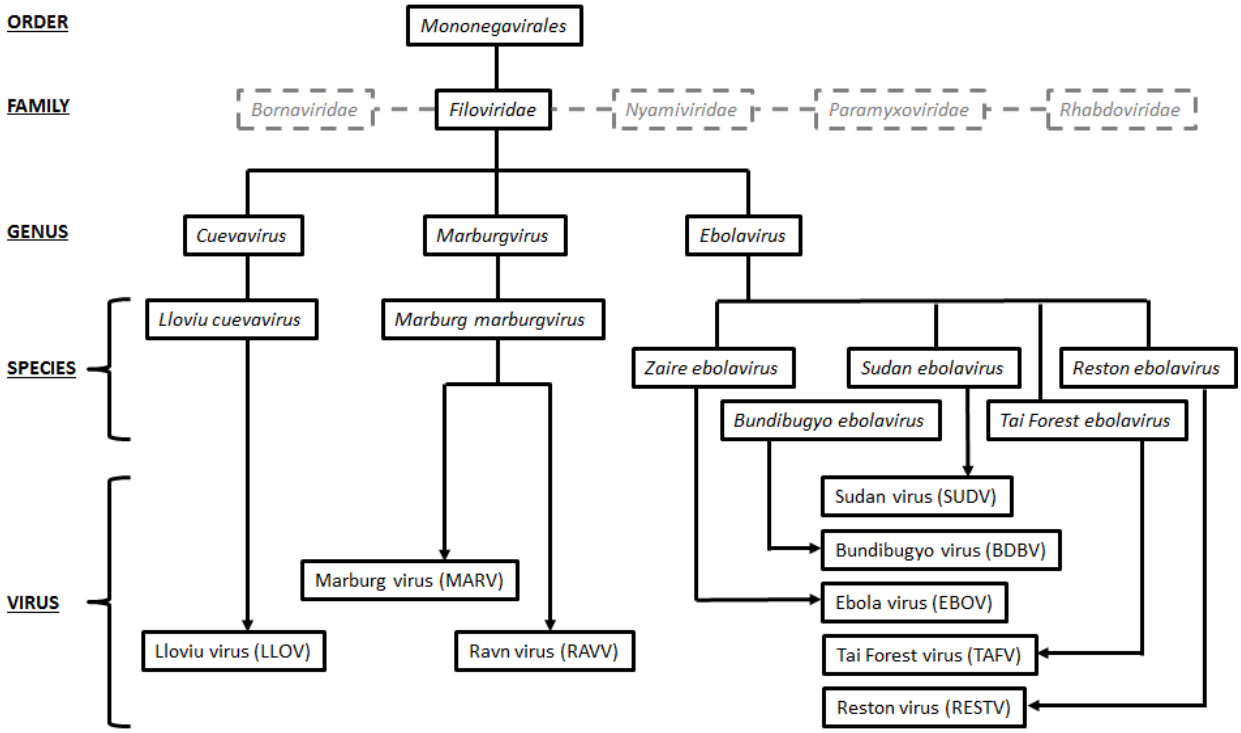

Figure 1.1. Taxonomic classification of the family *Filoviridae*. The family, genus and species of the viruses relevant to this thesis are shown in solid black boxes, whereas the other virus families of the order *Mononegaivrales* are shown in gray dashed boxes.

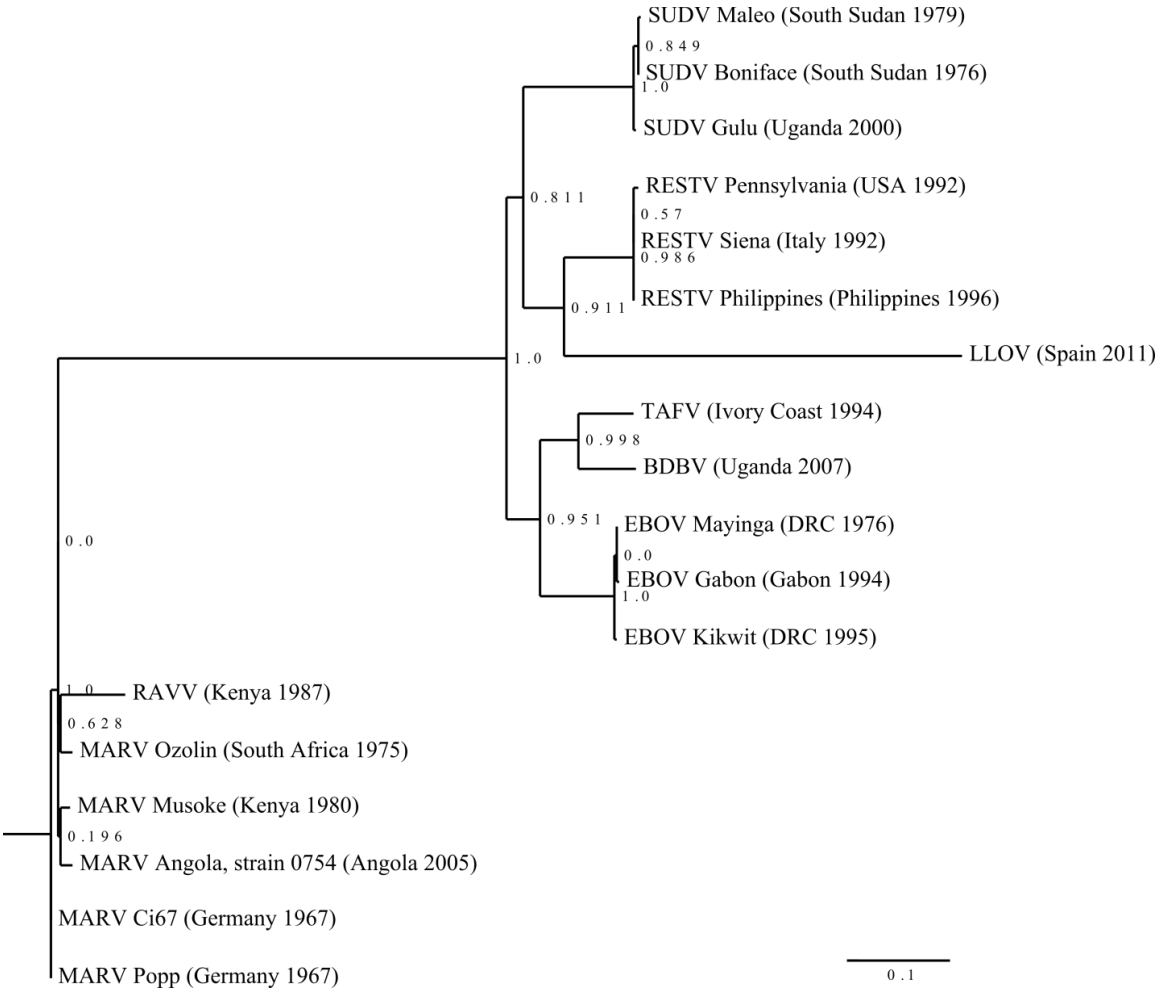

Figure 1.2. Phylogenetic classification of the family *Filoviridae*. Phylogenetic tree comparing the nucleotide sequences in the glycoprotein gene of selected filoviruses. Sequences were obtained from Genbank. Bootstrap proportions were obtained from 100 bootstraps and shown at the nodes, while the distance marked by the bar indicates number of mutations per 100 nucleotides.

1.2 Virus structure

1.2.1 Virion morphology

EBOV particles consist of a filamentous structure when viewed under the transmission electron microscope, and is the main reason why these organisms are named filoviruses (Latin: *filium = thread*). Virions are pleomorphic, and U-, 6-shaped as well as spherical particle configurations can be commonly found (Feldmann, Sanchez et al. 2013). Virions have a uniform diameter of 80 nanometers (nm) in addition to a variable length, with the most common class of virions measuring 982 ± 79 nm (Beniac, Melito et al. 2012). The virions are composed of: an internal helical ribonucleoprotein (RNP) complex, which contains the nucleocapsid (NC) as formed by the nucleoprotein (NP) encapsulating the viral genome, viral protein 35 (VP35), VP30 and RNA-dependent RNA polymerase (L), an outer membrane envelope consisting of VP40, GP and VP24 with only GP visible from the surface, and studded with heavily glycosylated, full length transmembrane GP ($GP_{1,2}$) spikes protruding approximately 10 nm from the surface of the virion (Feldmann, Sanchez et al. 2013) (Bharat, Noda et al. 2012).

1.2.2 Genome organization

The EBOV genome, similar to all other filovirus genomes, consists of a non-segmented, negative-sense, single-strand RNA molecule approximately 19 kilobases (kb) in length. The genome consists of seven genes arranged in a linear order from the 3’ to 5’ end (Figure 1.3). Noncoding regions exist between each gene, and gene overlaps are present between the VP35 and VP40, GP and VP30, as well as VP24 and the L genes (Feldmann, Sanchez et al. 2013). Each gene has its own conserved transcriptional signals, and begins at the 3’ end with a start site (3’CUC/ACUUCUAAUU) and end with a polyadenylation stop site at the 5’ end

(UAAUUCAAAAA(A)5') (Muhlberger, Trommer et al. 1996) (Muhlberger 2007). The genome is transcribed into seven monocistronic mRNA species, which are responsible for the production of all structural and non-structural viral proteins. Each mRNA codes for a single protein, with the exception of the GP mRNA, which codes for three different proteins due to RNA editing of the mRNA during transcription. The viral proteins produced by EBOV will be described in detail in the next section.

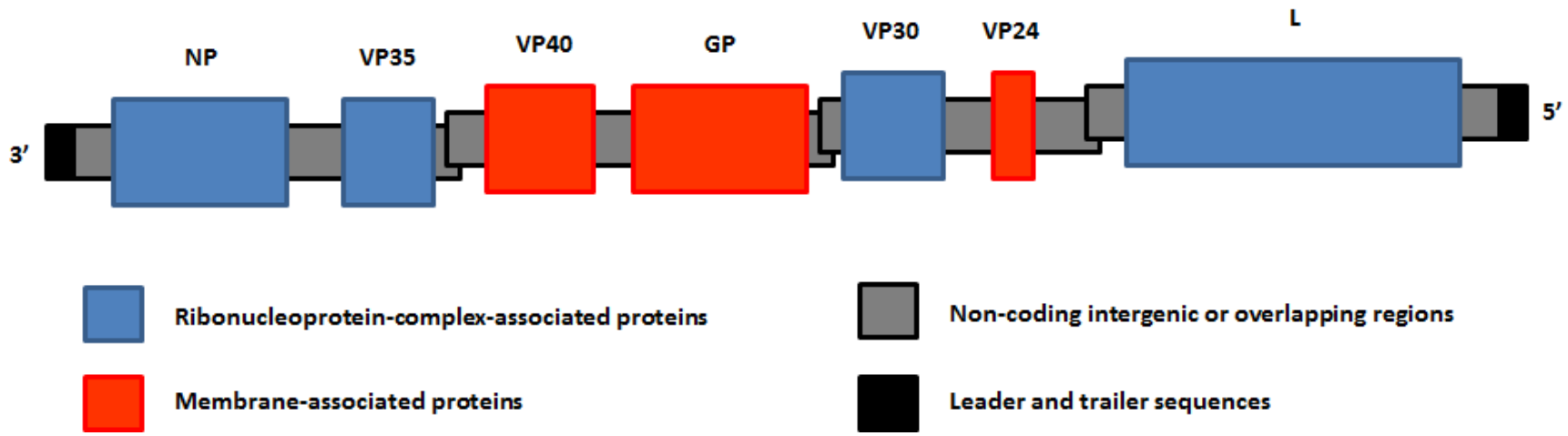

Figure 1.3. Schematic illustration of the Ebola virus genome. The negative-sense, single stranded EBOV genome contains seven genes and is ordered (from 3' to 5'): nucleoprotein (NP), viral protein (VP) 35, VP40, glycoprotein (GP), VP30, VP24, and RNA-dependent RNA polymerase (L).

1.2.3 Viral proteins

1.2.3.1 Nucleoproteins (NP and VP30)

The first gene on the 3' end of the EBOV RNA genome encodes for NP, a structural viral protein approximately 90-104 kiloDaltons (kDa) in size. NP is known as the major nucleoprotein, and plays a role in virus transcription, replication and assembly. When expressed alone, the hydrophobic N-terminus EBOV NP is able to self-assemble into helical tubes, which serves as the backbone for the NC (Watanabe, Noda et al. 2006). Mutation studies have indicated that NP is critical for virion capsid assembly and along with VP35, VP30 and L interacts with the genome RNA to form the RNP complex for transcription and replication purposes (Huang, Xu et al. 2002). Later during the infection, it is responsible for the formation of highly organized structures in the cytoplasm, called inclusion bodies, which accumulate the other RNP proteins for assembly.

The fifth gene from the 3' end of the EBOV RNA genome encodes for VP30, a structural viral protein approximately 27-30 kDa in size. VP30 is known as the minor nucleoprotein, and plays a role in virus transcription and assembly. VP30 can bind genomic RNA at the arginine-rich N-terminus to aid in genome encapsidation (John, Wang et al. 2007); and is also a transcriptional activator (Hartlieb, Muziol et al. 2007) whose activity is downregulated by phosphorylation (Modrof, Muhlberger et al. 2002). It has also been suggested that VP30 interacts with L to help form a bridge between the NP and L proteins in the formation of the NC (Groseth, Charton et al. 2009).

1.2.3.2 Other polymerase complex proteins (VP35 and L)

The second gene from the 3' end of the EBOV RNA genome encodes for VP35, a structural phosphoprotein, which is 35 kDa in size. VP35 is also known as a polymerase factor, and determines the mode of RNA synthesis between transcription and translation (Muhlberger, Weik et al. 1999). It plays a role in NC formation (Beniac, Melito et al. 2012), and has also been recognized as an interferon (IFN) agonist, which antagonizes the host Type I IFN response, and can effectively suppress RNA interference (Haasnoot, de Vries et al. 2007).

The last gene from the 3' end of the EBOV RNA genome encodes for L, which is a structural RNA-dependent RNA polymerase (RdRP) approximately 270 kDa in size. The RdRP is the enzymatic component of the RNP, responsible for driving the transcription and replication with the help of the other viral proteins within the RNP (Volchkov, Volchkova et al. 1999). Consistent with all *Mononegavirales*, the 2'-O-ribose methyltransferase domain activity facilitates the 5' capping of viral mRNAs (Ferron, Longhi et al. 2002).

1.2.3.3 Matrix proteins (VP40 and VP24)

The third gene from the 3' end of the EBOV RNA genome encodes for VP40, the main structural matrix protein approximately 35-40 kDa in size. VP40 is the most abundant protein in the virion, supporting the outer virion envelope and maintaining the structural integrity of the particle. VP40 is important for virus budding, as it interacts with both the RNP as well as the GP peplomers together near the membrane lipid rafts. VP40 was also reported to help regulate genome transcription and replication (Hoenen, Jung et al. 2010).

The sixth gene from the 3' end of the EBOV RNA genome encodes for VP24, a structural minor matrix protein approximately 24-25 kDa in size. VP24 serves several functions, including virus assembly by helping incorporate other viral proteins into the NC (Hoenen,

Groseth et al. 2006), as well as antagonizing the IFN response by inhibiting both Type I and II IFN signaling in the host early after infection. Interestingly, VP24 was shown to play an important role in the adaptation of wild-type EBOV to rodent animal models (Ebihara, Takada et al. 2006) (Volchkov, Chepurnov et al. 2000). VP24 was also reported to help regulate genome transcription and replication (Hoenen, Jung et al. 2010).

1.2.3.4 The glycoprotein gene products

The fourth gene from the 3' end of the EBOV RNA genome encodes for the precursor molecule for secreted GP (sGP), (precursor = pre-sGP). The insertion of one additional adenosine residue into the mRNA at the GP editing site (which normally contains 7 consecutive adenosine residues) results in the production of a precursor molecule for GP (pre-GP), due to a -1 shift in the open reading frame resulting in a later stop codon. The deletion of an adenosine residue or addition of two adenosine residues at the same editing site results in the production of a small, soluble glycoprotein (ssGP), due to a +1 or -2 shift in the open reading frame resulting in an earlier stop codon. The chance of transcripts encoding pre-sGP, pre-$GP_{1,2}$, and ssGP were estimated to be 70%, 25%, and 5%, respectively (Mehedi, Falzarano et al. 2011).

Pre-GP is cleaved by furin into $GP_{1,2}$, which is a 676-amino acid, structural transmembrane glycoprotein residing on the envelope of the glycoprotein, approximately 150-170 kDa in size depending on the level of glycosylation. $GP_{1,2}$ is present on the surface of the glycoprotein as spike structures (peplomers), and is cleaved by endosomal cathepsins B and L to give GP_1 and GP_2 subunits. GP_1 is responsible for EBOV entry through receptor binding, and GP_2 mediates membrane fusion (Takada, Robison et al. 1997). Disulfide bond instability between GP_1 and GP_2 may lead to the secretion of soluble GP_1, whereas cleavage of $GP_{1,2}$ by

tumour necrosis factor (TNF)-α converting enzyme leads to the secretion of another soluble, transmembrane-deleted GP variant ($GP_{1,2\Delta TM}$) (Dolnik, Volchkova et al. 2004). GP is a major virulence factor and the majority of the host immune response is directed towards GP; therefore it is also an attractive focus antigen for vaccine development.

Cleavage of pre-sGP by furin yields sGP and Δ-peptide. Δ-peptide is a small, non-structural, secreted glycopeptide of 40–48 amino acid residues. However, its molecular weight is approximately 10-14 kDa, due to glycosylation and sialylation (Volchkova, Klenk et al. 1999). The function of the Δ-peptide is currently unknown. sGP is a non-structural, secreted protein approximately 50-55 kDa in size, which shares an identical N-terminus with $GP_{1,2}$ (sharing the first 295 of 324 total amino acid residues), but has a unique C-terminus (Volchkov, Becker et al. 1995) (Sanchez, Trappier et al. 1996). sGP is also heavily glycosylated, and linked with disease progression, as large quantities could be detected in the serum of exposed, ill individuals (Sanchez, Trappier et al. 1996). A recent study shows that sGP is involved with immune evasion by subverting the pre-existing antibody response through cross-reacting with $GP_{1,2}$-specific antibodies, as well as influencing the immune system to produce a greater proportion of cross reactive antibodies (Mohan, Li et al. 2012).

ssGP is a non-structural, secreted EBOV protein recently found to be produced during infection of VeroE6 and Huh7 cells *in vitro*, as well as BALB/c mice *in vivo*. It is a slightly truncated version of sGP, and its molecular weight ranges between 50-55 kDa due to significant glycosylation. ssGP shares a common N-terminus with both $GP_{1,2}$ and sGP (the first 295 of 298 total amino acid residues), but distinct C-termini. Its function remains unknown, however unlike sGP, it does not appear to possess any anti-inflammatory properties (Mehedi, Falzarano et al. 2011).

1.3 Replication cycle

A number of cell types are susceptible to EBOV infection. EBOV has a lytic life cycle, which usually result in the lysis of infected cells, such as VeroE6 (Feldmann and Kiley 1999). However, persistent infection of cells is also possible with EBOV under certain conditions and has been demonstrated previously *in vitro* (Strong, Wong et al. 2008). EBOV are able to infect primary target cells such as monocytes and macrophages and endothelial cells (Geisbert, Young et al. 2003) (Stroher, West et al. 2001) (Wahl-Jensen, Kurz et al. 2005). EBOV share a similar life-cycle with the other filoviruses and can be generalized into the following steps: 1) GP-mediated attachment of the virion to the cell surface and subsequent entry, 2) release of the NC into the cytoplasm for transcription, translation and replication purposes and 3) virus assembly and then budding at the plasma membrane with subsequent release of progeny virus. The steps are described in greater detail in the following sections.

1.3.1 Attachment, entry and uncoating

The trimeric EBOV $GP_{1,2}$ is the only virus-derived protein on the virion surface and therefore responsible for mediating virus binding and entry into target cells. There is evidence supporting this as antibodies generated against GP are successful in neutralizing the virus from infection of target cells, and that expression of EBOV GP on recombinant vesicular stomatitis viruses (VSV) deleted for its wild-type surface protein alters cell tropism (Garbutt, Liebscher et al. 2004). Two separate studies have recently shown that Niemann-Pick C1 (NPC1), a 13-pass membrane protein involved in the lysosomal transport of cholesterol, is a receptor essential for EBOV entry. The first study used a small molecule compound to inhibit EBOV infection. When

Vero cells were treated with a novel benzylpiperazone adamantine diamide (3.0) *in vitro*, EBOV growth was decreased by more than 99% when sampled 96 hours (h) after infection. Using mutant cell lines and small, interfering RNA (siRNA) knockdown of receptors, NPC1 was found to be the target of 3.0. Knockout of the NPC1 receptor on normally susceptible Chinese hamster ovary cells resulted in complete resistance to EBOV infection, whereas NPC1 expression in the knockout cell line restored susceptibility to EBOV infection (Cote, Misasi et al. 2011). The second study evaluated the effect of NPC1 mutation in a lethal mouse model of infection. It was found that mice heterozygous for NPC1 ($NPC1^{-/+}$) demonstrated increased resistance to challenge with a mouse-adapted version of EBOV (MA-EBOV), whereas the homozygous NPC1 mice ($NPC1^{+/+}$) rapidly succumbed to MA-EBOV infection (Carette, Raaben et al. 2011). It was then shown that the luminal loop domain C of NPC1 binds directly and specifically to GP_1, and this was necessary and sufficient for EBOV entry into the target cell (Miller, Obernosterer et al. 2012).

It has been suggested that similar to most other enveloped viruses, EBOV enters the cell via the endocytic pathway; however the exact mechanisms have not yet been shown. An earlier study using *in vitro* EBOV infection of Vero cells showed that EBOV enters the host cell by clathrin-coated pits and caveolae (Sanchez 2007), however this was contradicted by a later study showing that EBOV entry is independent of clathrin, caveolae, and dynamin (Saeed, Kolokoltsov et al. 2010). It has now been suggested that EBOV internalization occurs by macropinocytosis since inhibition of macropinocytosis key regulators such as Pak1 and CtBP/BARS resulted in reduced EBOV entry (Saeed, Kolokoltsov et al. 2010), and that this process is $GP_{1,2}$ dependent (Nanbo, Imai et al. 2010).

Regardless, the EBOV envelope must fuse with the endosomal membrane next in order for the viral genome to leave the endosome and continue with replication. A decrease in the pH of the endosome is required for this fusion to occur (Takada, Robison et al. 1997), which enhance the activity of the cysteine proteases cathepsin B and cathepsin L and results in the proteolysis of the GP_1 subunit, removing the glycan cap, mucin-like domain and exposing core GP_2 residues (Hood, Abraham et al. 2010). It is believed that insertion of GP_2 into the endosome induces fusion of the two membranes, leading to NC release into the cytoplasm (Watanabe, Takada et al. 2000).

1.3.2 Transcription and replication

Similar to all filoviruses, EBOV transcription and replication occurs in the cytoplasm of the infected cell following NC release. The cytoplasm is the site for the transcription and replication of the EBOV genome and the expression of all viral proteins except for GP, which transit through the endoplasmic reticulum and Golgi bodies to reach the cell surface.

Transcription from the 3' to 5' direction on the viral genome template is the first obligatory process for all *Mononegavirales* after entry into the target cell. The negative-sense genome is not infectious, therefore it needs to be associated with the viral RNP complex (consisting of NP, VP35, VP30 and L) before positive-sense mRNAs can be produced from transcription (Muhlberger, Weik et al. 1999). Transcription is thought to start and stop as the polymerase complex encounters the conserved start and stop sequences in the genome, thereby producing separate mRNAs for each gene. The mRNA transcripts contain a poly(A) tail, as well as a 5' stem-loop cap in order to preserve transcript stability in addition to enhancing ribosome binding and translation (Sanchez and Kiley 1987) (Sanchez, Kiley et al. 1993). Translation of

the mRNA using the host cell machinery results in the production and accumulation of viral proteins, and it has been suggested that increasing levels of viral antigens, especially NP, triggers the change from transcription to replication (Whelan, Barr et al. 2004), and vice versa until an equilibrium is established where both processes are occurring simultaneously. Furthermore, the viral GP precursor (GP_0) is cleaved into GP_1 and GP_2, which assemble first as heterodimers, and then into trimers as surface peplomers. sGP precursor, produced by RNA stuttering during transcription of the GP gene, is cleaved into sGP and Δ-peptide, both of which are secreted from the cell.

Replication occurs with the 3' to 5' transcription of the positive-strand RNA antigenome by RdRP, producing a full length 5' to 3' RNA molecule. This full length antigenome is encapsidated with NP produced during transcription, and is used as a template to synthesize from 5' to 3', resulting in the negative-sense, full-length, progeny genome that will also be encapsidated with NP. This progeny may be used as a template for further transcription or replication purposes, resulting in its accumulation. During viral infection, it was observed NP induces the formation of inclusion bodies, which also accumulate the other NC proteins (Huang, Xu et al. 2002) for assembly of the RNP complex with the viral genome. Once sufficient levels are reached the immature virion is directed by an interaction between VP40 and the RNP to the plasma membrane to initiate the assembly process (Noda, Ebihara et al. 2006) (Jasenosky, Neumann et al. 2001).

1.3.3 Assembly, budding and egress

The virion is assembled at the lipid rafts of the plasma membrane once all the components are in one place (Suomalainen 2002). This process is believed to be facilitated by

VP40, which form interactions with both the cytoplasmic RNP (containing NP, VP35, VP30, L and the progeny genomic RNA) and the membrane-associated GP (Feldmann and Klenk 1996), drawing the two components together and allowing them to be enveloped as they exit the host cell. GP are directed to the plasma membrane and show an affinity for lipid rafts due to the palmitoylation of its transmembrane domain (Bavari, Bosio et al. 2002). VP24, which is also associated with the plasma membrane, was demonstrated to play a role for the correct assembly of the NC, including the incorporation of VP35 and VP30 (Hoenen, Groseth et al. 2006). Once assembled, the virus buds from the plasma membrane as live, infectious progeny virus, destroying the host cell in the process.

1.4 Epidemiology

The name 'Ebola' is derived from a small river located in northwestern Democratic Republic of the Congo, and infection with the Ebola viruses cause severe viral hemorrhagic fever in humans, commonly referred to as Ebola hemorrhagic fever. The first documented cases of infection in humans occurred in 1976, when EBOV and SUDV emerged almost simultaneously in Zaire (presently Democratic Republic of the Congo) and Sudan (presently South Sudan), respectively as two separate outbreaks (Anonymous 1978a) (Anonymous 1978b). The EBOV outbreak resulted in a case fatality rate (CFR) of 88% (280 deaths, 318 infected), which is only second in lethality to rabies virus infections. The SUDV outbreak resulted in a CFR of 53% (151 deaths, 284 infected). Outbreak viruses were isolated and found to be morphologically but antigenically distinct from the related Marburg virus (MARV), which causes similar symptoms of disease, but first appeared in 1967 when workers fell ill from handling infectious African green monkey tissues imported from Uganda (Martini and Siegert 1971). Sporadic and

unpredictable outbreaks of Ebola virus have since occurred mainly in sub-Saharan Africa, with EBOV and SUDV the two species responsible for most of the deaths. To date, the largest outbreak on record was the SUDV outbreak in Uganda during 2000-01, with a CFR of 53% (224 deaths, 425 infected). Furthermore, serological evidence of asymptomatic EBOV infections has been documented in endemic areas. A large-scale surveillance study involving 4,349 adults and 362 children across 220 randomly selected villages in Gabon discovered that the rural population is highly seropositive to EBOV, with an overall prevalence of 15.3% and rising to 32.4% to those living in deeply forested areas (Nkoghe, Padilla et al. 2011).

The remaining three Ebola species consist of BDBV, TAFV and RESTV, and outbreaks with these species in humans have not been as large in scale or frequency compared to EBOV and SUDV. BDBV was discovered during an outbreak in the Bundibugyo district of western Uganda during 2007-08 (Towner, Sealy et al. 2008), and only two BDBV outbreaks have been recorded thus far. Only one case of non-fatal human infection has been documented for TAFV, when an ethnologist fell ill after performing a necropsy on a dead chimpanzee at the Taï Forest reserve in the Ivory Coast in 1994 (Formenty, Hatz et al. 1999). RESTV was isolated during an investigation into unexplained nonhuman primate (NHP) deaths behind a shipment of cynomolgus macaques imported from the Philippines to a quarantine facility located in Reston, Virginia, USA in 1989 (Jahrling, Geisbert et al. 1990). It was subsequently found to be the cause of several outbreaks in primate facilities in Italy, the USA and the Philippines, in some cases causing asymptomatic infections in humans but lethal disease NHPs (Anonymous 1990) (Miranda, White et al. 1991). RESTV antibodies were isolated in 6 workers from the pig farm and slaughterhouse in the Philippines during 2009, but no signs or symptoms of infection were detected (Anonymous 2009).

Currently, the aggregate CFR is 76% for EBOV (1235 deaths, 1623 infected), 54% for SUDV (270 deaths, 502 infected) and 34% for BDBV (48 deaths, 141 infected) (summarized in Table 1.1).

Table 1.1. List of all documented Ebola virus disease outbreaks in humans, organized by year of outbreak and species responsible.

EBOV

Year	Location	Dead	Total	CFR (%)
1976	Democratic Republic of the Congo	280	318	88.0503
1977	Democratic Republic of the Congo	1	1	100
1994	Gabon	31	52	59.6154
1995	Democratic Republic of the Congo	250	315	79.3651
1996	Gabon	21	37	56.7568
1996-97	Gabon	45	60	75
1996	South Africa*	1	2	50
2001-02	Gabon, Republic of the Congo	96	122	78.6885
2002-03	Republic of the Congo	128	143	89.5105
2003	Republic of the Congo	29	35	82.8571
2005	Republic of the Congo	9	12	75
2007	Democratic Republic of the Congo	187	264	70.8333
2008-09	Democratic Republic of the Congo	15	32	46.875
2014 (ongoing)	Guinea, Liberia	142	230	61.7391
Total		1235	1623	76.0937

*Exported cases from the second 1996 Gabon outbreak

SUDV

Year	Location	Dead	Total	CFR (%)
1976	South Sudan	151	284	53.169
1976	England**	0	1	0
1979	South Sudan	22	34	64.7059
2000-01	Uganda	224	425	52.7059
2004	South Sudan	7	17	41.1765
2011	Uganda	1	1	100
2012	Uganda	16	24	66.6667
Total		270	502	53.7849

**Accidental laboratory infection by needle stick

BDBV

Year	Location	Dead	Total	CFR (%)
2007	Uganda	42	131	32.0611
2012	Democratic Republic of the Congo	6	10	60
Total		48	141	34.0426

TAFV

Year	Location	Dead	Total	CFR (%)
1994	Ivory Coast	0	1	0
Total		0	1	0

RESTV

Year	Location	Dead	Total	CFR (%)
1990	Philippines, USA***	0	7	0
2008	Philippines	0	6	0
Total		0	13	0

***Due to import of cynomolgus macaques from the Philippines

1.5 Ecology

Despite the increased number of recent Ebola virus outbreaks leading to increased opportunities to investigate their natural origins, the natural host reservoir species is still unknown. It has been postulated that EBOV is persisting in an unknown host within endemic areas as a zoonotic reservoir, where virus does not cause disease or only does so infrequently if subjected to certain specific circumstances (Groseth, Feldmann et al. 2007), and humans as well as NHPs are inadvertent dead end hosts resulting from EBOV spill-over. Over the past decade, accumulating evidence has pointed to bats as playing an important role in maintenance of virus persistence, and constituting one of the reservoir hosts. This is supported by the successful isolation of MARV from the Egyptian fruit bat (*Rosettus aegyptiacus*) (Towner, Amman et al. 2009), as well as the discovery of a novel Ebola-like virus, LLOV, amongst a species of insectivorous bat (*Miniopterus schreibersii*) residing in Spain (Negredo, Palacios et al. 2011).

The earliest indication that bats could play a possible role in the maintenance of Ebola was during the experimental infection of wild African fruit and insectivorous bats. It was shown that infection of these animals with EBOV supports the replication of virus to high titers without symptoms, where live virus was recovered from the feces of one infected fruit bat (Swanepoel, Leman et al. 1996). A study screening wild small vertebrates captured in Gabon and the Republic of the Congo found EBOV RNA in the liver and spleen, as well as evidence of seroconversion in three types of fruit bats (*Hypsignathus monstrosus*, *Epomops franqueti* and *Myonycteris torquata*) (Leroy, Kumulungui et al. 2005). However, live EBOV is yet to be isolated from an infected wild animal, despite experimentally infected bats showing high circulating levels of virus. One explanation for this discrepancy may be that bats infected naturally in the wild result in very low but persistent EBOV titers, and that a specific

physiological or environmental stimulus is needed to stimulate higher levels virus replication (Leroy, Kumulungui et al. 2005). This is supported by studies demonstrating increased EBOV production in persistently-infected bat lung cells, upon *in vitro* stimulation with lipopolysaccharides and phorbol 12-myristate 13-acetate (Strong, Wong et al. 2008). Further screening studies found that EBOV-specific antibodies can be detected from fruit bats in Ghana (Hayman, Yu et al. 2012) and Bangladesh (Olival, Islam et al. 2013). Interestingly, some dogs in Gabon were found to be asymptomatically-infected, and were likely exposed to Ebola virus by eating the carcasses of infected animals (Allela, Boury et al. 2005).

RESTV infection in animals appears to be more prevalent compared to EBOV. All RESTV cases were traceable to a single monkey breeding and export facility in the Philippines prior to 2008 (Miranda, Yoshikawa et al. 2002). However, after the serendipitous discovery of RESTV in domestic swine suffering from porcine reproductive and respiratory disease syndrome in the Philippines (Barrette, Metwally et al. 2009), bats in the Philippines (Taniguchi, Watanabe et al. 2011) and China (Yuan, Zhang et al. 2012), as well as orangutans in Indonesia (Nidom, Nakayama et al. 2012) were found to also be seropositive to RESTV.

1.6 Transmission

Direct physical contact with infectious tissue and fluids is generally accepted as the primary mode of transmission with Ebola viruses, and outbreaks can occasionally be traced back to an index case where the individual has handled infected bush meat (Peterson, Bauer et al. 2004), or come into direct contact with the reservoir species (Leroy, Epelboin et al. 2009). Amplification and transmission of the virus is then subsequently made possible within the human population via contact with infected tissue as well as bodily fluids such as blood, vomit, urine,

saliva, feces and semen (Bausch, Towner et al. 2007) (Cohen 2004). The improper use of needles as well as prolonged close contact within a nosocomial or laboratory setting, or with the deceased during traditional burial rituals also play a role in transmission to other family members and healthcare workers (Nkoghe, Formenty et al. 2004). In the laboratory, there have been reports that described the successful lethal infection of NHPs with aerosolized EBOV (Johnson, Jaax et al. 1995), where initial infection occurred in the respiratory lymphoid tissues before spreading to regional lymph nodes by infected dendritic cells (DC) and macrophages (Twenhafel, Mattix et al. 2013). In addition, recent studies have demonstrated that EBOV can infect pigs via the mucosal route, in which the infected pigs are then able to shed and transmit virus to other naive pigs (Kobinger, Leung et al. 2011) as well as to naïve NHPs (Weingartl, Embury-Hyatt et al. 2012). The establishment of interspecies airborne transmission without evidence of direct contact, in addition to past epidemiological observations (Roels, Bloom et al. 1999) supports the idea that airborne EBOV transmission may be contributing to the spread of disease during an outbreak.

1.7 Clinical manifestations

1.7.1 Incubation period

Ebola virus disease (EVD) has an incubation period of 2 to 21 days with an average of 4 to 10 days (Feldmann, Sanchez et al. 2013), which is dependent on factors including the infection dose, immune status of patient and the route of infection. EVD can be separated into three different phases: general symptoms (Phase I), specific symptoms (Phase II) and terminal disease (Phase III) (Nkoghe, Leroy et al. 2012). Depending on the disease outcome, survivors will undergo a convalescent phase, while non-survivors will progress to terminal disease.

1.7.2 Phase I: General symptoms

After the incubation period, patients infected with EBOV initially present non-specific, flu-like symptoms. These include: sudden onset of high fever (39 – 40^{o}C), violent headaches, muscle and joint pain in addition to general fatigue and malaise. These symptoms last typically from 2 to 4 days (Nkoghe, Leroy et al. 2012).

1.7.3 Phase II: Specific symptoms

EVD then subsequently progresses to more severe disease characterized by multisystem involvement. Manifestations include gastrointestinal (abdominal pain, nausea, vomiting, diarrhea, loss of appetite leading to weight loss and dehydration), respiratory (sore throat, chest pain, dry cough resulting in pharyngeal damage, difficulty swallowing and shortness of breath), vascular (edema and hypotension), as well as neurologic (headaches, seizures, behavioural changes including aggressiveness, confusion, delirium leading to coma) (Feldmann, Sanchez et al. 2013). A maculopapular rash accompanied by erythema appears between 5 to 7 days, accompanied by hemorrhagic symptoms such as petechiae or ecchymoses, as well as uncontrolled bleeding from puncture sites and the mucosa (Feldmann, Sanchez et al. 2013). These symptoms can last approximately 7 to 10 days (Nkoghe, Leroy et al. 2012).

1.7.4 Phase III: Terminal disease

The latter stages of EVD are characterized by severe metabolic imbalances, anuria, convulsions, and hypovolemic shock. Death occurs approximately 2 to 3 days afterwards due to multi-organ failure from massive tissue injury, as well as capillary extravasation from vascular

permeability and diffuse coagulopathy (Nkoghe, Leroy et al. 2012). Recovery for survivors of EVD is prolonged, lasting more than one month, as well as painful with intense fatigue, loss of appetite, weight and memory loss, and migratory joint pains (Nkoghe, Leroy et al. 2012). Sequelae from EVD are both physical and psychological in nature and can include orchitis, myelitis, recurrent hepatitis, uveitis, as well as psychosis (Feldmann, Sanchez et al. 2013). Shedding of live virus in bodily fluids is detectable for up to three months after disease onset (Rowe, Bertolli et al. 1999) (Rodriguez, De Roo et al. 1999).

1.8 Clinical management and infection control

Clinical care of patients with confirmed disease currently consists only of supportive management. However, provision of patient care can be challenging in rural, isolated settings where most filovirus outbreaks occur. In addition to some communities hiding ill patients and bodies out of fear and distrust for foreign medical workers (Ndayimirije and Kindhauser 2005), abandonment of suspected cases by healthcare workers may also occur from fear of infection, a perceived helplessness in altering the disease outcome, as well as a negative stigma from the community (Clark, Jahrling et al. 2012). Medical and laboratory equipment, supplies and infrastructure are often lacking (Clark, Jahrling et al. 2012). Therefore, the clinical care provided to patients during an outbreak varies widely in quality.

Since early signs of filovirus disease are general and difficult to distinguish from other types of infections, countermeasures are primarily symptom-based and the typical protocol for febrile illnesses was used. Initial treatments include anti-malarial drugs and antibiotics to eliminate the possibility of malaria, as well as prevent and treat secondary bacterial infections. The only antiviral drugs that had been used were acyclovir and ribavirin. Other treatments

include painkillers, sedatives, as well as anti-inflammatory, anti-diarrheal and anti-psychotic drugs, which were administered when needed at the medical doctor's discretion (Clark, Jahrling et al. 2012). Intravenous (IV) rehydration was routinely used in later outbreaks (Guimard, Bwaka et al. 1999). Coagulants such as fibrinogen and prothrombin were routinely given in order to counteract hemorrhaging in patients. In contrast, anti-coagulants such as heparin were also administered to some patients in response to certain disorders, such as disseminated intravascular coagulation (Clark, Jahrling et al. 2012). However, none of the strategies mentioned above have been rigorously tested in the laboratory for efficacy, therefore health benefits for the patient are unknown. Blood transfusions from convalescent to infected patients proved successful during the 1995 EBOV outbreak, where seven of eight recipients survived (Mupapa, Massamba et al. 1999), but this practice is controversial due to safety and practical concerns.

The principle of infection control during an outbreak is based on breaking the human-to-human transmission cycle. Healthcare workers are required to wear personal protective equipment, including scrubs, gowns, apron, rubber boots, head covering, mask, goggles, and at least two pairs of gloves (Raabea and Borcherta 2012). After confirmation of positive cases, patients are quarantined in an isolated building in order to minimize community exposure. Contact tracing is then initiated to identify and follow up on others who may be at high-risk for developing disease. Patients are monitored for at least 21 days, which is the maximum incubation period. In the event of death, the body is decontaminated with a 1:10 bleach solution and placed in a body bag, and then inside a coffin if available and culturally acceptable, and the burial conducted as soon as possible while incorporating traditional indigenous burial beliefs,

such as song and dance, that do not increase transmission risk (Raabea and Borcherta 2012) (Roddy, Weatherill et al. 2007).

1.9 Laboratory diagnosis

The initial symptoms of EVD are non-specific, and a differential diagnosis usually cannot be made with confidence in the clinic until the presentation of pathognomonic signs, such as hemorrhaging. By then it will be too late for effective medical intervention, and EBOV may have spread to other individuals in the meantime, expanding the number of potential cases and prolonging the outbreak. As such, rapid and sensitive virus detections are needed, particularly in the field.

There are several techniques used in the laboratory to detect EBOV, all of which are based on two different approaches. The first is focused on the detection of the virus particle or its components. Techniques that fall under this category include: quantitative reverse transcriptase polymerase chain reaction (RT-qPCR) to detect viral RNA (Towner, Rollin et al. 2004), electron microscopy and virus isolation from cell culture to detect virions, as well as immunohistochemistry, western blotting, immunofluorescence assays, and an antigen enzyme-linked immunosorbent assay (ELISA) to detect viral antigens. The second approach is focused on the detection of the host immune response to EBOV infection, and is performed by IgM or IgG capture ELISA using recombinant NP (Ikegami, Saijo et al. 2003) (Saijo, Niikura et al. 2001), or more recently recombinant GP as the capture antigen (Nakayama, Yokoyama et al. 2010). However, specific antibodies are not always detectable early in the course of EVD, and may not be detected at all in fatal cases due to breakdown of the immune response (Ftika and Maltezou 2013) (Leroy, Gonzalez et al. 2011).

Due to time and resource constraints in the field, antigen ELISA and RT-qPCR were selected as the optimal choices and have been used for the diagnosis of EBOV infections during outbreaks. ELISA is rapid, sensitive and capable of high throughput analysis, requiring approximately 5 hours for assay completion (Ksiazek, Rollin et al. 1992). However, a spectrophotometric plate reader would not be available in rural areas, therefore optical density values are read by the naked eye and interpretation of borderline samples may be subjective. RT-qPCR is also rapid, sensitive and offers a clearer cut-off between positive and negative samples, but a mobile real-time PCR system is needed for analysis. The development of a mobile laboratory unit containing all equipment required for viral RNA extraction and processing has shortened the response time considerably, with a turnaround time of less than 4 hours from the original receipt of clinical samples to the availability of results (Grolla, Jones et al. 2011).

1.10 General overview of the mammalian immune system

The immune system, composed of circulating white blood cells, is responsible for protecting the host against infections caused by foreign organisms, which include but are not limited to viruses, bacteria, fungi, protozoa and helminths. In mammals, the immune response is comprised of two distinct but linked systems: innate immunity and adaptive immunity.

1.10.1 Innate immunity

The innate immune response is the first line of defense against a variety of pathogens. When the physical barriers of the host, such as the skin or mucosa, are breached an inflammatory response is initiated. Neutrophils are the first responders to the site of infection. Neutrophils

first internalize the microorganisms, and then destroy the invading pathogen by producing oxygen radicals or hydrolytic enzymes, such as elastase and defensins (Segal 2005). Macrophages are the next responders and these cells are also crucial for host immunity. Macrophages are differentiated from monocytes after emigration from the endothelium of blood vessels, and are specialized in removing infected cells, including dead neutrophils via phagocytosis. After ingestion of the cell or pathogen, the resulting phagosome is fused with lysosomes inside the macrophage, in which the microorganism is digested by enzymes and reactive oxygen species. Compared to neutrophils, macrophages are longer-lived and able to secrete chemokines and cytokines which are important for the recruitment of other monocytes to the site of infection (Eming, Krieg et al. 2007). Natural killer cells are a lymphocyte subset that is also able to provide a rapid, non-specific response to tumours or infected cells by producing pro-inflammatory cytokines such as IFN-γ and TNF-α, which promote macrophage phagocytosis and direct lysis of infected cells or parasites, respectively (Robertson 2002).

Several components of the innate immune response are able to influence and shape the resulting adaptive immune response. After the digestion of invading pathogen, DCs along with macrophages are the primary cells that attach the digested peptide antigen to a MHCII molecule for presentation to the CD4 receptor of a corresponding helper T-cell. Therefore, these antigen-presenting cells represent a major link between innate and adaptive immunity (Palucka and Banchereau 1999). Furthermore, studies have shown that the CD16 receptor of natural killer cells can recognize the Fc region of the opsonizing antibodies that are produced by B-cells during the adaptive phase of the host immune response. The natural killer cells are activated by this process, releasing cytolytic granules which result in the apoptosis of the infected cell (Smyth, Hayakawa et al. 2002). Therefore, the function of the innate immune response is to

provide a rapid, non-specific response in hopes of containing the replication and spread of the pathogen, in addition to activating the adaptive immune response.

1.10.2 Adaptive immunity

If the innate immune system is unable to effectively control the infection, the adaptive immune response will be triggered to combat the pathogen. Compared to innate immunity, the adaptive immune system is a highly specialized host response that is tailored only to the foreign microorganism responsible for initially activating the immune response. Additionally, adaptive immunity typically results in immunological memory, in which the host is able to respond much more rapidly to infection with the same pathogen upon re-exposure in the future. This acquired immunity is the basis behind vaccinations. There are two different types of lymphocytes which mediate the adaptive immune response: T-cells and B-cells.

1.10.2.1 T-cells

T-lymphocytes are a heterogeneous population with different subsets, and are broadly split into $CD8^+$ or $CD4^+$ T-cells, also known as cytotoxic and helper T-lymphocytes, respectively. $CD8^+$ T-cells have the ability to recognize antigen bound to the MHCI molecules of infected cells. After activation and clonal expansion, these effector cytotoxic lymphocytes will secrete perforin and granulysin in order to kill infected cells. Antigen presenting cells can induce two types of effector $CD4^+$ T-cells responses: Th1 and Th2, which play a crucial role in the clearance of the invading pathogen (Mosmann, Cherwinski et al. 1986). The Th1 response is characterized by IFN-γ production, which leads to enhanced macrophage activity, and the proliferation of $CD8^+$ cytotoxic T-cells, resulting in cell-mediated immunity (Scott 1991). Th1

responses are typically associated with the clearance of intracellular pathogens, such as viruses, protozoa and several types of bacteria. The Th2 response is characterized by IL-4 production (Swain, Weinberg et al. 1990), which leads to B-cell proliferation, antibody-class switching, and increased neutralizing antibody production, resulting in humoural immunity (Kapsenberg 2003). Th2 responses are usually associated with the clearance of extracellular pathogens, such as parasites and extracellular bacteria.

1.10.2.2 B-cells

While T-cells can only recognize antigen fragments presented on the MHC molecules of either infected or professional antigen presenting cells, B-cells are able to recognize viral antigen in its native form (Janeway, Travers et al. 2001). A naïve mature B-cell is able to produce two immunoglobulin (Ig) classes, IgM and IgD. The pentamer IgM is a cell-surface molecule and is the first antibody to appear in response to the presence of an antigen (Janeway, Travers et al. 2001). When a B-cell encounters its matching antigen, the cell can be activated in a T-lymphocyte dependent or independent manner. In T-cell dependent activation, helper T-cells are needed to provide a signal via CD40 and cytokine receptors, which result in antibody class switching to produce IgG, IgA or IgE antibodies (Kracker and Radbruch 2004). During class switching, the constant region of the Ig heavy chain can be change with the variable region remaining constant, thereby allowing the same B-cell to produce different isotypes of antibodies (eg. IgG: IgG1 to IgG4; IgA: IgA1 and IgA2). In T-cell independent activation, the signals to activate the B-cell are provided by toll-like receptors, or by antigen cross-linking. Although this method results in a more rapid humoural immune response, affinity maturation and antibody class switching does not occur with T-cell independent activation. The majority of antigens are

T-cell dependent, and the monomeric IgG antibody is the main circulating isotype found in the host after an infection (Janeway, Travers et al. 2001).

1.11 Immunopathology of EBOV

EBOV favours monocytes, macrophages and immature DCs as initial sites of infection and replication (Geisbert and Hensley 2004). Infection of monocytes and macrophages lead to the uncontrolled release of pro-inflammatory cytokines and chemokines, including TNF-α, interleukin (IL)-1β, and macrophage inflammatory protein (MIP)-1α, as well as reactive oxygen and nitrogen species (Feldmann, Bugany et al. 1996) (Bray and Geisbert 2005). This attracts more monocytes, macrophages as well as neutrophils to the site of infection in a positive feedback loop, contributing to increased vascular permeability and vasodilation (Zampieri, Sullivan et al. 2007). Infected monocytes and macrophages overexpress cell surface tissue factor, which contribute to the coagulation abnormalities (Geisbert, Young et al. 2003). Furthermore, infected immature DCs do not secrete IFN-α, undergo full activation or maturation, nor up-regulate major histocompatibility complex (MHC) molecules to stimulate T-cells (Bosio, Aman et al. 2003) (Mahanty, Hutchinson et al. 2003), thereby impairing the resulting adaptive immune response. The virus has been suggested to disseminate in the host by using the lymphatic system as a mode of transport (Hensley, Young et al. 2002) to endothelial cells, as well as several cell types found in the liver, lung and spleen for replication and spread (Zampieri, Sullivan et al. 2007). The majority of the observed damage is caused by the uncontrolled viremia after infection. In addition to the dysregulated inflammatory response and the absence of adaptive immunity, an examination of human tissues show that tissue damage correlates with the presence of viral antigens and nucleic acid (Zampieri, Sullivan et al. 2007) (Zaki and

Goldsmith 1999), indicating that direct damage to the organs caused by viral replication plays a role in multi-organ failure. Viremia can exceed 10^6 plaque forming units (PFU) per millilitre (mL) of human sera (Anonymous 1978a), and the aggressiveness of EBOV means that most patients do not have sufficient time to mount a regulated immune response in order to control the infection before rapidly succumbing to the disease.

1.12 Immunoevasion of EBOV

EBOV has developed several methods to antagonize the IFN-α and -β responses in target cells such as macrophages, monocytes and DCs, which prevent the proper activation of host innate immunity. EBOV infection of human liver cells (Huh7) results in the antagonization of key antiviral responses, including Toll-like receptor (TLR)-, IFN regulatory factor (IRF)-3-, and protein kinase R-related pathways (Kash, Muhlberger et al. 2006). Conversely, RESTV infection of Huh7 cells results in a significant increase in the expression of IFN-stimulated genes instead (Kash, Muhlberger et al. 2006), which suggests an inverse correlation between the magnitude of Type I IFN responses and virulence (Kash, Muhlberger et al. 2006). Two EBOV structural proteins are important for the down-regulation of the IFN response. VP24 is known to desensitize host cells to the effects of IFN-α/β and IFN-γ. This is achieved by preventing the Janus kinase (JAK)-1 and Tyrosine kinase-2-mediated homo- or hetero-dimerization of Signal transducers of activation and transcription (STAT)-1 and STAT-2. This prevents JAK-STAT nuclear accumulation, which leads to the reduced expression of other IFN-stimulated genes (ISG) (Reid, Leung et al. 2006) (Reid, Valmas et al. 2007). VP35 can interfere with the synthesis and expression of IFN and ISGs in several ways. First, VP35 is known to block IRF-3 phosphorylation, which prevents its nuclear accumulation (Basler, Mikulasova et al. 2003) and

promotes the inactivation of IRF-7 through SUMOylation (Chang, Kubota et al. 2009). Second, VP35 binds viral double stranded RNA during the EBOV replication cycle and sequesters it away from recognition by retinoic acid-inducible gene (RIG)-I and Dicer (Cardenas, Loo et al. 2006) (Kimberlin, Bornholdt et al. 2010) (Leung, Prins et al. 2010), averting the downstream expression of ISGs and inhibiting double stranded RNA degradation through the RNA-induced silencing complex (Kuhl and Pohlmann 2012). Third, VP35 is also able to inhibit and reverse the activation of protein kinase R (Schumann, Gantke et al. 2009), which stops the translational arrest of viral mRNAs. Finally, expression of VP35 in immature mouse DCs has been shown to suppress the up-regulation of Cluster of differentiation (CD)40, CD80, CD86 and major histocompatibility complex (MHC)II in addition to the induction of cytokines such as IL-6, IL-12, TNF-α and IFN-α/β, preventing DC maturation and diminishing their ability to activate $CD4^+$ T-cells (Jin, Yan et al. 2010). The Type I IFN response is also crucial for *in vivo* control of Ebola virus. While immunocompetent mice are immune to EBOV infection, mice knockout for the STAT-1 or the IFN-α/β receptors, as well as wild-type mice treated with IFN-specific antibody become susceptible to the virus, and die from a disease with symptoms resembling that of filovirus infection in humans and NHPs (Bray 2001).

GP plays a role in viral pathogenesis by evading the immune response via epitope masking and steric shielding of the antigen. Structural modeling of GP reveals a surface heavily covered with N- and O-linked oligosaccharides as well as sialic acids (Cook and Lee 2013), which plays a key role in both strategies. The dense concentration of glycans creates a difficult environment for the binding of specific neutralizing antibodies, and instead the immune system is only able to produce antibodies against highly variable or non-protective epitopes. It has been shown in mice that cross-reactive antibodies targeting conserved areas of GP can be generated

after the removal of the glycosylated mucin-like domain (Ou, Delisle et al. 2012). The high clusters of glycans also prevent the proper interaction of GP with host MHCI and β1 integrin by steric occlusion (Francica, Varela-Rohena et al. 2010), resulting in the inhibition of the immune response. A follow-up study found that the efficiency of steric shielding between different Ebola species correlate with the difference in their relative pathogenicity (Noyori, Matsuno et al. 2013). The effect of GP-mediated virulence was demonstrated by *in vivo* studies in an IFN receptor knockout ($IFNAR^{-/-}$) mouse model of infection. Recombinant RESTV was generated, in which its wild-type GP was replaced with the EBOV GP (RESTVΔG/EBOVGP); and recombinant EBOV was generated, in which its wild-type GP was replaced with RESTV GP (EBOVΔG/RESTVGP). While mice challenged with EBOV/RESTVGP showed a prolonged average time to death and decreased mortality, those receiving RESTV/EBOVGP did not show any signs of disease (Groseth, Marzi et al. 2012).

sGP was recently demonstrated to play a role in viral immune evasion through a novel mechanism. In studies where mice has been co-immunized or sequentially immunized with sGP and full-length EBOV GP, the host humoural immune response was directed towards the production of antibodies against GP epitopes that cross-react with sGP, thereby allowing sGP to subvert the host antibody response by acting as a decoy antigen to absorb GP-specific antibodies (Mohan, Li et al. 2012). Surprisingly, the addition of sGP was also able to subvert an already existing antibody response established by vaccination with GP (Mohan, Li et al. 2012), which will have important implications for the design of an effective EBOV vaccine.

1.13 Animal models

Animal models that accurately recapitulate EBOV disease are needed for rapid and efficient screening to determine the efficacy of candidate vaccines and drugs. However, infection with wild-type EBOV does not result in lethal disease in adult, immunocompetent mice due to their strong Type I IFN response upon infection (Bray 2001), and only causes a transient, mild fever in guinea pigs (Ryabchikova, Kolesnikova et al. 1996). As a result, the wild type virus has been adapted to cause disease and death in its specific rodent host, but the hallmarks of human EBOV disease are not always observed in these animals. There are four candidate animal models available for EBOV disease to date, each with their own strengths and weaknesses.

1.13.1 Mice

An immunocompetent mouse model was developed by serial passaging of wild-type EBOV Mayinga variant in the livers and spleens of progressively older suckling mice. This resulted in a variant that has acquired lethal virulence to adult BALB/c and C56BL/6J mice, with the median lethal dose (LD_{50}) estimated to be approximately one virion (Bray, Davis et al. 1999). Intraperitoneal (IP) inoculation of this new EBOV variant, called mouse-adapted EBOV (MA-EBOV), caused disease symptoms including ruffled fur, reduced activity and weight loss 3-4 days post infection (dpi). Mice died at 5-7 dpi, where virus titers reached up to 10^9 PFU/gram (g) in the liver and spleen. Massive lymphocyte apoptosis was observed, but the process and morphology was different from that of NHPs and humans (Bradfute, Braun et al. 2007). Viremia was reported to peak at 10^7 PFU/mL, and elevated levels of liver enzymes including aspartate transaminase (AST) and alanine transaminase (ALT) was detected. However, there were only mild coagulation disorders, and inoculation of the immunocompetent mice through the subcutaneous (SC), intradermal (ID) or intramuscular (IM) routes did not cause disease (Bray,

Davis et al. 1999). Therefore, mice are only of limited value for mimicking clinical human EBOV disease and are not expected to have high predictive values for therapeutic efficacy in a higher animal model. Nevertheless, mice make valuable initial screening tools due to their low unit of cost. Reagents and knockout mice to study immune responses are readily available, and large numbers of mice can be used to achieve results with statistical significance.

1.13.2 Guinea pigs

A lethal guinea pig animal model was developed by serial passaging of wild-type EBOV Mayinga variant in the spleens of inbred strain 13 guinea pigs, resulting in a uniformly lethal virus at passage 4 (Connolly, Steele et al. 1999) that is also able to cause disease in outbred Hartley guinea pigs. Infection with the guinea pig-adapted EBOV (GA-EBOV) caused disease starting at 5 dpi, and is characterized by fever, anorexia and dehydration, leading to death by 8-11 dpi. Compared to mice, infected guinea pigs demonstrate increased fibrin deposition, which is coincident with a drop in platelet counts, leading to a prolonged prothrombin time (PT) and activated partial thromboplastin time (aPTT). However, the observed coagulation defects were not as severe as that of NHPs, and despite the observation of lymphopenia and neutrophilia starting at 2 dpi, lymphocyte bystander apoptosis was not detected. GA-EBOV replicated to high titers in the spleen liver, lung and adrenal glands in the host, and viremia was reported to be greater than 10^4 PFU/mL. Furthermore, GA-EBOV infection is lethal for guinea pigs regardless of inoculation route. Guinea pigs display more hallmarks of human EBOV disease compared to mice, and therefore are expected to be more predictive of therapeutic efficacy. However, a significant drawback is the lack of available reagent and tools to perform cytokine profiling and assay for T-cell activity, therefore only B-cell responses can be measured in this animal model.

Regardless, guinea pigs are a useful intermediate animal model to bridge findings and confirm experimental trends from mice before NHPs (Connolly, Steele et al. 1999).

1.13.3 Syrian golden hamsters

Syrian golden hamsters (*Mesocricetus auratus*) have already been broadly used in animal models for human infectious diseases. However, it has only been developed as an animal model for EBOV infection recently. While infection with wild-type EBOV does not cause lethal infection in hamsters, challenge of animals IP with 1000 focus forming units (FFU) of MA-EBOV causes lethal disease characterized by ruffled fur and decreased activity starting 3 dpi, resulting in death at 4-5 dpi (Ebihara, Zivcec et al. 2013). Target organs for MA-EBOV in the hamster were the mesenteric lymph nodes, the liver, spleen and adrenal glands. However, the animals do not lose weight and are resistant to infection if MA-EBOV was given SC. Infected hamsters display bystander lymphocyte apoptosis, in addition to severe coagulopathy with prolonged PT and aPTT at the late stages of infection (Ebihara, Zivcec et al. 2013).

Of the small animal models, the Syrian golden hamster displays pathological symptoms that are most similar to those observed in EBOV-infected NHPs and humans (Nakayama and Saijo 2013). Reagents to test for cytokine, chemokine and T-cell activity in hamsters have not been developed yet, but RT-qPCR based assays for the detection of 51 genes related to immune responses have been published for use in Syrian golden hamsters (Zivcec, Safronetz et al. 2011). Therefore, the Syrian golden hamster may offer higher predictive levels for therapeutic efficacy, but is currently not a commonly-used animal model for EBOV infections.

1.13.4 Nonhuman primates

A variety of NHP species have been used for studies with EBOV, including African green monkeys (*Chlorocebus aethiops*), baboons (*Papio hamadryas*), rhesus macaques (*Macaca mulatta*) and cynomolgus macaques (*Macaca fascicularis*). However, rhesus and cynomolgus macaques are extensively researched as the main NHP models for EBOV infections due to their increased susceptibility compared to other species (Bente, Gren et al. 2009), but the viral dose, variant, as well as the route of infection can play a role in affecting the progression of disease. Inoculation of rhesus or cynomolgus macaques IM with 1000 PFU of EBOV Kikwit variant leads to the development a high-grade fever with temperatures above 40^{o}C, in addition to viremia at 3 dpi (Nakayama and Saijo 2013). Lymphadenopathy in the peripheral lymph nodes occurs early in disease, with neutrophilia in addition to severe lymphopenia often detected in infected primates (Geisbert and Hensley 2004). Thrombocytopenia is also observed, resulting in a loss in the ability of blood to clot (Fisher-Hoch, Platt et al. 1983). EBOV can be detected in high amounts in the liver, spleen and lung, while also having lower affinity for the kidney, adrenal glands, testes, lymph nodes and the pancreas, resulting in organ titers of $10^{5.5\text{-}8.6}$ PFU/g at 6 dpi (Geisbert, Hensley et al. 2003). Ion levels in plasma drop during disease with a concomitant rise in urea and creatinine levels, indicating metabolic disorders. Furthermore, AST and ALT are observed to be elevated during the course of the disease (Fisher-Hoch, Platt et al. 1983). Animals develop a maculopapular rash around 4 dpi, and may lose up to 10% of their body weight due to dehydration and loss of appetite (Bente, Gren et al. 2009). Cynomolgus macaques are more susceptible to EBOV infection than rhesus macaques. On average, cynomolgus and rhesus macaques succumb to EBOV disease at 6.04 ± 0.82 dpi and 7.75 ± 1.26 dpi, respectively, after an IM challenge with 1000 PFU of EBOV (Qiu, Wong et al. 2013).

Prior to pursuing clinical trials, candidate treatments must be tested for protection in the rhesus or cynomolgus macaque animal models. These two NHP species exhibit many of the same hallmarks observed in human filovirus disease with no adaption of the virus needed (Nakayama and Saijo 2013) (Bente, Gren et al. 2009), and are considered to be the best animal models available for predicting the efficacy of candidate EBOV vaccines and post-exposure treatments in humans. However, practical and ethical considerations, such as the high unit cost per animal, labour-intensive husbandry, high maintenance costs, and the requirement of specialized facilities to house these animals have led to the restriction of experiments, in which experimental findings need to be first demonstrated in a small animal model before subsequent validation in NHPs.

1.14 Vaccines

Over the past decade, immunization with several experimental EBOV vaccine candidates have resulted in the induction of specific B- and T-cell responses, resulting in protection against EBOV disease in NHPs (Table 1.2). The earliest instance of 100% protection in NHPs came from a DNA vector expressing EBOV GP (DNA-GP) with boosting from a recombinant human adenovirus serotype 5 virus expressing EBOV GP (Ad5-GP). Three 100 μg doses of DNA-GP were administered IM every 4 weeks before an intramuscular (IM) Ad5-GP boost of 10^{10} PFU at 20 weeks after the first DNA dose. Challenge with EBOV at 32 weeks after the initiation of vaccination yielded protection in all vaccinated cynomolgus macaques (Sullivan, Sanchez et al. 2000). A subsequent study showed that a single vaccination of cynomolgus macaques with equal IM doses of Ad5-GP and Ad5 expressing EBOV NP at 2 x 10^{12} particles was fully protective when NHPs were challenged 4 weeks later (Sullivan, Geisbert et al. 2003). Phase I

clinical trials showed that the DNA- and Ad5-based vaccines were both safe and immunogenic in humans (Martin, Sullivan et al. 2006) (Ledgerwood, Costner et al. 2010). Concerns regarding host pre-existing immunity (PEI) to Ad5-specific antibodies can be overcome by multiple vaccinations or by administration of the vaccine via the mucosal route (Richardson, Abou et al. 2011) (Croyle, Patel et al. 2008).

Another group vaccinated cynomolgus macaques with three IM injections of EBOV virus-like particles (VLP) containing EBOV GP, NP and VP40, each dose containing 250 μg total protein and given at 6 week-intervals. Challenge at 4 weeks after the last injection also resulted in full protection (Warfield, Swenson et al. 2007).

A recombinant human parainfluenza virus type 3 virus expressing EBOV GP (HPIV3-EBOVGP) gave complete protection against challenge within 10 weeks amongst rhesus macaques, with two intranasal (IN) and intratracheal (IT) doses of 2×10^7 $TCID_{50}$ spaced 4 weeks apart, however concerns with host PEI against this vaccine platform still need to be addressed (Bukreyev, Rollin et al. 2007). A single IM injection of 10^7 PFU VSVΔG/EBOVGP was able to fully protect cynomolgus macaques if administered 4 weeks before challenge (Jones, Feldmann et al. 2005). Most recently, vaccination of rhesus macaques IM with 5×10^7 FFU of a live-attenuated, recombinant rabies virus (RABV) expressing EBOV GP resulted in complete protection, when the animals were challenged with EBOV 70 days after vaccination (Blaney, Marzi et al. 2013). However, with the exception of VSVΔG/EBOVGP, the candidate vaccines listed above have not been shown to provide post-exposure protection. As a result, there is a need for the development of strategies that are efficacious after EBOV infection.

Table 1.2. Summary of vaccine candidates in NHPs against EBOV infection.

Treatment	Dose	Number of doses and times of vaccination	Survival (%)	Clinical trials?	Reference
DNA-GP with Ad5-GP boost	100 µg DNA IM, 10^{10} PFU Ad5 IM	3 doses of DNA at 32, 28 and 24 weeks and 1 dose of Ad5 at 12 weeks before challenge	100% (4 of 4)	Yes (Phase I), NCT00072605 and NCT00374309	(Sullivan, Sanchez et al. 2000)
Ad5-EBOVNP and Ad5-EBOV GP	Equal amounts of each Ad5 totaling 2 x 10^{12} total particles	1 dose at 4 weeks before challenge	100% (4 of 4)	Yes (Phase I), NCT00374309 (Ad5-GP only)	(Sullivan, Geisbert et al. 2003)
VLPs	250 µg IM	3 doses at 16, 10 and 4 weeks before challenge	100% (5 of 5)	No	(Warfield, Swenson et al. 2007)
HPIV3-EBOVGP	2 x 10^7 $TCID_{50}$, IN/IT	2 doses at 14 and 10 weeks before challenge	100% (3 of 3)	No	(Bukreyev, Rollin et al. 2007)
VSVΔG-EBOVGP	1 x 10^7 PFU, IM	1 dose at 4 weeks before challenge	100% (4 of 4)	No	(Jones, Feldmann et al. 2005)
RABV-EBOVGP	5 x 10^7 FFU, IM	1 dose at 70 days before challenge	100% (4 of 4)	No	(Blaney, Marzi et al. 2013)

1.15 Post-exposure treatments

Current therapeutic strategies against EBOV disease can be separated into different categories based on their mechanism of action: 1) Recombinant nematode anticoagulant protein c2 (rNAPc2) and recombinant human activated protein C (rhAPC) are non-filovirus specific compounds aimed at treating the clinical symptoms of coagulopathy and sepsis, respectively, 2) siRNAs and positively-charged phosphorodiamidate morpholino oligomers (PMO*plus*) are compounds specifically designed to inhibit viral replication and translation, respectively; and 3) VSVΔG/EBOVGP to boost host immune responses in order to fight disease. The candidates are discussed in further detail below (summarized in Table 1.3).

rNAPc2 inhibits tissue factor VIIa-mediated coagulation by preventing thrombin formation (Moons, Peters et al. 2002), and is utilized to counter thrombosis-related organ failure. It has already completed Phase I (Vlasuk, Bradbury et al. 2003) and II clinical trials (Lee, Agnelli et al. 2001) (Moons, Peters et al. 2003). Rhesus macaques were administered daily SC injections of rNAPc2 at 30 μg/kg, starting either 10 minutes (n=6) or 24 hours (n=3) after EBOV exposure for 14 and 8 days, respectively. Both treatments prolonged survival with an increase of mean time-to-death of 3.4 days, and 33% of NHPs were protected in each group (Geisbert, Hensley et al. 2003). rhAPC is a clinically approved compound used to treat severe sepsis in humans (Hensley, Stevens et al. 2007). Rhesus macaques (n=11) were given rhAPC as a continuous intravenous (IV) infusion beginning 30-60 minutes after infection for 7 days, resulting in prolonged survival with an increase of mean time-to-death of 4.3 days and survival rates of 18% (2 of 11) (Hensley, Stevens et al. 2007).

siRNAs can be designed with homology against specific viral targets upon knowledge of the desired target sequence. First, siRNAs targeting EBOV VP24, VP35 and L were generated

behind the rationale of preventing the down-regulation of Type I IFN responses and suppressing virus replication. Pooled siRNAs were delivered at 2 mg/kg to rhesus macaques as a bolus IV infusion, starting 30 minutes after EBOV challenge and then either on days 1, 3 and 5 (n=3) or daily on days 1 to 6 (n=4). This approach protected 66% and 100% of animals given four and seven doses, respectively (Geisbert, Lee et al. 2010) and are approaching Phase I clinical trials, pending the reformulation of its product (ClinicalTrials.gov 2014a). PMO*plus* are an improved class of positively-charged compounds based on phosphorodiamidate morpholino oligomers, which are neutrally-charged, synthetic antisense oligonucleotide analogs resistant to degradation by RNase H (Warren, Shurtleff et al. 2012). PMOs can also be designed to target any desired viral targets, and inhibits translation through steric hindrance by binding to viral mRNA. Pooled PMO*plus* designed against EBOV VP24, VP35 and L (AVI-6002) was delivered daily at a dose of 40 mg/kg to rhesus macaques via the subcutaneous (SC) and IP routes over 10 (n=4) and 14 days (n=4), starting between 30–60 minutes of infection. This strategy protected a combined 63% (5 of 8) NHPs. In a follow-up study, AVI-6002 was administered daily at a dose of 28 or 40 mg/kg to rhesus macaques (n=5) via the IV route, beginning 30-60 minutes after infection and spanning 14 days. This strategy protected 60% (3 of 5) NHPs (Warren, Warfield et al. 2010). AVI-6002 completed Phase I clinical trials in late 2011 (ClinicalTrials.gov 2014b).

The live-attenuated VSVΔG/EBOVGP is designed to rapidly elicit potent, specific B- and T-cell immune responses in the recipient. A single intramuscular (IM) injection of VSVΔG/EBOVGP at a dose of 2×10^7 PFU to rhesus macaques (n=8) protected 50% (4 of 8) animals if given 30 minutes after challenge (Feldmann, Jones et al. 2007). Recombinant VSV-based vaccines are not yet slated for clinical trials.

Table 1.3. Summary of post-exposure treatments in NHPs against EBOV infection.

Treatment	Time of first intervention (after exposure)	Dose	Number of doses (days of treatment)	Survival (%)	Clinical trials?	Reference
rhAPC	30-60 minutes	Continuous infusion over 7 days		2/11 (18%)	Approved for human use	(Hensley, Stevens et al. 2007)
rNAPc2	10 minutes	30 µg/kg	15 (0-14)	2/6 (33%)	Yes (Phase II)*	(Geisbert, Hensley et al. 2003)
	24 hours	30 µg/kg	9 (0-8)	1/3 (33%)		
siRNA	30-60 minutes	2 mg/kg	4 (0, 1, 3, and 5)	2/3 (67%)	Pending (Phase I), NCT01518881	(Geisbert, Lee et al. 2010)
			7 (0-6)	4/4 (100%)		
PMO*plus*	30-60 minutes	40 mg/kg, IP and SC	11 (0-10), n=4	5/8 (63%)	Yes (Phase I), NCT01353027	(Warren, Warfield et al. 2010)
			15 (0-14), n=4			
		40 mg/kg, IV	15 (0-14), n=5	3/5 (60%)		
VSVΔG-EBOVGP	20-30 minutes	2 x 10^7 PFU, IM	1	4/8 (50%)	No	(Feldmann, Jones et al. 2007)

* For coronary disease. (see: http://clinicaltrials.gov/ct2/show/NCT00116012)

1.16 Immune correlates of protection

An immune correlate of protection (CoP) is defined as "a specific immune response to a vaccine that is closely related to protection against infection, disease, or other defined end point" (Plotkin 2010). In practice, it is neither realistic nor necessary to elucidate a complete immunological profile from every patient to determine protection against every type of disease, therefore the identification of the immune CoP after natural infection, vaccination, or post-exposure treatment is an important research topic. Besides basic immunological interest, characterizing these immune responses give researchers valuable knowledge in choosing the correct antigens to include in a candidate vaccine, predicting protection on an individual and population level without having to challenge the patients with live pathogens, revealing trends in previously collected data on survivors versus non-survivors of disease, and may be used to discourage experiments or clinical trials that are deemed to have a low chance of success (Plotkin and Gilbert 2012). The immune CoP is a marker of immune function that is consistently and reliably related to protection, as evidenced by statistical analysis. The immune response in question may then be a non-mechanistic CoP, which does not induce protection on its own but nonetheless is still predictive through its relationship with another immune response that is responsible for survival, or a mechanistic CoP, which is the immune component critical for survival from disease (Plotkin and Gilbert 2012), but not necessarily the same as the mechanism that eliminates the pathogen from the host (Plotkin 2008).

The immune CoP against survival from EBOV is poorly defined to date and has been a matter of intense debate. Immune responses that correlate to protection from EBOV have typically been deduced in the past from studies of passive antibody or adoptive cell transfer, determining protection efficacy in immunocompromised subjects or inferred from surviving

animals of challenge experiments. However, there is a split between the reports on the nature of the immune responses necessary to induce protection. From vaccination studies, a DNA plasmid encoding GP or sGP was successful in protecting immunized guinea pigs from lethal challenge with GA-EBOV. Subsequent analysis of immune responses showed that both levels of IgG as well as T-cell responses specific against the GP and sGP antigens correlate to protection (Xu, Sanchez et al. 1998). Venezuelan equine encephalitis virus (VEEV)-based RNA replicons expressing GP or NP were also successful in protecting BALB/c mice, as well as strain 2 and strain 13 guinea pigs from challenge, and EBOV-specific IgG levels were correlated with survival in vaccinated animals (Pushko, Bray et al. 2000). In vaccination studies involving NHPs, robust humoural and cell-mediated responses were detected in many survivors of EBOV challenge. EBOV-specific IgG and IFN-γ^+ producing $CD8^+$ T-cells were detected in NHP survivors vaccinated with Ad5-GP and boosted with DNA-GP (Sullivan, Sanchez et al. 2000) (Sullivan, Geisbert et al. 2003). High IgG levels specific for GP, NP and VP40, as well as vigorous $CD4^+$ and $CD8^+/CD44^+$ T-cell responses expressing TNF-α were associated with a favourable outcome in NHPs vaccinated with EBOV VLPs (Warfield, Swenson et al. 2007). Survivor NHPs mucosally vaccinated with human parainfluenza virus type 3 (HPIV3)-EBOVGP demonstrated high IgG and IgA levels against GP, as well as $CD4^+$ and $CD8^+$ T-cells secreting TNF-α and IFN-γ from *in vitro* stimulation of the peripheral mononuclear blood cells (PBMC) (Bukreyev, Rollin et al. 2007). Strong EBOV-specific IgG responses, in addition to specific $CD4^+$ and $CD8^+$ T-cells expressing TNF-α and IFN-γ were also detected in VSVΔG/EBOVGP vaccinated NHPs that survived EBOV challenge (Jones, Feldmann et al. 2005).

From immunity transfer studies, it was reported that the adoptive transfer of $CD8^+$ T-cells specific for EBOV NP from C57BL/6J mice vaccinated with the VEEV-based vaccine to naïve

animals was protective against MA-EBOV challenge (Wilson and Hart 2001), whereas passive transfer of IgG sera from immunized to naïve animals did not protect mice and only 1 of 5 recipient guinea pigs survived infection (Pushko, Bray et al. 2000). In another study, mice infected SC with MA-EBOV survived infection and were shown to have high virus-specific IgG titers. The passive transfer of their immune sera into naïve and SCID mice resulted in complete protection and a delay in the peak level of viral replication, suggesting antibodies alone can protect from disease (Gupta, Mahanty et al. 2001). The monoclonal antibody (mAb) KZ52, isolated from a recovering patient of EBOV infection, was highly neutralizing *in vitro* (Maruyama, Rodriguez et al. 1999) and demonstrated non-sterilizing immunity in strain 13 guinea pigs, leading to protection if administered 1 hour before or after GA-EBOV challenge (Parren, Geisbert et al. 2002). However, in NHPs the passive transfer of KZ52 intravenously (IV) at two doses of 50 mg/kg administered 1 day before exposure and 4 dpi failed to control viremia, impact the course of disease and did not provide protection (Oswald, Geisbert et al. 2007). Furthermore, passive transfer of concentrated polyclonal antibodies from Ad5-GP vaccinated NHPs to naïve animals only protected 1 of 4 NHPs, suggesting that the role of humoural immunity may be limited in protection (Sullivan, Hensley et al. 2011).

Studies were also performed in immunocompromised animals in order to elucidate an immunological trend important for survival from EBOV. CD4- ($CD4^{-/-}$), CD8- ($CD8^{-/-}$) and B-cell ($B\text{-cell}^{-/-}$) deficient mice from a C57BL/6J background were infected SC with MA-EBOV. While $CD4^{-/-}$ and $B\text{-cell}^{-/-}$ mice cleared infection and survived, $CD8^{-/-}$ mice succumbed to infection (Gupta, Mahanty et al. 2004). Immunodepletion of these $B\text{-cell}^{-/-}$ survivor mice with CD4-specific antibodies resulted in survival from IP re-challenge with MA-EBOV, whereas the same mice treated with CD8-specific antibodies did not survive IP re-challenge (Gupta, Mahanty

et al. 2004). In NHP studies, animals vaccinated with Ad5-GP were depleted of $CD3^+$ or $CD8^+$ T-cells *in vivo*. While vaccinated NHPs not immunodepleted with antibodies survived challenge, administration of the anti-$CD3^+$ antibody abrogated protection in 2 of 2 NHPs, whereas 4 of 5 animals given anti-$CD8^+$ antibody cM-T807 did not survive challenge (Sullivan, Hensley et al. 2011).

1.17 Knowledge gap

Based on the literature at the time, it appears that the surviving animals in successful vaccination studies always demonstrated strong levels of both the B- and T-cell responses. In other studies, the observation that immunodepletion of $CD8^+$ T-cells in NHPs abrogated protective immunity, coupled with the failure of KZ52 to generate protection in NHPs meant that there is a significant bias towards cell-mediated immunity being the critical component for protection, and therefore the mechanistic CoP towards EBOV. However, two critical studies are still needed to prove beyond any doubt that the cell-mediated immune response is essential for protection from EBOV. The first is the survival of naïve NHPs from EBOV challenge, with protection conferred by the adoptive transfer of EBOV-specific $CD8^+$ T-cells, which would indicate that $CD8^+$ T-cells are required and sufficient for protection within the individual. The second is that the large-scale comparison of immune responses between surviving and non-surviving NHPs of EBOV infection must demonstrate a clear difference in the $CD8^+$ T-cell response, which would indicate that the cell-mediated immune response correlates with protection in a genetically diverse population.

1.18 Hypothesis

The hypothesis for this thesis is: ***specific CD8$^+$ T-cell responses are responsible for the protection observed in surviving animals of EBOV, and therefore constitute the immune correlates of protection.***

1.19 Objectives

The immune correlates to protection to EBOV will be demonstrated in three commonly used animal models: mice, guinea pigs and NHPs, using the strengths of each model.

1) ***To determine the immune responses important for survival in mice.*** Groups of transgenic/knockout mice with ablation of selected immune pathways will be vaccinated with Ad5-GP and then challenged with MA-EBOV at 28 dpi, after the vaccine has been given sufficient time to establish immunity. Survival proportions will indicate the relative contribution of each immune response compartment to protection.

2) ***To confirm immunological trends derived from mice in guinea pigs.*** Guinea pig sera from past experiments have been grouped based on survival outcome from GA-EBOV challenge. While T-cell responses cannot be measured in this animal model, testing of antibody responses by IgG ELISA or neutralizing antibody assays is still possible in order to determine the effect of humoural responses on survival with statistical significance.

3) ***To confirm immunological trends derived from rodents in NHPs.*** NHPs from previous experiments with different vaccine platforms have been separated based on

survival outcome from EBOV challenge, in order to increase the number of animals for statistical analysis. Specific B- and T-cell responses will be evaluated before and after challenge, and immune responses that correlate with and predict protection will be highlighted.

4) ***To determine if the immune response is a mechanistic or non-mechanistic correlate of protection.*** NHPs will be administered the purified immune component as determined in the first three objectives as a prophylactic or post-exposure therapy, and then exposed to a lethal dose of EBOV. Survival of the treated NHPs will indicate that the immune marker is a mechanistic correlate of protection, whereas non-survival will suggest that the immune marker does not constitute the mechanism of protection, but nevertheless will still be useful for predicting protection from EBOV.

CHAPTER II: MATERIALS AND METHODS

2.1 Cell lines

VeroE6 (ATCC CRL-1586) are African green monkey (*Cercopithecus aethiops*) kidney cells. They were maintained in Dulbecco's Modified Eagle's Medium (Sigma), supplemented with 10% (v/v) fetal bovine serum (FBS) that was heat inactivated at 30 minutes at 56^{o}C (Sigma), 2 mM L-glutamine (Gibco), 100 units/mL of penicillin (Gibco), and 100 μg/mL of streptomycin (Gibco).

Human embryonic kidney (HEK) 293 (ATCC CRL-1573) are human kidney carcinoma cells. Cells were maintained in Dulbecco's Modified Eagle's Medium (Sigma), supplemented with 10% (v/v) fetal bovine serum (FBS) that was heat inactivated at 30 minutes at 56^{o}C (Sigma), 2 mM L-glutamine (Gibco), 100 units/mL of penicillin (Gibco), and 100 μg/mL of streptomycin (Gibco).

All cell lines were grown and maintained in 37^{o}C and 5% CO_2 in a humidified incubator, and passaged every 3-4 days so that the cell confluence does not exceed 95%.

2.2 Ebola viruses

2.2.1 Challenge viruses

Mouse-adapted *Zaire ebolavirus*, Mayinga variant (MA-EBOV), known officially as Ebola virus mouse-hhp/COD/1976/Mayinga (Genbank accession number AF499101.1), was kindly provided by the Special Pathogens Branch of the Centers for Disease Control and Prevention (Atlanta, Georgia). MA-EBOV was previously developed by another research group (Bray, Davis et al. 1998) and used in this thesis for challenge studies involving mice.

Guinea pig-adapted *Zaire ebolavirus*, Mayinga variant (GA-EBOV), known officially as Ebola virus guinea pig-hhp/COD/1976/Mayinga (Genbank accession number AF272001.1), was kindly provided by the Special Pathogens Branch of the Centers for Disease Control and Prevention (Atlanta Georgia). GA-EBOV was previously developed by another research group (Connolly, Steele et al. 1999) and used in this thesis for challenge studies involving guinea pigs.

Wild-type *Zaire ebolavirus*, Kikwit variant (EBOV), known officially as Ebola virus H.sapiens-tc/COD/1995/Kikwit-9510621 (Genbank accession number AY354458), was kindly provided by the Special Pathogens Branch of the Centers for Disease Control and Prevention (Atlanta, Georgia), in which the passage 3 stock virus was cultured from VeroE6 cells in complete minimal essential medium supplemented with 2% FBS (Sigma), 100 units/mL of penicillin (Gibco), and 100 μg/mL of streptomycin (Gibco). EBOV was used for challenge studies involving NHPs.

2.2.2 Reporter virus

EBOV expressing the enhanced green fluorescent protein eGFP (EBOV-eGFP), known officially as Ebola virus H.sapiens-lab/COD/1976/Mayinga-eGFP-p3, was derived from an Ebola virus isolated during the 1976 outbreak (GenBank accession number NC_002549). The eGFP reporter gene is cloned between the NP and VP35 open reading frame. EBOV-eGFP was used in neutralizing antibody assays.

2.3 Vaccines

2.3.1 Construction and production of adenovirus vectors

The construction of an optimized expression cassette containing the chicken-β-actin (CAG) promoter and cytomegalovirus enhancer, as well as the gene synthesis of the human codon-optimized EBOV GP were performed previously in our research group as described in this reference (Richardson, Yao et al. 2009), resulting in a pCAGα expression cassette expressing the codon-optimized GP. This expression cassette was inserted into the transfer vector pShuttle2 using the restriction enzymes *SpeI* and *NheI*, and then inserted into the E1 and E3-deleted pAdenoX expression vector (BD Biosciences) at the E1 deletion region using the unique restriction homing endonucleases *I-CeuI*/*PI-SceI* and ligation of complementary ends with T4 DNA ligase (Invitrogen). The integrity of the clones were confirmed by sequencing as well as *EcoRI* digests, and the recombinant virus was rescued by transfecting the linearized DNA into HEK 293 cells, incubated at 37^{o}C, 5% CO_2, and harvested after cytopathic effects (CPE) were observed. The rescued virus was called Ad5-optGP. Large-scale infections were initiated by infecting fifty 150 mm tissue culture dishes (NUNC) seeded with HEK293 cells and infected with rescued Ad5-optGP. The virus and cells were harvested following the appearance of 3+ CPE (~20% of the cell monolayer still intact) at approximately 48 hours after infection, centrifuged at 4000 rpm for 5 minutes, and re-suspended in a 10 mM Tris-HCl solution. Cell lysates were freeze-thawed three times and purified by a standard cesium chloride gradient sedimentation process using high (1.45 g/mL) and low density (1.25 g/mL) cesium chloride density gradients, first at 72000 times gravity (xg) for 3 hours with no brake, and then at 72000 xg overnight. The Ad5-optGP band was removed using a 21½ gauge needle and the contents applied into a 3 mL dialysis cassette (Pierce), and then dialyzed in 2 liters of PBS for 2 hours, and then in 2 liters of 10mM Tris-HCl overnight. The purified Ad5-optGP was then removed from the dialysis cassette and combined with a glycerol-based vaccine solution and stored at -

80°C. The total particle number was determined by standard optical density at 260 nm, whereas the infectivity of vectors was performed by the immunodetection of the Ad5 hexon protein (Clontech) following infection of HEK 293 cells with limiting dilutions of Ad5-optGP following recommendations by the manufacturer and expressed in infectious forming units. Several Ad5-optGP preparations were generated and quantified for both infectious particle and total particle number, and preparations with a ratio of at least 1:200 infectious to total particles were used in the studies presented in this thesis.

The recombinant Ad5 virus expressing recombinant IFN-α is known commercially as DEF201 (Defyrus Incorporated). It was generously provided by Jeffrey D. Turner and Jane Ennis and manufactured as described in the following reference (Wu, Barabe et al. 2007).

2.3.2 Production of vesicular stomatitis virus vectors

The replication-competent, recombinant VSV vector expressing EBOV GP (VSVΔG/EBOVGP) was previously generated and characterized (Garbutt, Liebscher et al. 2004) by researchers from the Special Pathogens Program at the Public Health Agency of Canada, based on the reverse genetics system originally developed by John K. Rose and colleagues (Lawson, Stillman et al. 1995). Stock VSVΔG/EBOVGP vaccine was prepared by infection of VeroE6 cells. Briefly, VeroE6 cells were split into T-150 tissue culture flasks (Corning) one day before infection. The virus was diluted in DMEM supplemented with 2% FBS (Sigma), 2 mM L-glutamine, as well as 100 units/mL of penicillin (Gibco), and 100 μg/mL of streptomycin (Gibco), then inoculated onto cells at a multiplicity of infection (MOI) of 0.0001 for 1 hour at 37°C. The inoculum was removed and replaced with DMEM supplemented with 2% FBS (Sigma), 2 mM L-glutamine, as well as 100 units/mL of penicillin (Gibco), and 100 μg/mL of

streptomycin (Gibco). The flasks were incubated at 37^{o}C, 5% CO_2 and harvested after 3+ CPE. Supernatants were harvested, centrifuged at 2500 rpm for 10 minutes at 4^{o}C, transferred to a fresh tube and heat-inactivated FBS was added to adjust the final concentration to 10%. The stock virus was then aliquoted and stored at -80^{o}C.

2.4 Production of murine monoclonal antibodies

The development and characterization of the individual EBOV GP-specific neutralizing mAbs (1H3, 2G4 and 4G7) comprising the ZMAb treatment was done previously by researchers from the Special Pathogens Program and described in the following reference (Qiu, Alimonti et al. 2011). For the purification of mAbs, initial mouse hybridoma cell cultures were grown in Roswell Park Memorial Institute 1640 medium supplemented with 10% FBS (Sigma), 2 mM L-glutamine, as well as 100 units/mL of penicillin (Gibco), and 100 μg/mL of streptomycin (Gibco). The hybridomas were expanded in Hybridoma serum free media (Invitrogen) supplemented with 1 mM L-glutamine and 1x antibiotic-antimycotic (Invitrogen), incubated in roller bottles at 37^{o}C and 5% CO_2 for 7 to 14 days. The supernatant was clarified by centrifugation and concentrated 10-fold with a 30-kD molecular weight cutoff filter (Millipore). The mAbs were then purified on a HiTrap Protein G high performance column (GE Healthcare) with protein A binding buffer and IgG elution buffer (Thermo Scientific), according to manufacturer instructions. The fractions positive for IgG mAb were pooled and dialyzed by Centriprep units containing a 30-kD molecular weight cutoff filter (Millipore). The antibody purity was determined by a standard SDS-polyacrylamide gel electrophoresis and determined to be >98%.

2.5 Animal sources and scoring criteria

6-8 week old female C57BL/6J and various transgenic/knockout mice based on the same background (Jackson Laboratories), as well as female Hartley strain of guinea pigs (Charles River) between 6-8 weeks of age were used for the rodent studies presented in this thesis. The animals received commercial mouse or guinea pig food and water. The severity of disease was estimated with an internal scoring protocol that had been approved by the Canadian Science Centre for Human and Animal Health Animal Care Committee. Animals scores can range between 0 to 3 (Table 2.1).

Table 2.1. Clinical scoring criteria for mice and guinea pigs. If animals reach a clinical score between 2 and 3 (animal lying on side, not moving despite prodding) the animal will be euthanized according to guidelines.

Score	Description
0	No symptoms
1	Ruffled fur and decreased activity
2	Laboured breathing, hunched posture, bleeding
3	Death

Cynomolgus macaques (Health Canada Animal Resources Division or Primus Bio-Resources) received commercial monkey chow, water, treats, vegetables, and fruits. Environmental enrichment consisted of commercial toys and visual stimulation. The animals were monitored daily and scored for disease progression with an internal filovirus scoring protocol, which was previously approved by the Canadian Science Centre for Human and Animal Health Animal Care Committee. The scoring system rated changes from normal in the subject's posture/activity, attitude, activity level, feces/urine output, food/water intake, weight, temperature, respiration, and scored disease manifestations such as a visible rash, hemorrhage,

cyanosis, or flushed skin and assigns a score estimating disease severity, ranging from 0 to 64 (Table 2.2).

Table 2.2. Clinical scoring criteria for nonhuman primates. If treated animals reach a clinical score of 25 the investigator is required to consult a veterinarian regarding euthanasia. Control animals will only be allowed to reach a score of 20 before a decision is made regarding euthanasia.

Parameter	Degree of parameter	Possible Score
Posture	Normal	0
	Decreasing activity, Decreasing normal behaviour, pilo-erection	3
	Huddled when in room, shaking, toes and hands clenched	5
Temperature	Increase in body temperature above 2°C	5
Weight	Decrease in body weight of more than 10%	10
Respiration	Normal	0
	Increased or Decreased	2
	Laboured, breathing through mouth	10
	Cough or sneeze	2
Feces + Urine	Normal consistency volume / Soft normal stool	0
	Feces absent or dry / Decreased urine output / Cloudy urine	2
	Wet pasty / Small very dry stool	2
	Liquid stool / blood in stool or urine No urine > twice	10
Food + water	Normal	0
	Slightly decreased - still eating fruit and treats, 25% or greater reduction in pellets / water	1
	Moderately decreased - reduced intake of fruits and treats, 25 - 50% reduction in pellets / water	3
	Severely decreased - reduced intake of fruits and treats	4
	Seriously decreased - refusing all food, dehydration apparent > 2 days	10
Recumbent	No symptoms	0
	Huddled on camera, active when people in room	3

	Lies down, will get up when approached or prompted, uses cage for support	15
	Lies down, will not get up when approached	25
Attitude	Normal	0
	Hyperactive or mildly depressed, responds to treats and toys	1
	Moderately depressed, response requires prodding, loses interest in treats and toys,	3
	Severely depressed, no interest in treats, does not respond to human presence	10
Other	Flushed appearance to skin	2
	Nasal discharge	2
	Visible Rash	5
	Cyanosis	5
	Haemorrhage (subcutaneous)	10
	Haemorrhage (orifices)	15
Total score		0-64

2.6 Ethics statement

All animal procedures, manipulations and scoring criteria were approved by the Institutional Animal Care Committee at the National Microbiology Laboratory of the Public Health Agency of Canada according to the guidelines of the Canadian Council on Animal Care. All infectious work was performed in the Biosafety Level 4 facility located at the National Microbiology Laboratory.

2.7 Animal experiments

2.7.1 Mice

Groups of 11 or 12 wild-type and transgenic/knockout C57BL/6J mice, including B-/T-cell$^{-/-}$ (Rag-1), IFN-$\gamma^{-/-}$ (IFN-γ), CD8^{+} T-cell$^{-/-}$ (B2μG), CD4^{+} T-cell$^{-/-}$ (Cd4^{tm1Knw}) and B-cell$^{-/-}$ (Igh6) were used for this study. The mice were immunized by an intramuscular (IM) injection of 1 x 10^{10} total particles of Ad5-optGP diluted in PBS, and then challenged 28 days later by two intraperitoneal (IP) injections carrying a total 1000 x LD_{50} of MA-EBOV. Splenocytes were harvested from three sacrificed mice at 10 days after vaccination for assaying T-cell responses, whereas sera were harvested from trial bleeds of the remaining mice just before challenge for GP-specific IgG ELISA and NAb assays. The mice were weighed every day for 28 days and monitored for clinical signs of disease following challenge.

2.7.2 Guinea pigs

Guinea pigs were administered IM or IN with 1 x 10^{10} total particles of Ad5-optGP diluted in PBS, either in the presence or absence of pre-existing immunity (PEI), which was induced IM or IN with 1 x 10^{11} total particles of Ad5-lacZ, 28 days prior to vaccination. Guinea pigs were challenged at 28 days following vaccination by two IP injections carrying a total 1000 x LD_{50} of GA-EBOV. Sera were harvested from trial bleeds of the animals just before challenge for GP- and EBOV-specific IgG ELISA and NAb assays. The guinea pigs were weighed every day for 28 days and monitored for clinical signs of disease following exposure, and results were grouped by survival outcome.

2.7.3 Nonhuman primates

For determining the immune correlates of protection against EBOV, healthy male and female cynomolgus macaques (*Macaca fascicularis*) weighing between 2.5 to 11 kg were administered Ad5-optGP ranging between 1 x 10^{10} - 4 x 10^{10} infectious forming units, with or without Ad5-IFN-α (3 x 10^{9} - 2 x 10^{9} PFU/kg/NHP) via the IM, IN or the IN/intratracheal (IT) routes, either in the presence or absence of induced PEI against Ad5. The NHPs used in the post-exposure experiments were administered 0.44 μg/kg of recombinant universal type I IFN-α (PBL Interferon Source) IM on days 5 to 21 after challenge in addition to the Ad5-optGP vaccine. In the VSV study, animals were vaccinated IM, IN or orally (OR) with 2 x 10^{7} PFU VSVΔG/EBOVGP. Macaques were challenged with two IM injections totaling 1000 PFU EBOV either at least 28 days after vaccination, or 30 minutes before the initiation of treatment. Sera were sampled from the animals at 0 and 6-7 dpi for quantitation of IgG and NAb levels. Sera were also harvested at 0 and 7 dpv as well as 0 and 6-7 dpi for quantitation of cytokine/chemokine levels. Whole blood was harvested at 14dpv and 7 dpi for assaying T-cell responses. In addition, terminal samples were harvested from moribund NHPs prior to euthanasia.

For the ZMAb experiments, nine healthy male or female cynomolgus macaques weighing between 2.5 to 4.9 kg were randomized into two groups of four on the basis of treatment regimens after 10 days acclimatization. One NHP (Group C) received PBS in place of ZMAb as a positive control for infection. Each macaque received two IM injections totaling 1000 PFU EBOV. Beginning at 24 (Group A) or 48 (Group B) hours after challenge, the subjects were treated intravenously with 25 mg/kg of ZMAb, which contained three EBOV-GP–specific neutralizing mAbs (1H3, 2G4, and 4G7) administered as a 5 mL slow bolus into the saphenous vein. On examination dates before the animals received the ZMAb bolus (1, 4, 7, 14, 21, and 28

dpi for Group A, and at 2, 5, 8, 14, 21, and 28 dpi for Group B), a number of parameters relevant to survival were recorded and measured, including clinical score, viremia by RT-qPCR and $TCID_{50}$ titrations, hematology, blood chemistry in addition to the magnitude of humoural and cellular immune responses by IgG and IgM ELISAs, neutralizing antibody assays, IFN-γ ELISpot and flow cytometry. The study was not blinded, and the data presented were performed in triplicate with the average value shown, with the exception of FACS, which were performed in singles.

2.8 Blood counts and blood biochemistry analysis

Complete blood counts were performed on the VetScan HM5 (Abaxis Veterinary Diagnostics) and the blood biochemistry performed on the VetScan VS2 (Abaxis Veterinary Diagnostics). For blood counts, whole blood was collected in K2 ethylenediaminetetraacetic acid plus blood collection tubes (BD Biosciences), in which 1 mL of blood was aliquoted to a 2 mL cryovial (Sarstedt) for processing. The following parameters were analyzed, but only parameters demonstrating significant changes after infection were presented: levels of white blood cells (WBC), lymphocytes (LYM), monocytes (MON), neutrophils (NEU), eosinophils (EOS), basophils (BAS), percentage of lymphocytes (LY%), monocytes (MO%), neutrophils (NE%), eosinophils (EO%), basophils (BA%), levels of red blood cells (RBC), hemoglobin (HGB), hematocrit (HCT), red blood cell indices including mean corpuscular volume (MCV), mean corpuscular hemoglobin (MCH), mean corpuscular hemoglobin concentration (MCHC), red cell distribution width (RDW), levels of platelets (PLT), procalcitonin (PCT), mean platelet volume (MPV), and platelet distribution width (PDW).

For blood biochemistry, whole blood was collected in SST plus blood collection tubes (BD Biosciences). Samples were spun at 2500 xg for 10 minutes at room temperature to isolate the serum, in which 100 μL of serum was added to the VetScan comprehensive diagnostic profile rotor (Abaxis Veterinary Diagnostics) for processing. The following parameters were analyzed, but only parameters demonstrating significant changes after infection were presented: levels of albumin (ALB), alkaline phosphatase (ALP), alanine aminotransferase (ALT), amylase (AMY), total bilirubin (TBIL), blood urea nitrogen (BUN), calcium (CA), phosphates (PHOS), creatinine (CRE), glucose (GLU), sodium (NA^+), potassium (K^+), total protein (TP), and globulin (GLOB).

2.9 EBOV titration

The whole blood, which was collected as described previously, was measured for viremia using either real-time reverse-transcription PCR (RT-qPCR) or titration of live virus for each time point. For genomic quantification, 140 μL of blood was added to 560 μL of Buffer AVL (Qiagen) and the total RNA was extracted using the QIAamp viral RNA mini kit (Qiagen) according to manufacturer instructions. EBOV RNA was detected with the LightCycler 480 Master Hydrolysis Probes kit (Roche) under the following RT-qPCR reaction conditions: reverse transcription at 63°C for 3 minutes, enzyme activation at 95°C for 30 seconds, and then 45 cycles, which includes nucleic acid denaturation at 95°C for 15 seconds, as well as primer annealing and extension at 60°C for 30 seconds with StepOne Plus (Applied Biosystems). The lower detection limit for this assay is 1 virus particle/mL. The following primer and probe set was used for this experiment (Table 2.3).

Table 2.3. Sequences of the primer and probe set used in detection of EBOV RNA.

Name	Sequence (5' → 3')
EBOVLF2	CAGCCAGCAATTTCTTCCAT
EBLVLR2	TTTCGGTTGCTGTTTCTGTG
EBOVLP2FAM	[6-FAM]ATCATTGGCGTACTGGAGGAGCAG[BHQ1]

For live virus titrations, the EBOV median tissue culture infectious dose 50 ($TCID_{50}$) virus titers were determined by first serially diluting whole blood 10-fold, 500 µL sample in 4.5 mL DMEM + 2% FBS. 100 µL of the dilution were then added in four replicates to a 96-well plate (Corning) of pre-seeded VeroE6 cells at 95% confluence and incubated at 37^{o}C for 1 hour. The samples were then removed and 100 µL of fresh DMEM + 2% FBS was added to the wells and incubated for 14 days. The plates were scored for the presence of cytopathic effects (CPE) at 14 dpi, and titers were calculated with the Reed and Muench method (Reed and Muench 1938) and expressed as $TCID_{50}$/mL. The lower detection limit for this assay is 10 $TCID_{50}$/mL.

2.10 Isolation of splenocytes

Spleens from mice were removed for assays measuring T-cell responses. First, groups of three Ad5-GP vaccinated mice were euthanized at 10 dpi by an overdose of inhalational isofluorane and cervical dislocation. Spleens were removed and placed in a 60 mm petri dish containing fine metal mesh (50 mesh, Bellco Glass) submerged in 5 mL of Leibovitz's medium (L-15 media, Thermo Scientific). Splenocytes were then separated by mechanically disruption against the metal mesh with a sterile syringe plunger and filtered through a 40 µM cell strainer (BD Biosciences) and collected in a 50 mL Falcon tube. The metal mesh was washed once with 10 mL of L-15 media and added to the Falcon tube after passing the contents through the

strainer. The splenocytes were spun at 485 xg for 7 minutes at room temperature and the resulting pellet re-suspended in 10 mL of L-15 media for further processing with the mouse IFN-γ ELISpot assay kit.

2.11 Isolation of peripheral blood mononuclear cells

Whole blood was collected as described previously for peripheral blood mononuclear cell (PBMC) isolations. The blood was first diluted 1:1 with sterile phosphate buffered saline (PBS) and mixed well. 7.5 mL of the sample was then overlaid onto 5 mL of 60% Ficoll (GE Healthcare) diluted in PBS, and the same was done with the other 7.5 mL. The tubes were centrifuged at 750 xg for 45 minutes at 20^{o}C, with the centrifuge brake turned off. PBMCs residing at the band located at the medium-Ficoll interface were collected with a pipette and washed once with RPMI-1640 media before re-suspension in RPMI-1640 supplemented with 0.1 mM MEM nonessential amino acids, 1 mM sodium pyruvate, 10 mM 4-(2-hydroxyethyl)-1-piperazineethanesulfonic acid, 2 mM L-glutamine, 55 μM β-mercaptoethanol, 10% FBS, and 1% penicillin/streptomycin, called complete RPMI (cRPMI). The number of PBMCs was counted by adding 10 μL of the cell suspension to 90 μL of ammonium-chloride-potassium lysing buffer, incubating for 5 minutes, loaded onto a hemocytometer (Hausser Scientific) and enumerated. The cell suspension was then pelleted at 100 xg for 10 minutes, and re-suspended in cRPMI such that the concentration is 5 x 10^6 cells/mL. The cells will be processed using the monkey IFN-γ ELISpot assay kit or fluorescence-activated cell sorting (FACS).

2.12 Immunological assays

2.12.1 Neutralizing antibody assays

Harvested sera samples were first inactivated at 56^{o}C for 45 minutes to denature complement. The samples were first diluted 1:10 with DMEM supplemented with 2% FBS, 1% L-glutamine and 1% penicillin/streptomycin, and then serially diluted 2-fold in 50 µL DMEM supplemented with 2% FBS, 1% L-glutamine and 1% penicillin/streptomycin. Each serum sample was diluted in triplicate. The dilutions were mixed with an equal volume of EBOV-eGFP at 100 transducing units per well, and incubated at 37^{o}C, 5% CO_2 for 60 minutes. Control wells were infected with equal amounts of EBOV-eGFP with PBS added in place of sera. The mixture was then added to 90-95% confluent VeroE6 cells and incubated at 37^{o}C, 5% CO_2 for 60 minutes. 100 µL of DMEM supplemented with 2% FBS, 1% L-glutamine and 1% penicillin/streptomycin was added to each well and incubated at 37^{o}C, 5% CO_2 for 48 hours. Dilutions were scored as positive for NAb activity if there was a greater than 50% reduction in the number of cells expressing eGFP when enumerated under a fluorescent plate reader (Advanced Imaging Devices). The highest serum dilution that satisfies this condition was recorded and reported as the reciprocal of the dilution.

2.12.2 Enzyme-linked immunosorbent assay

2.12.2.1 GP-specific IgM or IgG ELISA

Immulon 2 HB flat bottom MicroTiter 96-well ELISA Plates (Thermo Scientific) were coated with 50 nanograms (ng) of Histidine-tagged GP lacking the transmembrane (TM) domain His-$GP_{1,2\Delta TM}$ capture antigen diluted in PBS and incubated at 4^{o}C overnight. Plates were washed three times with wash buffer (PBS 0.1% TWEEN 20), and then blocked for 90 minutes with blocking buffer (5% skim milk powder/PBS/0.2% Tween 20) at 37ºC in accordance to instructions from the researchers that developed the assay (Nakayama, Yokoyama et al. 2010)

(His-$GP_{1,2\Delta TM}$ later made commercially available from IBT Bioservices). Plates were washed three times with wash buffer. For Ad5 vaccinated samples, serum was either diluted at 1:1600 for the samples harvested before challenge, or 1:50 after challenge in blocking buffer. 50 µL of the diluted sera were added to each well in triplicate, and incubated for 60 minutes at 37°C. For VSV vaccinated samples, sera were first diluted 1:10 in blocking buffer, and then serially diluted 1:2 with each dilution added in triplicate, and incubated for 60 minutes at 37°C. The plates were washed three times with wash buffer. A secondary antibody for mouse (horseradish peroxidase (HRP)-conjugated rat anti-mouse antibody to mouse IgG) (Jackson Laboratories), guinea pig (HRP-conjugated goat anti-guinea pig antibody to guinea pig IgG), (KPL) or NHPs (HRP-conjugated Goat anti-Human antibody to IgG or IgM) (KPL) was added where appropriate and then incubated for 60 minutes at 37°C. Horseradish peroxidase substrate [3% hydrogen peroxide solution with 2, 2'-azinobis(3-ethylbenzthiazolinesulfonic acid)] was added as a substrate and incubated at room temperature for 30 minutes. The plates were read using a VMax Kinetic ELISA Microplate Reader (Molecular Devices) and the data were analyzed using CellMaxPro software. For Ad5 vaccinated samples, the data were reported as the optical density measured by absorbance at 405 nm (A_{405}). For VSV vaccinated samples, the data were reported as endpoint dilutions.

2.12.2.2 EBOV-specific IgG ELISA

Gamma irradiated sucrose gradient-purified EBOV was used instead of the recombinant GP as the capture antigen. Heat inactivated guinea pig or NHP sera were diluted at 1:50 with blocking buffer. All other steps were performed as described previously and the results were reported as A_{405}.

2.12.3 ELISpot assays

The frequency of pooled mouse splenocytes secreting IFN-γ was measured with the mouse IFN-γ ELISpot assays (BD Bioscience) following manufacturer instructions. Briefly, 96-well ELISpot plates were coated with purified anti-mouse IFN-γ antibody and left at 4^{o}C overnight. Unspecific binding sites were blocked with cRPMI for 2 hours at room temperature, and 5 x 10^5 purified splenocytes were added to each well. 15mer peptides with 10 amino acid overlaps that spanned the entire EBOV GP (167 peptides total) were purchased (Genscript), and split into 17 individual pools. Splenocytes were stimulated with 2.5 μg/mL of each individual peptide pool diluted in cRPMI in singles (no replicates) and incubated for 18 hours at 37^{o}C, 5% CO_2. Cells were then washed and incubated with the biotinylated anti-mouse IFN-γ for 2 hours at room temperature, followed incubation with HRP-conjugated streptavidin (BD Biosciences) for 1 hour at room temperature. The spots were visualized using 3-amino-9-ethylcarbazole as the substrate (BD Biosciences) and enumerated using an ELISpot Plate Reader (Advanced Imaging Devices).

The frequency of PBMCs secreting IFN-γ was measured with the monkey IFN-γ ELISpot assay (Mabtech) in triplicate according to manufacturer instructions. 96-well plates pre-coated with anti-human IFN-γ antibody were first reconstituted in Dulbecco's PBS (DPBS), blocked with cRPMI for 2 hours at room temperature, and then 5 x 10^5 purified PBMCs were added to each well. Peptides consisted of 15mers with 11 amino acid overlaps that spanned the entire EBOV GP (Mimitopes). The peptides were combined into four pools each containing 42 peptides. Pool 1 consists of peptides spanning amino acids 1 to 179, pool 2 consists of peptides spanning amino acids 180 to 347, pool 3 consists of peptides spanning amino acids 348 to 495,

and pool 4 consists of peptides spanning amino acids 496 to 676. PBMCs were stimulated with 2.5 μg/mL of each peptide and incubated for 18 hours. Spots indicating the presence of IFN-γ secreting cells were visualized by addition of the 3-amino-9-ethylcarbazole substrate and quantified using the ELISpot Plate Reader.

2.12.4 Flow cytometry analysis

The frequency of $CD4^+$ or $CD8^+$ T-cells secreting IFN-γ and IL-2 was assessed by flow cytometry. Purified PBMCs were seeded at 1 x 10^6 cells per well in cRPMI media. Cells were then stimulated with 5 μg/mL of the four previously-mentioned EBOV GP peptide pools (Mimotopes) overnight at 37°C, 5% CO_2, in the presence of 1 μL/mL of GolgiPlug (BD Biosciences). PBMCs were then stained with the anti-human CD4–peridinin chlorophyll protein–Cy5.5 and CD8-allophycocyanin mouse antibodies (clones L200 and RPA-T8, respectively), followed by 20 minutes incubation in Cytofix/Cytoperm (BD Biosciences). Intracellular cytokines were then detected by staining with the anti-human IFN-γ–fluorescein isothiocyanate and IL-2–phycoerythrin mouse antibodies (clones B27 and MQ1-17H12, respectively) diluted in PermWash buffer (BD Biosciences). At least 300,000 events were acquired on the four-colour Accuri C6 cytometer (BD Biosciences) in the Biosafety Level 4 laboratory of the Public Health Agency of Canada, and the resulting data was analyzed with FCS Express 4 (DeNovo Software).

2.12.5 Cytokine and chemokine single and multiplex analysis

The Cytokine Monkey Magnetic 28-Plex Panel (Invitrogen) was used following manufacturer instructions for the simultaneous quantitative determination of serum levels various

cytokines and chemokines. First, serial 3-fold dilutions of cytokine standards were prepared in assay diluent and added to a Multiscreen BV filter plate (Millipore), in parallel with 100 μL of serum sample that was diluted 1:2 with assay diluent. 25 μL of fluorescent magnetic antibody beads were added to each well and washed twice with working wash solution. 50 μL of incubation buffer was added to each well, and left in the dark on a plate shaker at 500 rpm for 2 hours at room temperature. The plate was then applied to a magnetic separator (Invitrogen) and washed twice with wash solution. 100 μL of biotinylated anti-human multi-cytokine reporter was added to each well and left in the dark on a plate shaker at 500 rpm 1 hour at room temperature. The plate was then applied to the magnetic separator and washed twice with wash solution. 100 μL of streptavidin-phycoerythrin was added to each well after a 10-fold dilution in strepavidin diluent. The plate was incubated in the dark on a plate shaker at 500 rpm for 30 minutes at room temperature, applied to the magnetic separator, washed twice with wash buffer, re-suspended in wash buffer and then shaken for 1 minute. The plate was read on the Qiagen Liquichip 200 Workstation (Qiagen), and cytokine concentrations were calculated using the Luminex xPONENT 3.1 software. The following cytokines and chemokines were detected (Table 2.4). Only those that demonstrated a statistically significant difference between surviving and non-surviving animals were included in this thesis.

Table 2.4. List of cytokines and chemokines detected in the Luminex assay.

Epidermal growth factor (EGF)	IL-8
Eotaxin	IL-10
Fibroblast growth factor-basic (FGF-basic)	IL-12
Granulocyte-colony stimulating factor (G-CSF)	IL-15
Granulocyte macrophage-colony stimulating factor (GM-CSF)	IL-17
Hepatocyte growth factor (HGF)	Monocyte chemoattractant protein (MCP)-1
IFN-γ	Macrophage-derived chemokine (MDC)
IFN-inducible T-cell alpha chemoattractant (I-TAC)	Macrophage migration inhibitory factor (MIF)
IL-1β	Macrophage induced gene (MIG)
IL-1RA	macrophage inflammatory protein (MIP)-1α
IL-2	MIP-1β
IL-4	Regulated on activation, normal T cell expressed and secreted (RANTES)
IL-5	TNF-α
IL-6	Vascular endothelial growth factor (VEGF)

2.13 Sequencing of EBOV GP

Sequencing of EBOV GP was carried out in order to detect escape mutations. Briefly, total RNA was extracted from whole blood samples collected at 8 dpi from NHP B2, B3, as well as the challenge virus, using the QIAamp Viral RNA Mini Kit (Qiagen) according to manufacturer instructions. The EBOV GP gene was then amplified with the OneStep reverse transcription PCR (RT-PCR) Kit (Qiagen) according to manufacturer instructions. Reaction conditions were as follows: reverse transcription at 50°C for 30 minutes, enzyme activation at 95°C for 15 minutes, and then 39 cycles, which includes nucleic acid denaturation at 95°C for 15 seconds, as well as primer annealing at 50°C for 30 seconds, and then extension at 72^{o}C for 30 seconds. The RT-PCR product was purified with the QIAquick PCR Purification kit (Qiagen) following manufacturer instructions, and then sequenced on the ABI 3720XL DNA Sequencer with Applied Biosystems BigDye Terminator Version 3.1 Chemistry. The resulting sequences were assembled with the DNASTAR Lasergene 9 SeqMan software. The primer sequences used in this protocol are as follows (Table 2.5).

Table 2.5. List of sequencing primers for EBOV GP.

Name	GP gene region (base pair)	Sequence (5' → 3')
$GP_{1,2}$ XhoI Fwd	1 to 18	GACCTCGAGATGGGCGTTACAGGAATATTG
$GP_{1,2}$ Nhe I Rev	2030 to 2014	GACGCTAGCCTAAAAGACAAATTTGC
$GP_{1,2}$ Fwd01	264 to 285	CAGGTCCGGTGTCCCACCAAAGG
$GP_{1,2}$ Fwd02	528 to 546	CGCTGAAGGTGTCGTTGC
$GP_{1,2}$ Rev02	546 to 528	GCAACGACACCTTCAGCG
$GP_{1,2}$ Fwd03	757 to 776	CTGCTCCAGCTGAATGAGAC
$GP_{1,2}$ Rev03	746 to 721	GTGAATCTTGATTACCGTTGGACG
$GP_{1,2}$ Fwd04	1051 to 1070	GTTCAAGTGCACAGTCAAGG
$GP_{1,2}$ Rev04	1070 to 1051	CCTTGACTGTGCACTTGAAC
$GP_{1,2}$ Fwd05	1311 to 1330	GAGCAAGGGTACCGACTTCC
$GP_{1,2}$ Rev05	1330 to 1311	GGAGGTCGGTACCCTTGCTC
$GP_{1,2}$ Fwd06	1563 to 1582	GGATGAAGGTGCTGCAATCG
$GP_{1,2}$ Rev06	1582 to 1563	CGATTGCAGCACCTTCATCC
$GP_{1,2}$ Rev07	1835 to 1817	GGTTCGATACAGCAGTCCG

2.14 Statistics

For absorbance IgG ELISAs, graphed results were an average of three independent raw absorbance readings from the same serum sample. For endpoint IgM and IgG ELISAs, results were considered positive when the reading was higher than the mean by at least 2 standard deviations above a similar dilution of serum from the same animal that was taken before challenge. Therefore, positive results indicate $p<0.05$.

Results between the different groups were compared using the two-tailed Mann Whitney non-parametric t-test, which does not assume that biological sample values conform to a Gaussian distribution. Significance values of $p<0.05$ were considered significant (*), $p<0.01$ were considered highly significant (**), and $p<0.001$ were considered extremely significant (***). All statistical analysis was performed on GraphPad Prism v.5.01 software. Error bars

indicate either one standard deviation or 95% confidence interval from the arithmetic or geometric mean, respectively.

CHAPTER III: IMMUNE RESPONSES CORRELATING TO PROTECTION FROM EBOLA VIRUS IN RODENTS

3.1 Introduction

Human adenovirus serotype-5 (Ad5) belongs to the family *Adenoviridae* and is used as a delivery vehicle for therapeutic transgenes to combat genetic diseases. Ad5 has many properties that make it an attractive vaccine candidate, including its ability to elicit a strong sustained T-cell immune response in both immunocompetent and immunocompromised humans (Richardson, Dekker et al. 2010), and to tolerate the introduction of up to approximately 8kb in large foreign DNA fragments expressing viral antigens (Richardson, Dekker et al. 2010). The Ad5 vector is highly versatile and has been used in a number of wide-ranging applications. In addition to EBOV studies, Ad5 has been tested in the laboratory against other well-known pathogens, including H5N1 *influenzavirus* (Patel, Tikoo et al. 2010), simian immunodeficiency virus (Gabitzsch, Xu et al. 2011), and MARV (Geisbert, Bailey et al. 2010). Interestingly, it has also been used as a vehicle for treating cocaine addictions (Koob, Hicks et al. 2011). Furthermore, it has been tested in humans for a variety of conditions, including several types of cancers (ClinicalTrials.gov 2014c) (ClinicalTrials.gov 2014d) (ClinicalTrials.gov 2014e) (ClinicalTrials.gov 2014f), heart disease (ClinicalTrials.gov 2014g), and human immunodeficiency virus infections (ClinicalTrials.gov 2014h), and is a well-known entity in clinical trials. Most importantly, wild-type Ad5 is not associated with severe disease in humans.

However, PEI to the Ad5 vector backbone has previously been associated with undesirable clinical outcomes, including lack of efficacy and increased risk of infections (Buchbinder, Mehrotra et al. 2008), which led to the suspension or redesign of several clinical trials (Buchbinder, Mehrotra et al. 2008) (Gray, Allen et al. 2011). It is estimated that 30-50% of

the North American population and over 90% of the population in developing countries are seropositive for Ad5-neutralizing antibodies (Chirmule, Propert et al. 1999). This significantly compromises the utility of Ad5-based vaccines, especially if the homologous vectors were to be re-administered. Although PEI can be bypassed with an increased dosage of Ad5, systemic administrations of high doses can be toxic to both animals and humans leading to pathology, including extensive liver damage (Brunetti-Pierri, Palmer et al. 2004) and has played a part in the death in one individual during a clinical trial (Lehrman 1999).

Despite these setbacks, there remains substantial interest in the use of Ad5 for medical applications, and of all experimental EBOV vaccines Ad5-GP is currently the candidate that is furthest in clinical trials. Our research group has recently developed a significantly improved Ad5-based EBOV vaccine containing a new expression cassette with a cytomegalovirus early enhancer/chicken β actin (CAG) promoter, and codon optimized EBOV GP (Ad5-optGP). This vaccine has been shown to elicit post-exposure protection in mice, in addition to stronger immune responses at doses 100 times lower than the previously generated Ad5-GP vaccine that has completed Phase I clinical trials (Richardson, Yao et al. 2009).

The goal of this thesis chapter is to determine the individual components of the immune response necessary for establishing protection as elicited by the Ad5-optGP vaccine in mice and guinea pigs. In mice studies, transgenic/knockout mice with ablation for a specific component in the adaptive immune response were obtained commercially. These include: Rag-1 (B-/T-cell$^{-/-}$), B2μG (CD8^{+} T-cell$^{-/-}$), Cd4^{tm1knw} (CD4^{+} T-cell$^{-/-}$), Igh6 (B-cell$^{-/-}$) and IFN-γ (IFN-γ$^{-/-}$). Vaccinated or mock vaccinated wild type C57BL/6J (WT vacc or WT unvacc, respectively) mice served as controls (Figure 3.1). Phosphate buffered saline (PBS) were used in mock treatments. The groups of mice (n=11 or 12 per group) were immunized by an IM injection of 1 x 10^{10} total

particles of Ad5-optGP 28 days prior to IP challenge with 1000 x LD_{50} of MA-EBOV. In addition to monitoring for survival and weight loss for 28 days after challenge, splenocytes were harvested from three mice of each group at 10 days post-vaccination (dpv) and measured for specific T-cell responses by IFN-γ ELISpot assay. Sera were harvested from the remaining mice of each group at 28 dpv, to measure for specific B-cell responses by neutralizing antibody (NAb) assays and GP-specific IgG ELISAs (Figure 3.2).

Based on the hypothesis, it is expected that the deletion of B- and T-cells, as well as the deletion of $CD8^+$ T-cells in mice will completely abrogate protection as induced by the Ad5-optGP vaccine. Partial survival can be expected from IFN-$\gamma^{-/-}$ and $CD4^+$ T-cell$^{-/-}$ mice, since $CD8^+$ T-cell killing is not completely dependent on IFN-$\gamma^{-/-}$ secretion and $CD4^+$ T-cells are not the only activators of Th1-biased immunity. B-cell$^{-/-}$ mice are expected to survive MA-EBOV challenge. The magnitude of the specific T-cell response as measured by IFN-γ ELISpot assays is expected to be predictive of survival, whereas antibody levels stimulated by the vaccine will not be indicative of protection.

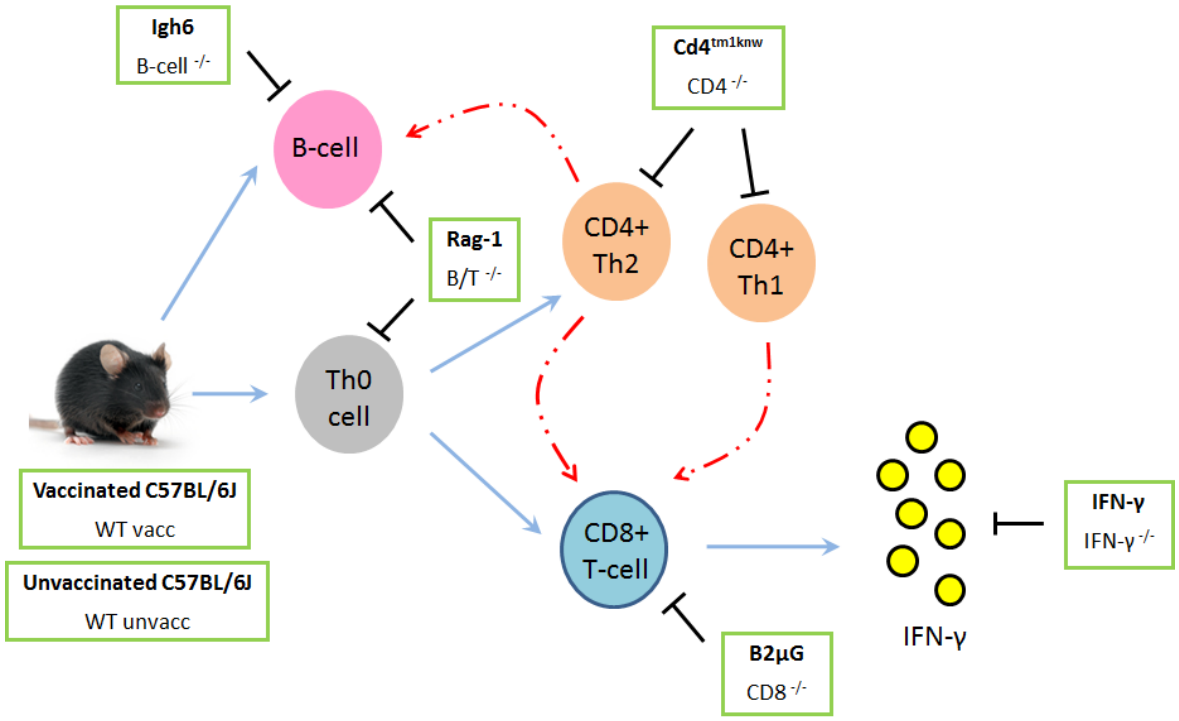

Figure 3.1. Immune pathways and deficiencies of immunocompetent and transgenic/knockout mice. A simplified schematic of the adaptive immune system in immunocompetent mice, and the effects on the immune response from each knockout presented in the thesis.

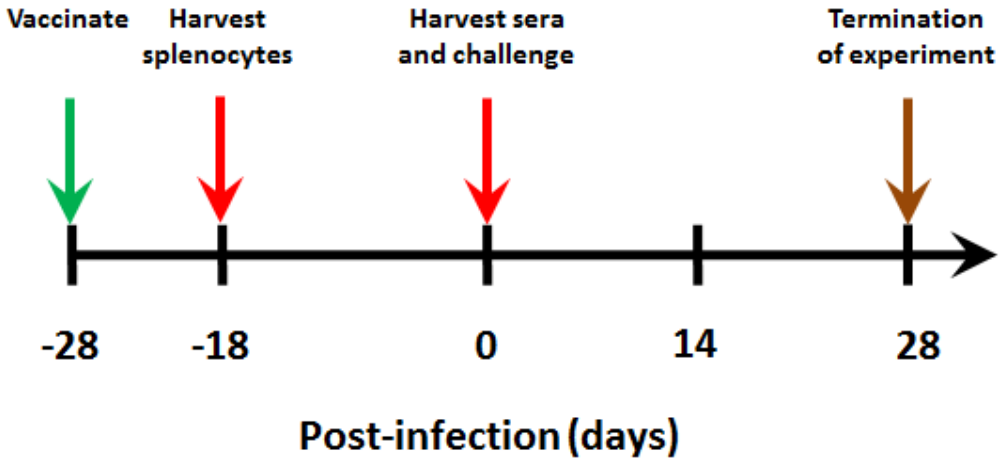

Figure 3.2. Timeline of Ad5-optGP treatment, harvest or MA-EBOV challenge in wild type C57BL/6J or transgenic/knockout mice. Major events over the course of the experiment are indicated by the arrows on the timeline.

In the guinea pig model, PEI to the Ad5 vector backbone was either mock induced with PBS, or stimulated by IM or IN administration of 1 x 10^{11} total particles of Ad5 expressing *lacZ* (Ad5-lacZ) 56 days before challenge. 1 x 10^{10} total particles of Ad5-optGP were then administered IM or IN 28 days before challenge with 1000 x LD_{50} of GA-EBOV. Challenged animals were monitored for survival and weight loss for 28 days after challenge and grouped as survivors or non-survivors based on outcome of disease. Sera were harvested from all animals at 28 dpv (Figure 3.3), where specific B-cell responses were monitored by a NAb assay, and virus-specific as well as GP-specific IgG ELISAs. Several experiments were combined for the purpose of potentially producing statistically significant trends, resulting in aggregate totals of 40 surviving and 9 non-surviving guinea pigs. Based on the hypothesis, it is expected that differences in antibody levels between survivors and non-survivors of GA-EBOV infection will not be statistically significant.

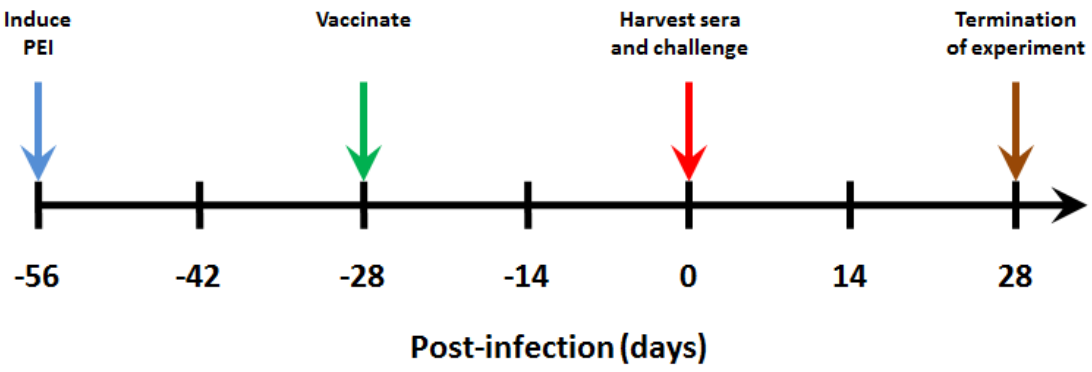

Figure 3.3. Timeline of Ad5-lacZ or Ad5-optGP treatment, sample or GA-EBOV challenge in guinea pigs. Major events over the course of the experiment are indicated by the arrows on the timeline.

3.2 Results

3.2.1 Survival and weight loss in wild-type and transgenic/knockout mice

Unvaccinated C57BL/6J mice were susceptible to lethal MA-EBOV challenge, resulting in rapid weight loss and resulting in no survival, with a mean time to death of 7.1 ± 0.3 days after challenge. Conversely, C57BL/6J mice vaccinated with Ad5-optGP all survived challenge without significant weight loss. Vaccinated B-/T-cell$^{-/-}$ mice failed to survive challenge, with weight loss and a mean time to death of 7.0 ± 1.3 days. Complete protection was achieved in immunized CD8^{+} T-cell$^{-/-}$ mice without significant weight loss (Figures 3.4A and B). IFN-$\gamma^{-/-}$ and CD4^{+} T-cell$^{-/-}$ mice immunized with Ad5-optGP were able to mount a partially protective immune response with 78% (7 of 9) mice and 33% (3 of 9) mice surviving the lethal challenge with a mean time to death of 10.0 ± 1.4 days and 6.5 ± 0.5 days, respectively. Ad5-optGP vaccinated IFN-$\gamma^{-/-}$ survivors did not lose weight during challenge, suggesting complete protection; conversely, vaccinated CD4^{+} T-cell$^{-/-}$ survivors did lose weight during challenge, suggesting that the protection was not complete for this group (Figures 3.4C and D). Vaccination of B-cell$^{-/-}$ mice was ineffective in protecting against EBOV challenge, with observed weight loss resulting in no survival and a mean time to death of 8.0 ± 0.5 days (Figures 3.4E and F).

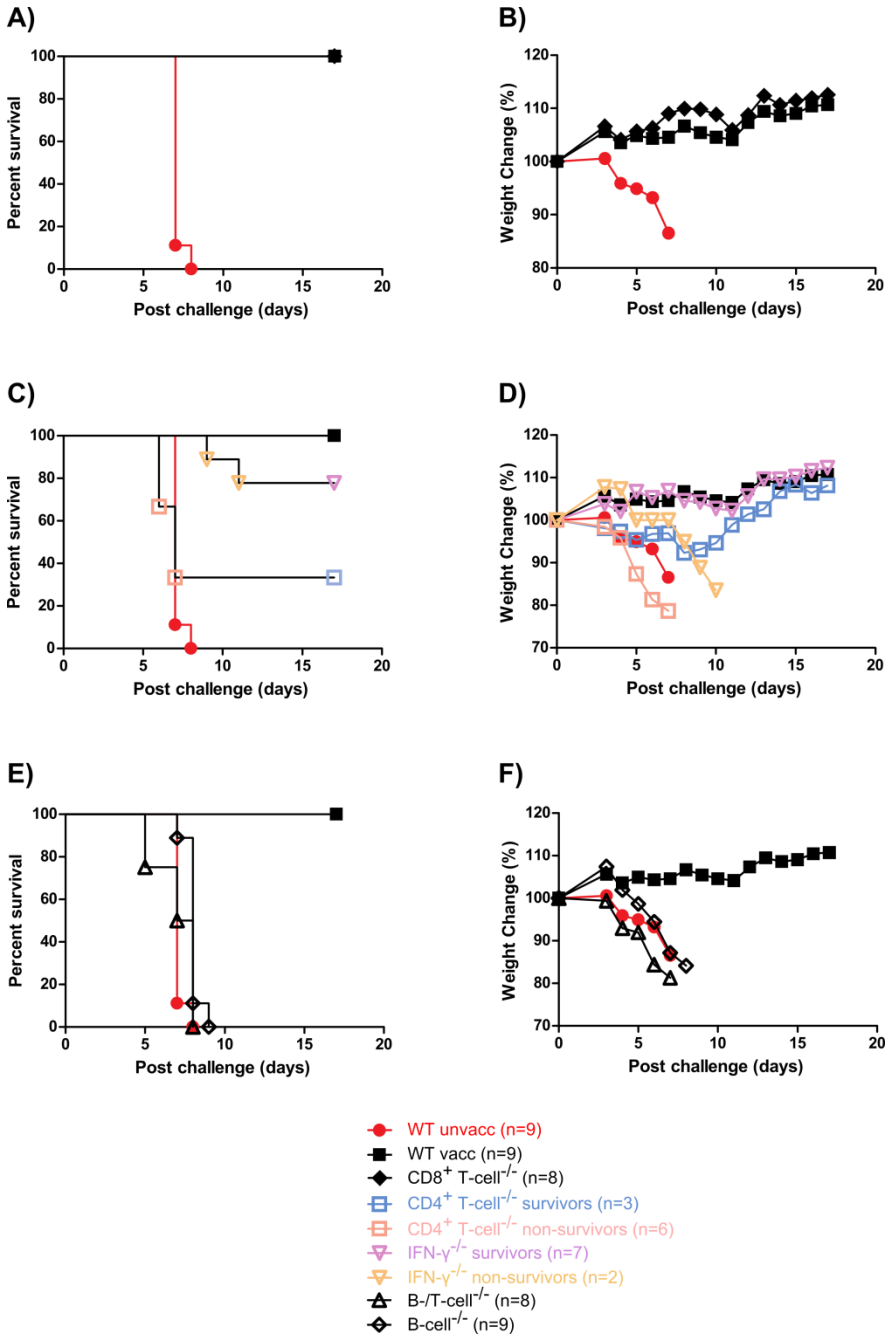

Figure 3.4. B-cells are important for vaccine-induced survival of mice against MA-EBOV challenge. Survival and weight loss graphs of wild-type and transgenic/knockout mice after MA-EBOV challenge. (A and B) represent mice that showed 100% survival, (C and D) represent mice that showed partial survival, and (E and F) represent mice that did not survive. The various groups were immunized with the Ad5-optGP vaccine 28 days before challenge. Protective efficacy and weight loss were expressed as percentage survival and percentage weight change, respectively. The WT unvacc and WT vacc control groups were shown in each graph as a comparison.

3.2.2 Cell-mediated responses in wild-type and transgenic/knockout mice

The numbers of GP-specific splenocytes secreting IFN-γ were measured by IFN-γ ELISpot assay. Groups of mice (n=3) were sacrificed and their harvested spleens pooled before purification and stimulation *ex vivo* with a GP peptide library at 10 dpv. The total number of spot-forming cells (SFC) per 1 x 10^6 splenocytes for each group was adjusted for background levels, in which the WT unvacc group was set at zero. Specific T-cell responses were not detected for B-/T-cell$^{-/-}$ and IFN-γ$^{-/-}$ mice. However, robust levels of GP-specific IFN-γ secreting cells were observed in the WT vacc, B-cell$^{-/-}$ and CD4$^+$ T-cell$^{-/-}$ mice, with 1738, 1440, and 1594 SFC per 1 x 10^6 splenocytes, respectively. CD8$^+$ T-cell$^{-/-}$ mice demonstrated reduced but detectable IFN-γ responses, at a level of 456 SFC per 1 x 10^6 splenocytes (Figure 3.5).

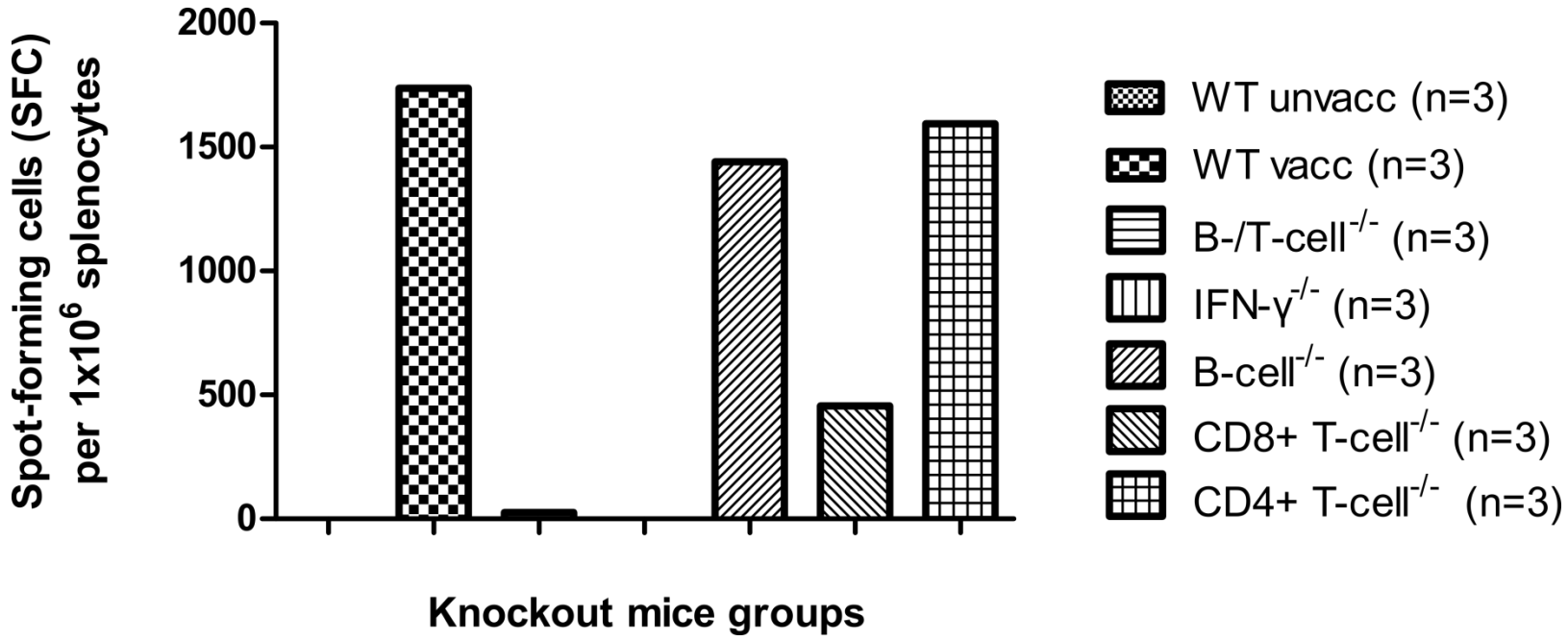

Figure 3.5. T-cell responses after vaccination do not correlate with survival from MA-EBOV challenge in mice. Specific T-cell responses in wild-type and transgenic/knockout mice measured after 10 days after Ad5-optGP vaccination, as determined by IFN-γ ELISpot assay from harvested splenocytes. The number of IFN-γ^+ cells is expressed as spot-forming cells per 1 x 10^6 splenocytes.

3.2.3 Humoural responses in wild-type and transgenic/knockout mice

The antibody response induced by Ad5-optGP immunization was measured on sera sampled at 28 dpv for levels of NAbs with the neutralizing antibody assay, and levels of total anti-GP IgG by ELISA. The limit of detection with the NAb assay is 10 reciprocal dilutions, and background NAb titers were detected from WT unvacc, B-/T-cell$^{-/-}$ and B-cell$^{-/-}$ mice, using the WT unvacc group as the control group for statistical analysis. NAbs resulting from vaccination were detectable in the WT vacc, CD8^{+} T-cell$^{-/-}$, IFN-$\gamma^{-/-}$ and CD4^{+} T-cell$^{-/-}$ groups, with levels of 111 ± 48 ($p=0.0003$), 90 ± 47 ($p=0.0005$), 68 ± 58 ($p=0.0007$), and 47 ± 36 ($p=0.0034$), respectively (Figure 3.6A). For IgG ELISAs, the WT unvacc group was utilized as the control group for statistical analysis. An average absorbance of 0.17 ± 0.04 at 405 nm (A_{405}) was detected for the WT unvacc mice. Non-zero optical density readings were observed for B-/T-cell$^{-/-}$ and B-cell$^{-/-}$ mice, which were not statistically significant from the WT unvacc group. However, high levels of anti-GP IgG were detected for the WT vacc, CD8^{+} T-cell$^{-/-}$ and IFN-$\gamma^{-/-}$ groups, with corresponding A_{405} values of 1.22 ± 0.02, 1.05 ± 0.15, and 1.15 ± 0.50, respectively (all $p<0.0001$). Interestingly, while all surviving IFN-$\gamma^{-/-}$ demonstrated robust GP-specific antibody levels, the 2 non-surviving IFN-$\gamma^{-/-}$ mice had comparatively lower IgG levels. CD4^{+} T-cell$^{-/-}$ mice demonstrated a severely compromised IgG antibody response, with an average A_{405} value of 0.20 ± 0.26 ($p>0.05$) and only 2 survivors out of 9 total mice testing positive for levels of GP-specific antibodies (Figure 3.6B). Taken together, the results from transgenic/knockout mice studies suggest that following vaccination with Ad5-optGP, the development of a protective immune response against MA-EBOV infection is reliant on IFN-γ, CD4^{+} T-cells, and most critically B-cells. Levels of EBOV NAbs and GP-specific IgG both correlate to survival, however IgGs were shown to be the superior indicator of protection.

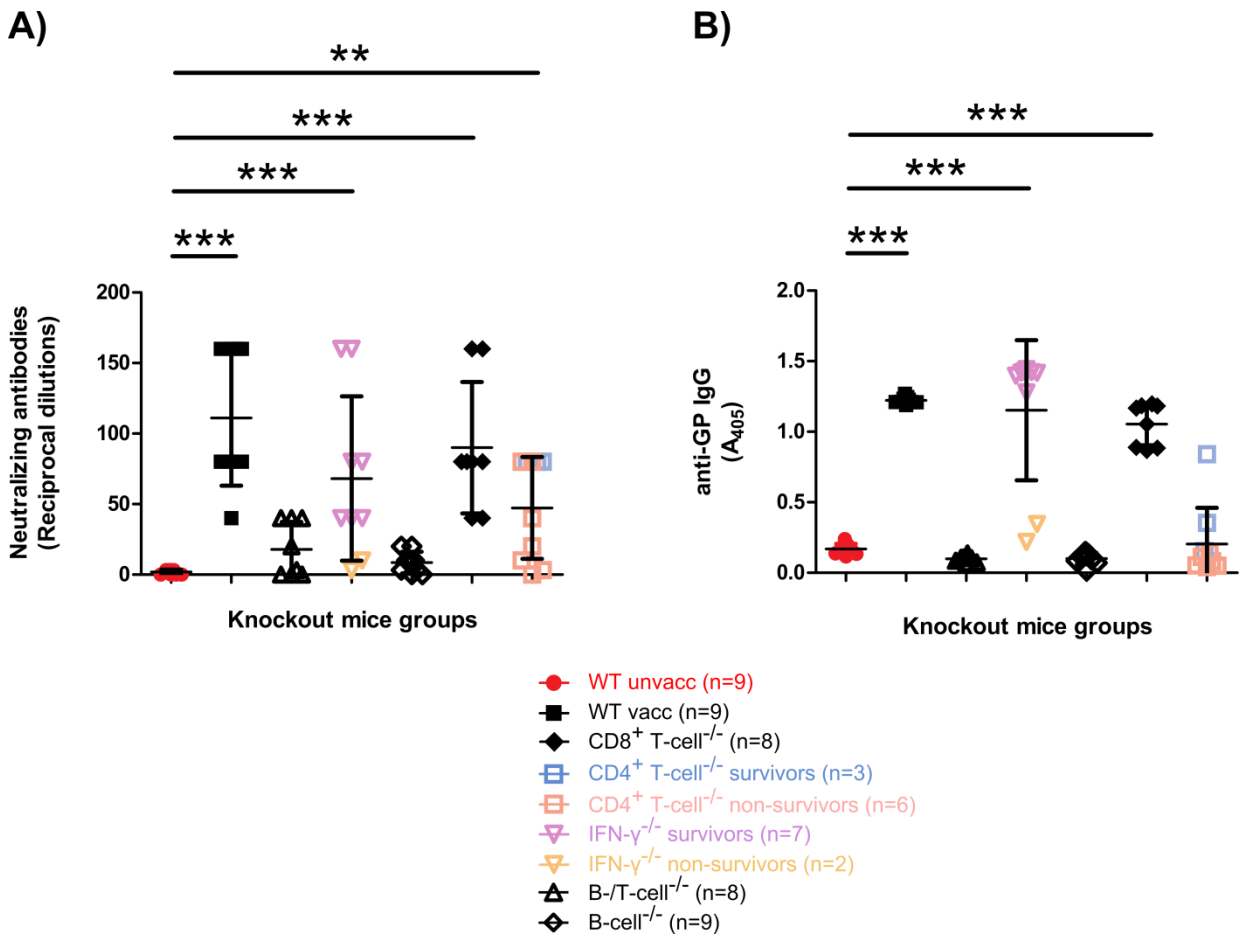

Figure 3.6. Antibody responses after vaccination correlate with survival from MA-EBOV challenge in mice. Specific B-cell responses were measured from the serum of wild type and transgenic/knockout mice 28 days after Ad5-optGP vaccination. (A) Neutralizing antibody levels and (B) Total GP-specific IgG levels reported as reciprocal dilutions and A_{405}, respectively. Error bars represent ± standard deviation.

3.2.4 Survival and weight loss in guinea pigs

Guinea pigs were used to further characterize immune responses correlating with survival from EBOV infection, and to confirm the experimental trends observed from mice. Animals were grouped based on survival outcome and only antibody responses were monitored, due to the unavailability of molecular tools to evaluate T-cell responses in guinea pigs. Guinea pigs were challenged with 1000 x LD_{50} GA-EBOV, 28 days after Ad5-optGP vaccination in the presence or absence of Ad5-lacZ induced PEI. Untreated, control animals typically succumb to disease between 7 to 9 days in untreated animals (data not shown), whereas treated moribund guinea pigs developed rapid weight loss and have been observed to perish between 7 and 10 dpi, with one animal lasting as long as 20 dpi. The data generated for this particular animal has been highlighted in green for clarity. The mean time to death for treated non-survivors is 9.4 ± 4.1 days (Figure 3.7).

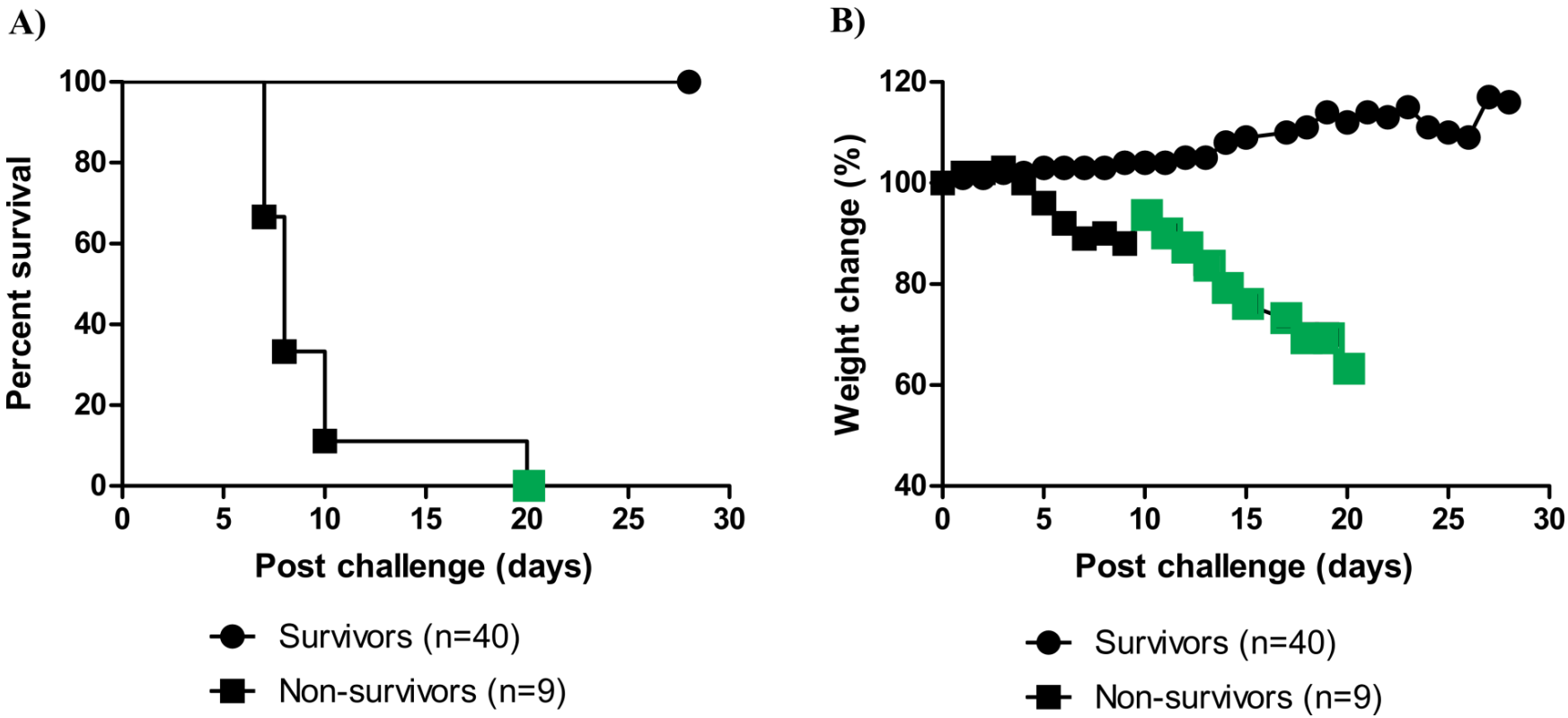

Figure 3.7. Moribund guinea pigs typically rapidly succumb to GA-EBOV infection. Survival and weight loss in guinea pigs after GA-EBOV challenge. (A) The protective efficacy and (B) weight loss from surviving and non-surviving animals are expressed as percentage survival and weight change, respectively. The animal that succumbed to GA-EBOV at 20 dpi is highlighted in green.

3.2.5 Humoural responses in guinea pigs

The magnitude of the antibody response was evaluated on sera sampled at 28 dpv for levels of NAbs with the neutralizing antibody assay, and levels of total anti GA-EBOV or anti-GP IgG by ELISA. Total anti-EBOV IgG used GA-EBOV as a capture antigen and measures the total IgG response towards all GA-EBOV antigens, whereas total anti-GP IgG measures the total IgG response towards only the EBOV GP. Statistically significant differences could be detected and correlated to protection between surviving and non-surviving guinea pigs using all three assays. For neutralizing antibody assays, average levels of EBOV-specific NAbs were 38 ± 31 reciprocal dilutions in survivors, while it was 17 ± 23 in non-survivors (p=0.0221) (Figure 3.8A). For GA-EBOV specific ELISAs, average IgG levels between survivors and non-survivors were 0.56 ± 0.28 and 0.28 ± 0.31 $A_{405,}$ respectively (p=0.0054) (Figure 3.8B). For GP-specific ELISAs, average circulating IgG levels between surviving and non-surviving animals were 1.31 ± 0.47 compared to 0.45 ± 0.39 $A_{405,}$ respectively (p=0.0002) (Figure 3.8C). Interpreting the above results using a 95% confidence interval, the range of GA-EBOV specific and GP-specific IgG levels for survivors are 0.47–0.65 and 1.16–1.46 $A_{405,}$ respectively, while the range of GA-EBOV specific and GP-specific IgG levels for non-survivors is between 0.04–0.52 and 0.15–0.75 $A_{405,}$ respectively. Furthermore, GP-specific ELISAs offer the most precise measurements of the specific humoural immune response, and should be utilized in subsequent studies.

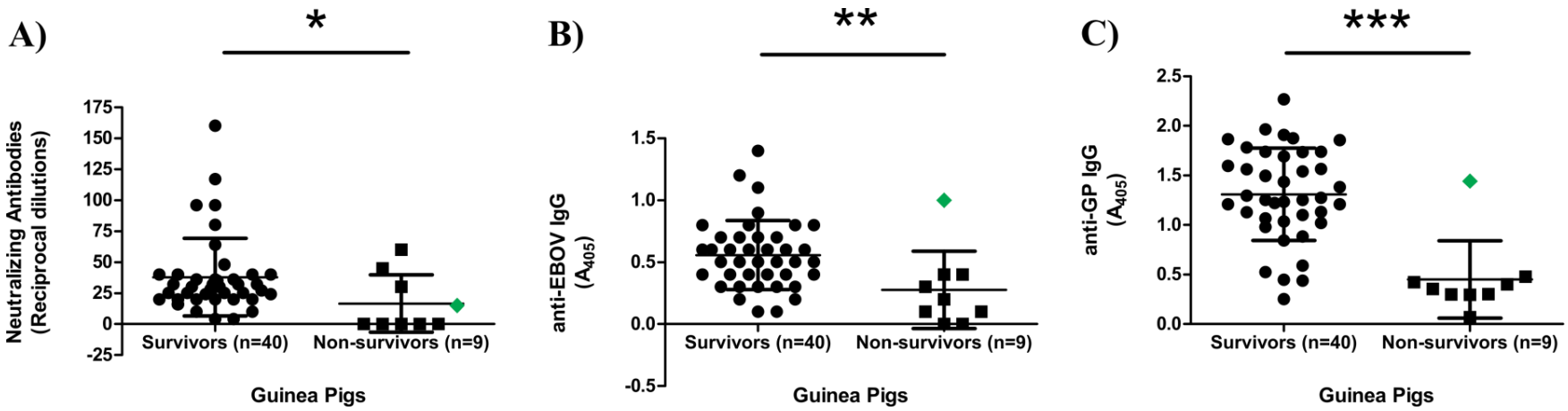

Figure 3.8. Antibody responses after vaccination correlate with survival from GA-EBOV challenge in guinea pigs. Specific B-cell responses in guinea pigs as measured 28 days after Ad5-optGP vaccination, in the presence or absence of induced pre-existing immunity. (A) Neutralizing antibody levels (B) Total EBOV-specific and (C) Total GP-specific IgG levels. Neutralizing antibodies are reported as reciprocal dilutions, whereas IgG levels are reported as A_{405}. Arithmetic means are shown and error bars represent ± standard deviation. The animal that succumbed to GA-EBOV at 20 dpi is highlighted in green.

3.3 Discussion

The experimental results from mice and guinea pigs strongly contradict the hypothesis. Surprisingly, vaccinated B-cell$^{-/-}$ mice did not survive challenge or demonstrate prolonged survival, highlighting the importance of humoural immunity for the Ad5-optGP vaccine in order to establish protective immunity. A robust cell-mediated response was observed in these B-cell$^{-/-}$ mice, as evidenced by the production of IFN-γ from splenocytes upon stimulation with the GP peptide, but this response was not sufficient for survival. CD8^{+} T-cell$^{-/-}$ mice did not produce a very strong IFN-γ response but did produce comparable levels of NAbs and anti-GP IgG to the WT vacc group, yet the CD8^{+} T-cell$^{-/-}$ mice survived infection. Therefore, a correlation cannot be drawn between the cell-mediated response and survival. Conversely, in mice the presence of NAb or the anti-GP IgG response positively correlated with survival. In groups with partial survival, IgG antibody was not detected in the two IFN-γ$^{-/-}$ mice that did not survive challenge, whereas specific antibodies were detected in two of three CD4^{+} T-cell$^{-/-}$ survivors.

In guinea pigs, levels of NAbs correlated weakly with survival with significant overlap between the range of survivors and non-survivors, however both GA-EBOV specific and GP-specific IgG levels varied significantly and positively correlated with protection. Indeed, the guinea pig highlighted in green demonstrated a significant GP-specific IgG response and succumbed to GA-EBOV disease much later than the other treated animals in its group, presumably due to the higher level of serum antibodies. In the absence of T-cell data, conclusions cannot be drawn regarding the role of cell-mediated immunity to protection in this animal model. However, it cannot be denied that the antibody response definitely does correlate to survival for both mice and guinea pigs. Although these results are promising, both MA-EBOV and GA-EBOV are viruses that have been specifically adapted to kill its host, and may

not accurately reflect the true nature of EBOV infections. Therefore, the next step is to observe whether the same trends hold true in NHP studies.

CHAPTER IV: IMMUNE RESPONSES CORRELATING TO PROTECTION FROM EBOLA VIRUS IN NONHUMAN PRIMATES

4.1 New hypothesis

Since the original hypothesis was inconsistent with the experimental results, a new hypothesis is necessary. Due to revelations in the previous chapter, the latest hypothesis is as follows: ***specific B-cell responses, in particular GP-specific IgG levels, are predictive of survival from EBOV and therefore constitute the immune correlates of protection.***

4.2 Introduction

Using outbred cynomolgus macaques as the model NHP, Chapter IV builds on the experimental trends that were established in the previous chapter, in order to demonstrate that the findings also hold true with wild-type EBOV infections. Similar to guinea pigs, NHPs from different past vaccination and post-exposure therapy experiments were grouped together based on survival outcome, in order to increase the power and significance of the results from statistical analysis. It was also done in part to provide an immunologic marker for non-protection that is independent of the reasons behind vaccine or treatment failure, whether it is the presence of PEI, insufficient dosage, inadequate route of administration, presence or absence of adjuvant, or the timing of medical intervention. In past vaccine studies, prophylactics were always administered 28 days before EBOV challenge, whereas in past post-exposure studies, treatments were initiated 30 minutes after challenge.

In Ad5-optGP studies, NHPs were given IM, IN, or IN/IT with 1 x 10^{10} to 4 x 10^{10} infectious forming units of Ad5-optGP in the presence or absence of PEI induced by 1 x 10^{11} total particles of Ad5-lacZ. 2 x 10^{9} PFU/kilogram (kg) of adenovirus vectored-IFN-α (Ad5-IFN-α) was used in some NHPs as a vaccine adjuvant administered along with Ad5-optGP. Recombinant universal type I IFN-α was also administered IM at a dose of 0.44 μg/kg in some NHPs. In the VSV study, NHPs were immunized IM, IN or OR with a single administration of 2 x 10^{7} PFU of VSVΔG/EBOVGP (Figure 4.1A).

To compare innate and adaptive immune responses between surviving and non-surviving NHPs, PBMCs and sera were collected from available animals whenever appropriate and possible. To characterize humoural immunity in vaccination and post-exposure therapy studies, sera were collected at 28 dpv (0 dpi) and at 6-7 dpi, and then measured for antibody levels via NAb assays, or GP-specific IgG via ELISA. For cell-mediated immunity in vaccination and post-exposure therapy studies, peripheral blood mononuclear cells (PBMC) were sampled at 14 dpv and 7 dpi, and then measured for specific T-cell activity either by IFN-γ ELISpot assays or fluorescence-activated cell sorting (FACS). The identification of an early, innate immune marker correlating with increased vaccine efficacy or early signs of immune dysregulation is also critical for survival. To measure and compare between NHPs the levels of cytokine and chemokine after vaccination as well as before and after EBOV challenge, sera was harvested at 7 dpv, 28 dpv and between 6-10 dpi before single and multiplex analysis (Figure 4.1B). In total, 24 and 50 cynomolgus macaques were included for Ad5-optGP vaccination and post-exposure studies, respectively. A total of 22 NHPs were included for the VSVΔG/EBOVGP vaccine study.

Based on the most recent hypothesis, it is expected that high levels of GP-specific IgG induced by vaccination will be predictive of survival from EBOV. Furthermore, a rapid IgG response after EBOV challenge will correlate with the observed post-exposure protection from EBOV in NHPs. It is also expected that the aggressiveness and speediness of EBOV from infection to onset of disease will require all arms of the immune response in order to effectively combat the pathogen. Therefore, increased T-cell responses as well as early induction of pro-inflammatory cytokines are expected to play a role in protection from EBOV.

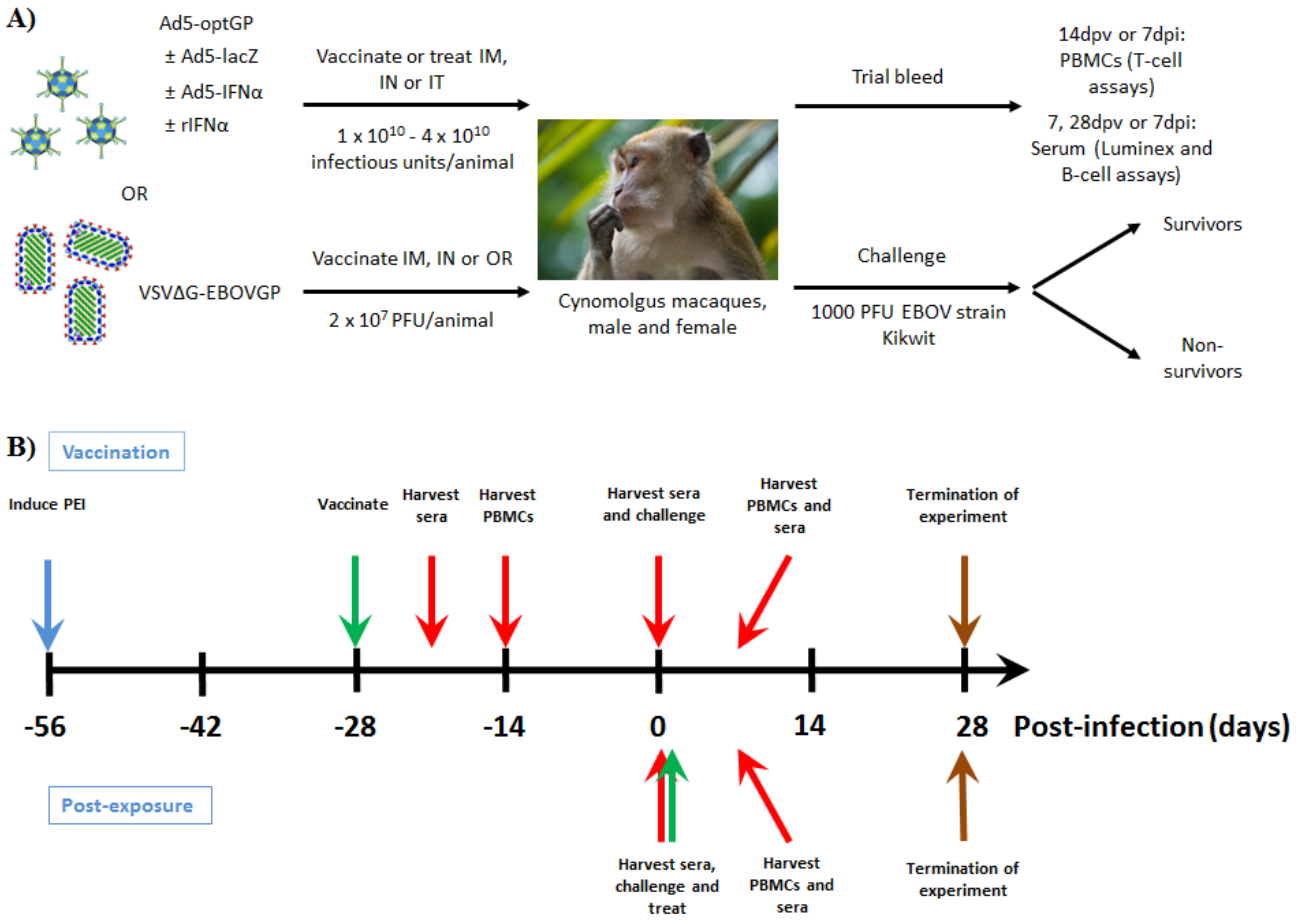

Figure 4.1. Experimental flow and timeline of NHP studies. (A) An aggregated plan of the various NHP experiments, in which PMBC and sera samples were collected and (B) Timeline of vaccinations, treatments, challenge, and sample collections. Major events over the course of the experiment are indicated by the arrows on the timeline.

4.3 Results

4.3.1 B-cell responses in nonhuman primates before EBOV challenge

Humoral immune responses were first evaluated between surviving (n=8) and non-surviving (n=16) NHPs from the Ad5-optGP experiments, immediately before lethal challenge with EBOV, which represent antibody levels generated as a result of vaccination. For determination of serum IgG levels in NHPs, ELISA studies were only performed with the recombinant GP as the capture antigen, as previous studies with guinea pigs described in Chapter III demonstrated that GP-specific immune responses correlated with survival to a higher degree than EBOV-specific immune responses. Significant levels of circulating NAbs could not be detected before challenge (Figure 4.2A). Serum GP-specific IgG levels before challenge were measured to be 2.00 ± 0.18 and 0.12 ± 0.17 A_{405} for surviving and non-surviving NHPs, respectively ($p<0.0001$) (Figure 4.2B). The range of total GP-specific IgG before challenge was between 1.85–2.16 for survivors, and 0.03–0.21 A_{405} for non-survivors of lethal EBOV infection using a 95% confidence interval.

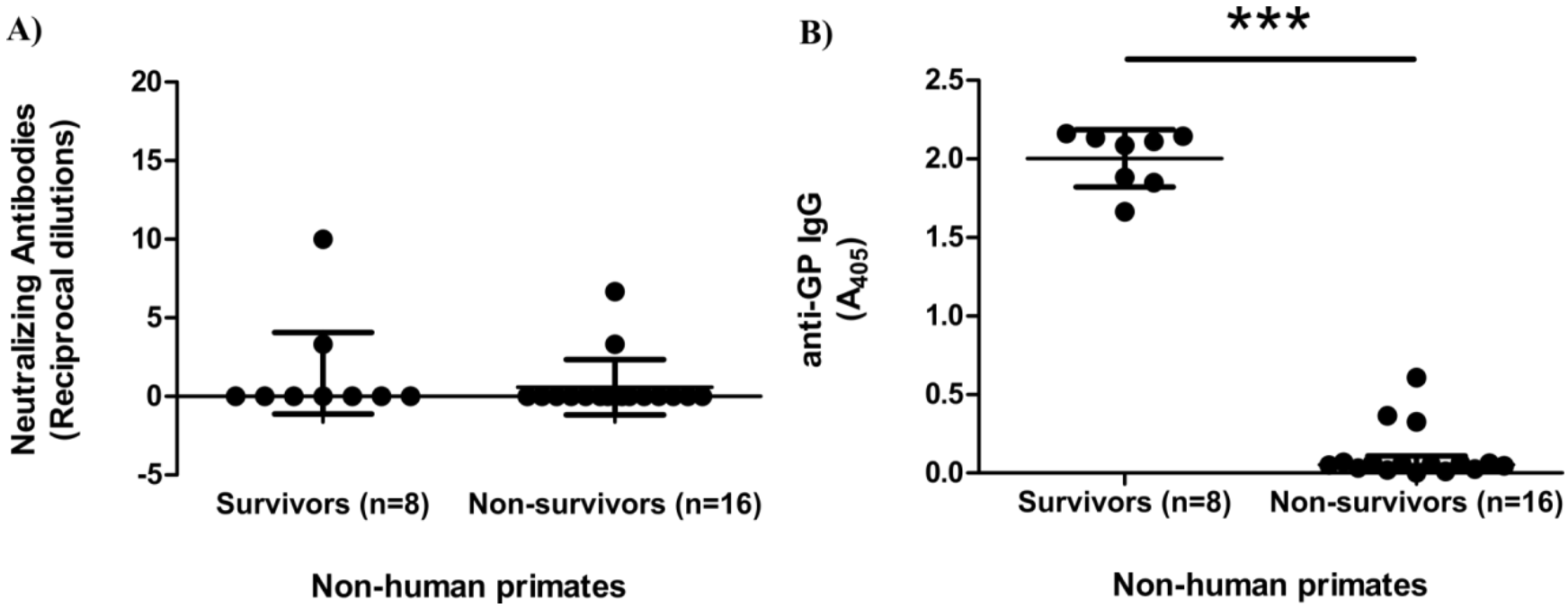

Figure 4.2. EBOV glycoprotein-specific IgG antibodies correlate with survival in Ad5-optGP vaccinated NHPs after immunization. Humoural immune responses from the sera of cynomolgus macaques, measured 28 days after vaccination with Ad5-optGP. (A) Neutralizing antibody levels and (B) Total GP-specific IgG levels reported as reciprocal dilutions and A_{405}, respectively. Arithmetic means are shown and error bars represent ± standard deviation.

4.3.2 B-cell responses in nonhuman primates after EBOV challenge

Antibody responses were then measured and compared between surviving (n=17) and non-surviving (n=57) NHPs from the Ad5-optGP experiments, 7 days after lethal EBOV challenge, which represent antibody levels generated as a result of treatment and EBOV exposure. NAb levels for surviving animals were determined to be 35 ± 69 reciprocal dilutions, whereas non-surviving NHPs had levels of 70 ± 110. The difference in NAb levels between survivors and non-survivors was not statistically significant ($p>0.05$) (Figure 4.3A). Total GP-specific IgG levels from surviving NHPs were 1.45 ± 0.51 A_{405}, compared to non-surviving animals, which had 0.18 ± 0.23 A_{405}. The difference in GP-specific levels between the two groups was statistically significant ($p<0.0001$) (Figure 4.3B). The range of GP-specific IgG levels after EBOV challenge was between 1.19–1.71 and 0.12–0.25 A_{405} for survivors and non-survivors, respectively, and survivors treated 30 minutes after challenge were found to exhibit lowered GP-specific IgG titers than most animals that were vaccinated 28 days before challenge.

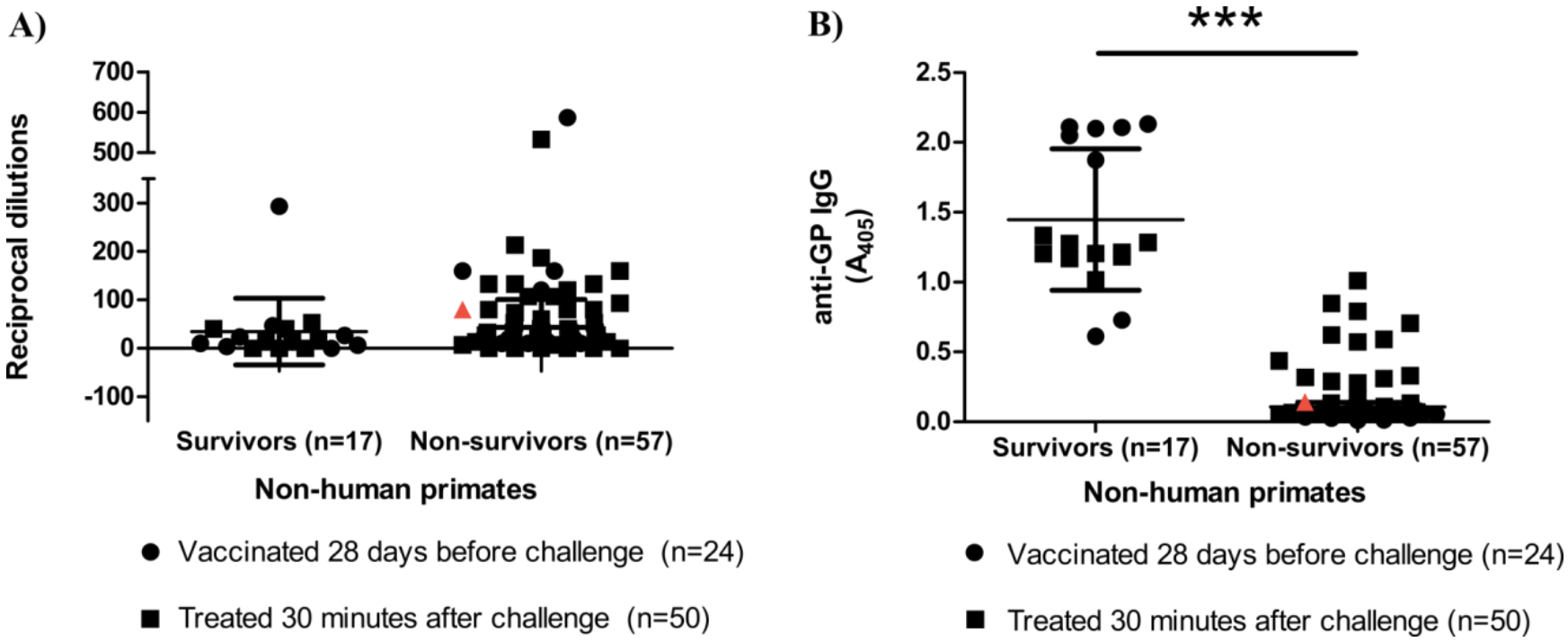

Figure 4.3. EBOV glycoprotein-specific IgG antibodies correlate with survival in Ad5-optGP vaccinated NHPs after challenge. Humoural immune responses from the sera of cynomolgus macaques, measured 7 days after EBOV challenge. (A) Neutralizing antibody levels and (B) Total GP-specific IgG levels reported as reciprocal dilutions and A_{405}, respectively. Black circles and squares represent animals from vaccination and post-exposure studies, respectively. An infected, untreated control animal (red square) is included to demonstrate immune responses during disease progression. Arithmetic means are shown and error bars represent ± standard deviation.

4.3.3 B-cell responses in VSV-treated nonhuman primates

To determine if this observation was also true for candidate EBOV vaccines that were constructed on other platforms, serum samples from an independent study with VSVΔG/EBOVGP were also analyzed with respect to GP-specific IgG levels, either immediately before or 7 days after challenge. The endpoint dilution titers of surviving (n=11) and non-surviving (n=11) NHPs immediately before challenge were determined to be 12805 ± 29905 and 64 ± 59 reciprocal dilutions, respectively. This difference was statistically significant (p=0.0003) (Figure 4.4A). The endpoint dilution titers of the same surviving and non-surviving NHPs 7 days after challenge were determined to be 6491 ± 4616 and 136 ± 100, respectively. This difference was also statistically significant (p=0.0001) (Figure 4.4B).

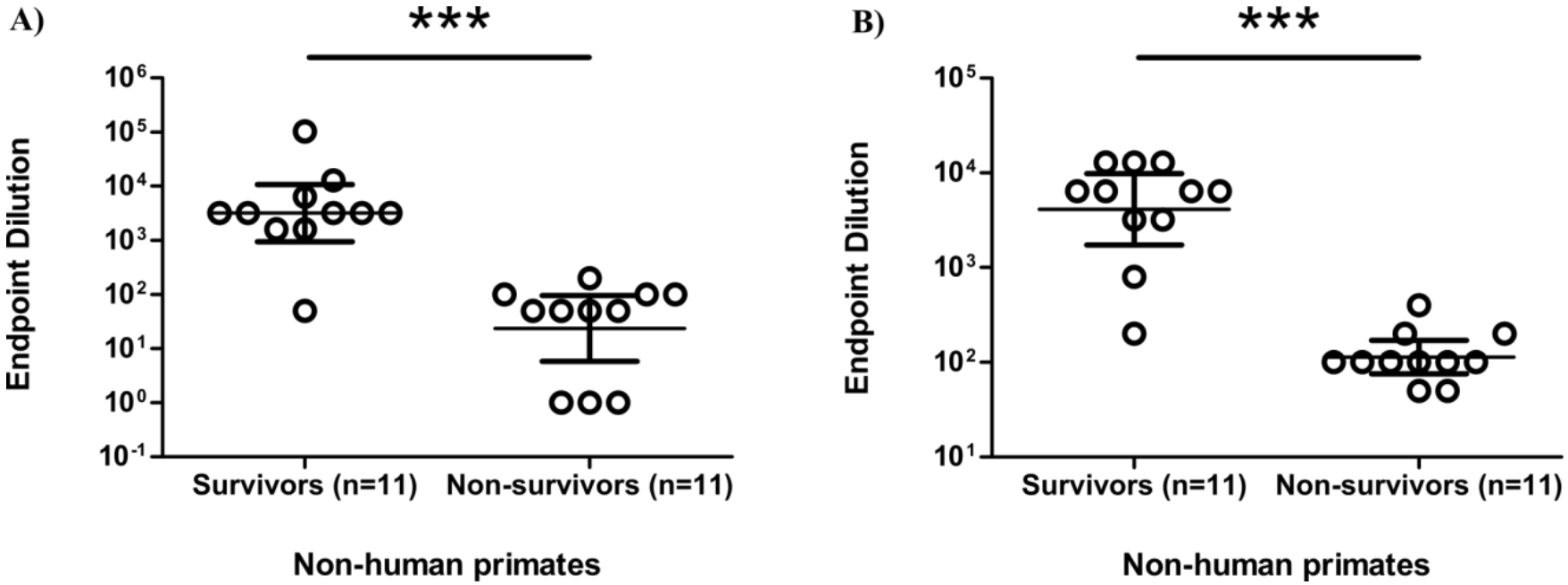

Figure 4.4. EBOV glycoprotein-specific IgG antibodies correlate with survival in VSVΔG/EBOVGP vaccinated NHPs after immunization as well as after challenge. Humoural immune responses from the sera of cynomolgus macaques, measured after vaccination with VSVΔG/EBOVGP or infection with EBOV. Total serum GP-specific IgG levels were measured (A) immediately before or (B) at 6 days after challenge. Antibody levels are reported as endpoint dilutions. Geometric means are shown and error bars represent 95% confidence intervals.

4.3.4 T-cell responses in nonhuman primates before EBOV challenge

The cellular immune response to Ad5-optGP vaccination was then compared between surviving (n=8) and non-surviving (n=6) NHPs with blood harvested 14 days after immunization. The numbers of IFN-γ secreting PBMCs were measured in parallel with the combined IFN-γ expression levels of CD4 and CD8 T-lymphocyte markers. After *ex vivo* stimulation of PBMCs by GP peptide pools, the occurrence of IFN-γ secreting cells in survivors compared to non-survivors was 127 ± 112 and 29 ± 29 SFC per million PBMCs, respectively, as measured by ELISpot. This difference was not statistically different between the two groups ($p>0.05$) (Figure 4.5A). However, the combined number of IFN-γ secreting cells from $CD4^+$ and $CD8^+$ T-cells after vaccination was statistically significant between survivors and non-survivors, at 660 ± 324 and 142 ± 72 IFN-γ secreting cells per million lymphocytes, respectively ($p=0.0013$) (Figure 4.5B).

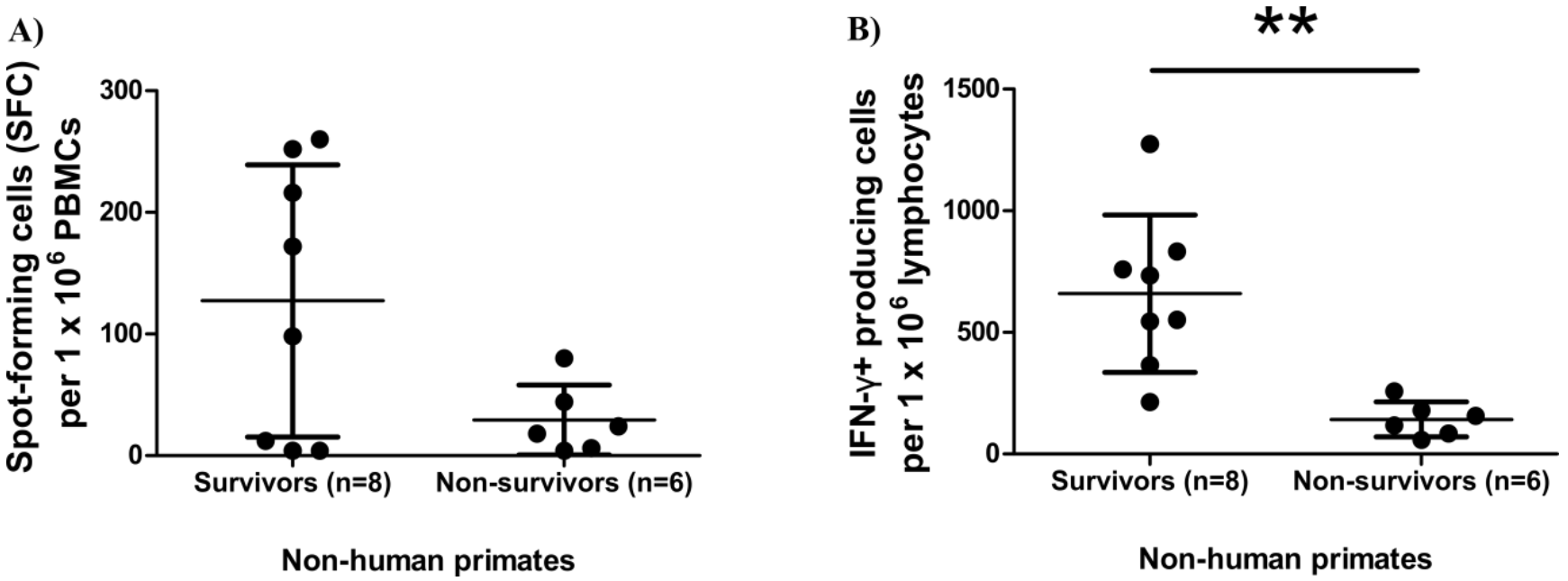

Figure 4.5. T-cell responses after vaccination correlate with survival from EBOV challenge in NHPs. Cellular immune responses from purified PBMCs or lymphocytes of cynomolgus macaques, measured 14 days after vaccination with Ad5-optGP. (A) Total number of IFN-γ secreting cells per million PBMCs and (B) Number of IFN-γ secreting cells per million lymphocytes after *ex vivo* stimulation by EBOV GP peptides, as measured by ELISpot and flow cytometry, respectively. Arithmetic means are shown and error bars represent ± standard deviation.

4.3.5 T-cell responses in nonhuman primates after EBOV challenge

Cell-mediated responses were then measured between surviving and non-surviving NHPs from Ad5-optGP experiments, 7 days after lethal EBOV challenge, which represent immune responses generated as a result of treatment and EBOV exposure. The number of IFN-γ secreting PBMCs after *ex vivo* stimulation by GP peptide pools in survivors (n=9) compared to non-survivors (n=12) was 152 ± 105 and 18 ± 27 SFC per million PBMCs, respectively, as measured by ELISpot. The difference observed between the two groups was statistically significant (p=0.0013) (Figure 4.6A). It should be noted that the blood samples from non-survivors contain a significantly higher proportion of granulocytes than their survivor counterparts (Figure 4.6B). This caveat makes the comparison of T-cell responses between survivors and non-survivor animals after EBOV challenge difficult, if not inappropriate. Furthermore, the differing blood profiles between the two groups may be responsible for the lowered amount of IFN-γ secreting cells in non-surviving animals. In order to estimate the impact of cell-mediated immunity after challenge, the proportion of T-cells as a percentage of IFN-γ producing PMBCs was calculated instead. In surviving NHPs (n=9), IFN-γ was mainly produced by T-cells at 69 ± 24%, which is higher compared to non-survivors (n=10), where T-cells only represent 34 ± 24% of IFN-γ positive cells. This difference was statistically significant (p=0.0057) (Figure 4.6C).

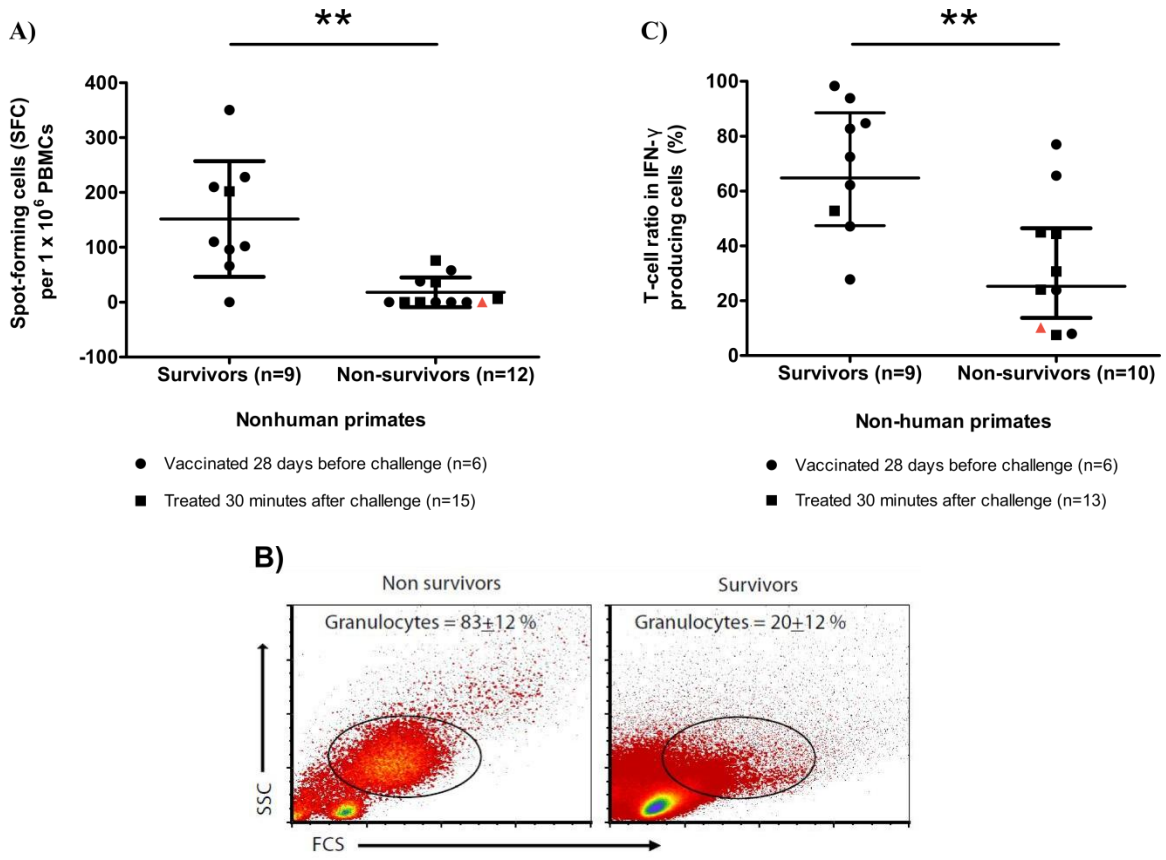

Figure 4.6. T-cell responses after challenge correlate with survival from EBOV challenge in NHPs. Cellular immune responses from purified PBMCs of cynomolgus macaques, measured 7 days after EBOV challenge. (A) Number of IFN-γ secreting cells per million PBMCs as determined by ELISpot; (B) Percentage of T-cells in IFN-γ producing cells as determined by FACS and (C) flow cytometry analysis of cell populations between survivors and non-survivors of EBOV infection. Arithmetic means are shown for ELISpot data and error bars represent ± standard deviation. Geometric means are shown for FACS data and error bars represent ± 95% confidence intervals.

4.3.6 Innate immune responses in nonhuman primates before challenge

To elucidate other host immune determinants of survival outcome after vaccination, the expression profile of several cytokines and chemokines were evaluated from NHP serum samples collected at 7 days after immunization with Ad5-optGP. MCP-1 levels between the survivor (n=8) and non-survivor (n=8) did not differ significantly immediately before vaccination (Figure 4.7A). At 7 days after Ad5-optGP administration, an increase in MCP-1 levels was observed for survivors compared to non-survivors, with average levels of 549 ± 282 and 295 ± 85 picograms (pg)/mL, respectively. This difference was statistically significant (p=0.0451) (Figure 4.7B).

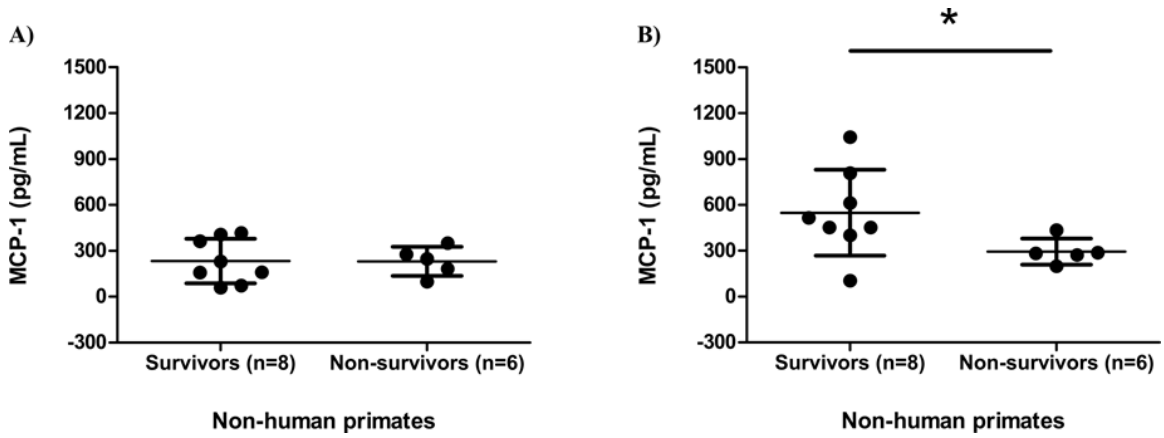

Figure 4.7. MCP-1 levels correlate with survival in NHPs after immunization. Chemokine levels in surviving and non-surviving cynomolgus macaques after vaccination. MCP-1 levels were measured from sera taken (A) immediately before vaccination and (B) 7 days after vaccination with Ad5-optGP. Arithmetic means are shown and error bars represent ± standard deviation.

4.3.7 Innate immune responses in nonhuman primates after challenge

Several cytokines and chemokines were also measured 6-10 days after EBOV exposure to determine alternative immune markers, which could predict positive versus negative outcomes after infection. While the survivor (n=9) and non-survivor (n=15) groups did not show differences in IL-6, MIP-1α and MCP-1 levels immediately before challenge (Figures 4.8A, C, E), the moribund animals demonstrated increased levels following EBOV exposure, which were statistically significant. For surviving and non-surviving NHPs, IL-6 levels were 1720 ± 2437 and 40 ± 92, respectively ($p=0.0001$) (Figure 4.8B); MIP-1α levels were 174 ± 164 and 28 ± 26, respectively ($p=0.0003$) (Figure 4.8D); and MCP-1 levels were 39575 ± 91741 and 383 ± 255 pg/mL, respectively ($p<0.0001$) (Figure 4.8F).

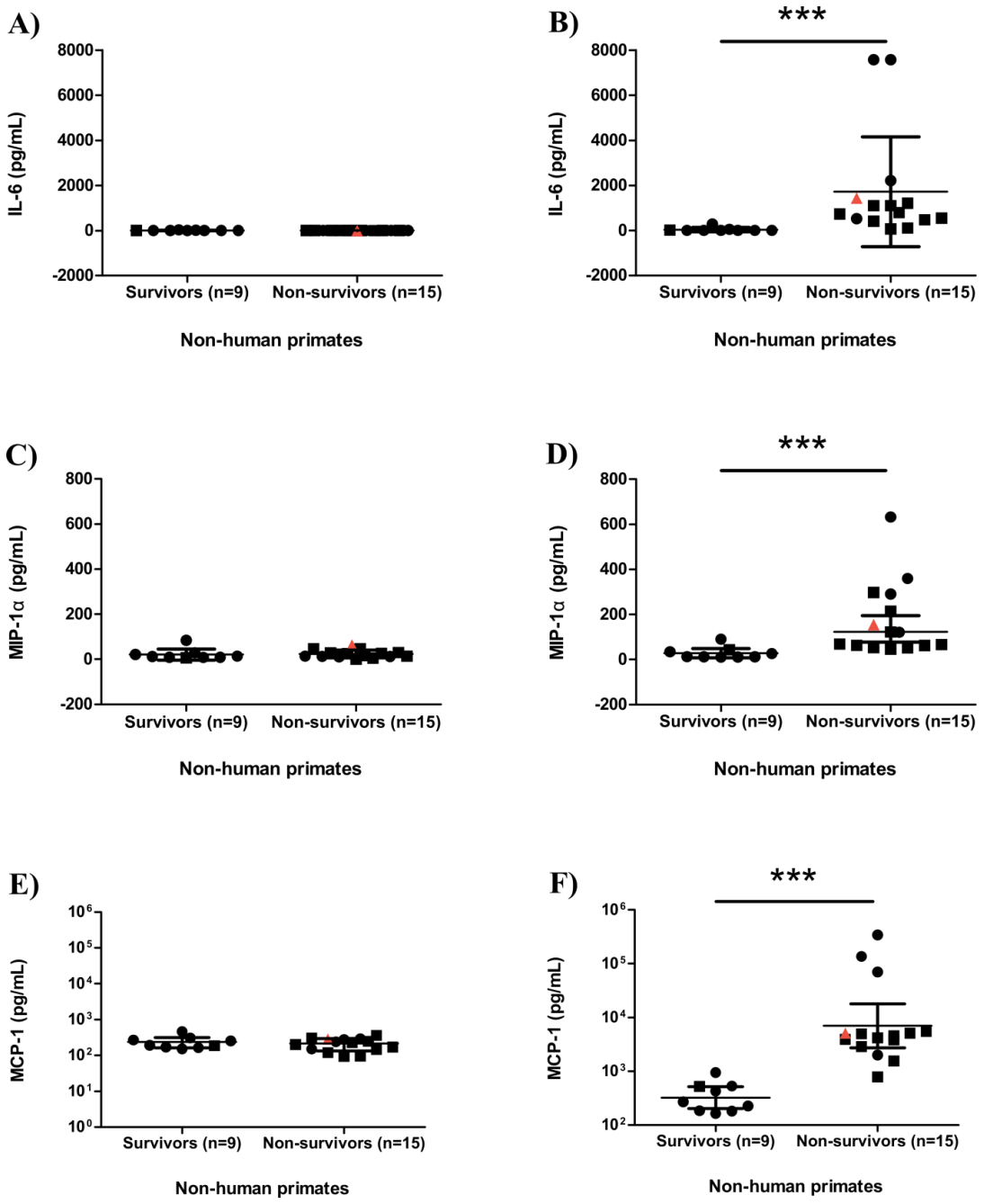

Figure 4.8. IL-6, MIP-1α and MCP-1 levels correlate with survival in NHPs after challenge. Chemokine and cytokine levels were compared between surviving and non-surviving cynomolgus macaques (A, C, E) immediately before challenge or (B, D, F) 6-10 days after EBOV challenge. An infected, untreated control animal (red triangle) is included to demonstrate chemokine and cytokine responses during disease progression. Arithmetic means are shown for IL-6 and MIP-1α, in which error bars represent ± standard deviation. Geometric means are shown for MCP-1 levels, in which error bars represent ± 95% confidence intervals.

4.4 Discussion

The experimental results from NHPs support the new hypothesis as established in the beginning of Chapter IV. Over 96 outbred NHPs in total, serum NAb levels against EBOV could not be statistically associated with protection; therefore antibody-mediated virus neutralization does not appear to play a major role. However, increased levels of GP-specific IgG levels were predictive and correlate to the highest degree of statistical significance with survival of the host to EBOV infection. Furthermore, GP-specific levels can be used to predict a positive or negative survival outcome with greater than 99.9% confidence, and holds true regardless of the vaccine platform choice (Ad5 versus VSV) and the timing of exposure (before or after challenge with EBOV). It appears that the initiation of an early antibody response specific to EBOV is important and at the minimum statistically correlates with survival from infection, which is consistent with previously published data (Sullivan 2009). EBOV GP is known to be the main determinant of pathogenicity, where $GP_{1,2}$ is responsible for initiating attachment and fusion of the viral and host membranes, leading to endothelial cell disruption and cytotoxicity (Lee, Fusco et al. 2008) (Yang, Delgado et al. 1998), and sGP can inhibit neutrophil activation and thereby host immune responses (Yang, Delgado et al. 1998). Therefore, GP-specific IgG may be able to control EBOV disease through the disruption of several essential viral functions.

The importance of the T-cell response to survival was also investigated. While the number of IFN-γ secreting PBMCs did not demonstrate a statistical association with survival, an increased number of IFN-γ secreting $CD4^+$ and $CD8^+$ T-cells positively correlated with survival when measured 14 days after Ad5-optGP vaccination. After

EBOV challenge, the number of IFN-γ secreting PBMCs showed a statistically significant difference in the number of IFN-γ producing cells between surviving and non-surviving animals. However, the cellular composition of the blood sampled between surviving and non-surviving NHPs were significantly different from each other. Moribund NHPs demonstrated an unusually high proportion of granulocytes, presumably induced by EBOV disease progression. Since lymphocytes are the main IFN-γ producers, it cannot be ruled out that the abundance of granulocytes may be responsible for the lowered rate of IFN-γ producing cells as observed in non-survivors. Furthermore, due to massive lymphocyte apoptosis stemming from EBOV disease it was difficult to obtain sufficient counts of IFN-γ secreting T-cells after challenge. Therefore, the proportion of IFN-γ producing T-cells was calculated instead and its levels found to be positively correlated with survival. These results are in agreement with a previous study, which links the cell-mediated response with a reduction in viral load resulting in a better outcome against EBOV infection (Bradfute, Warfield et al. 2008). However, the significant overlap between the values between survivors and non-survivors may limit the overall usefulness of this measure in practice.

NHP survivors showing detectable clinical signs of disease exhibited a decreased humoral but not cell-mediated immune response, and were mainly associated with NHPs treated 30 minutes after EBOV challenge. This could be explained by the fact that NHPs vaccinated 28 days before challenge had more time to establish a complete and specific antibody response, which is beneficial for survival. On the other hand, animals treated 30 minutes after EBOV challenge have very little time to establish a robust IgG response, and thus have to rely on other additional immune components to limit viral spread and

disease progression early during infection, until the activation and amplification of the humoural response.

The adaptive immune response is a very complex network of highly regulated interactions and optimal cross-talk between T- and B-cells essential for antibody production (Clark and Ledbetter 1994), but its establishment is dependent on an functional innate immune response, in which its dysregulation has been postulated as a possible cause of fatal outcome in EBOV patients (Wauquier, Becquart et al. 2010). Characterization of early innate immune markers early post-vaccination or after EBOV challenge yielded several cytokines and chemokines, which correlate with survival. Early after Ad5-optGP vaccination, increased expression of MCP-1 is associated with survival. However, up-regulation of MCP-1 after lethal challenge was observed largely from non-survivors, suggesting that increased MCP-1 levels has a beneficial role following vaccination but a detrimental one after challenge. The expression of pro-inflammatory markers IL-6 and MIP-1α were also significantly increased in non-survivors after EBOV challenge, and may be indicative of disease progression. Monitoring these parameters, in addition to the cell-mediated response, will help complement the antibody data to illustrate a complete picture of the resulting immune responses after vaccination and post-exposure, and may help with critical decision making for patient management.

To summarize, the results strongly reinforce the idea that the B-cell response is a superior predictor of survival from EBOV disease compared to the T-cell response, and suggest that antibodies play the major role in protection, whereas cell-mediated immunity plays a supporting role and becomes more prominent when specific antibody levels are

suboptimal. Therefore, candidate vaccines and therapeutics that elicit robust levels of GP-specific IgG are more likely to be efficacious. For instance, vaccination with a higher antigen dose (Kaur, Kaur et al. 2008), administration of vaccine via IP as opposed to the IN, IT or OR routes (Kurono, Yamamoto et al. 1999), or the use of a strong Th2 adjuvant such as MF59 oil-in-water emulsion or alum (Mosca, Tritto et al. 2008) (Brewer, Conacher et al. 1999) can all promote increased antibody responses and it will be interesting to combine these strategies with current experimental EBOV vaccines in order to increase efficacy. Furthermore, the level of GP-specific IgG is a reliable predictor of protection against EBOV infection, and should be the method of choice for routine testing after vaccination in addition to assessing prognosis in patients during outbreak situations.

The findings from these experiments are supported by two independent NHP studies that were published in approximately the same timeframe. The first study showed that protection of naïve NHPs is possible by passive transfer of species-matched antibodies from vaccinated rhesus macaques, which had previously survived EBOV infection (Dye, Herbert et al. 2012). Purified polyclonal IgG antibodies from survivors were administered to naïve macaques at a concentration of 70–100 mg/kg beginning at 48 hours after challenge, with further injections at 4 and 8 days after EBOV infection. All NHPs survived the challenge despite the delayed initiation of the treatment (Dye, Herbert et al. 2012); one NHP developed mild and delayed signs of disease, but this was followed by a full recovery.

The second study investigated the impact of selectively depleting various immune cell subsets in VSVΔG/EBOVGP vaccinated cynomolgus macaques before and during

vaccination. By using specific antibodies to reduce the number of $CD4^+$, $CD8^+$ T-cells or $CD20^+$ B-cells *in vivo*, this resulted in severely compromised antibody levels accompanied by a robust $CD8^+$ T-cell response in $CD4^+$ T-cell depleted NHPs; and a lack of $CD8^+$ T-cell response but robust IgG antibody levels in $CD8^+$ T-cell depleted NHPs. All $CD8^+$ T-cell depleted NHPs survived challenge, whereas all $CD4^+$ T-cell depleted animals died. The $CD20^+$ B-cell depleted animals still exhibited robust antibody levels, and therefore $CD4^+$ T-cells were depleted during the EBOV challenge. The survival of $CD4^+$ depleted NHPs indicated that $CD4^+$ T-cells also play a minimal role in protection once the antibody response is established, and it was therefore recognized that antibodies play the crucial role for VSVΔG/EBOVGP mediated protection (Marzi, Engelmann et al. 2013).

These developments in NHPs strongly have implicated the antibody response in protection against EBOV infection in three different ways, and it is clear that humoural immunity correlates with and plays a significant role in survival. The passive transfer of polyclonal IgG supported the viability of using antibody-based treatments against EBOV infections, the depletion of immune cell subsets isolated the component responsible for protection, and the results presented in this thesis chapter provide a large-scale, statistically powered study, which supports these trends over a small outbred NHP population. More animals will be needed in order to investigate a number of factors, such as precisely determining the minimum levels of GP-specific IgG required conferring protection, and establishing whether IgG-mediated protection is also independent of vaccine dosage, routes of vaccination or choice of vaccine platform outside of Ad5 and VSV. However, the number of NHPs required for these studies is outside the financial

constraints of the typical academic and government research laboratory and the nature of these experiments are more suited to the industry. Rather, the important task at hand is to investigate whether antibodies generated against EBOV GP are able to confer protection in rodents and NHPs from lethal challenge. In addition to the potential development of a valuable prophylactic or post-exposure candidate, this will also determine whether antibodies are a mechanistic or non-mechanistic correlation of protection, which will further help define the components required for an effective EBOV vaccine or treatment.

CHAPTER V: MONOCLONAL ANTIBODIES AS A CANDIDATE TREATMENT FOR EBOLA VIRUS DISEASE

5.1 Introduction

Therapy with mAbs has been utilized in the past against a wide range of human conditions, including cancer, cardiovascular disease, autoimmune disorders, and transplant rejection with high success rates. In contrast, mAb treatments are rarely employed against infectious diseases and remain an unknown quantity for this particular purpose. The only clinically approved mAb to date against infectious diseases is Palivizumab, which is used for the prevention of Respiratory Syncytial Virus infections (FDA.gov 2014). The earliest indication that passive immunotherapy may be feasible for treatment of EBOV infections was during the 1995 EBOV outbreak in Kikwit. Blood from convalescent patients was transfused to 8 patients from the latter stages of the outbreak, resulting in 7 survivals (Mupapa, Massamba et al. 1999). In the laboratory, treatment of infected cynomolgus macaques with polyclonal equine IgG prepared from hyperimmunized horses (Krasnianskii, Mikhailov et al. 1995) at 0 and 5 dpi also resulted in partial protection of 1 in 3 animals (Jahrling, Geisbert et al. 1999), and suggests a role for antibodies in survival from EBOV disease. The practice of blood transfusions is however dangerous and controversial, and it is difficult to confirm consistent specificity and purity of polyclonal antibody treatments. These factors limit their usefulness in the clinic and as a result efforts were then focused on generating mAbs by recombinant DNA technology for the treatment of EBOV infections.

The first mAbs against EBOV infection were developed by constructing phage display libraries from the RNA of recovering patients during the 1995 EBOV outbreak in

Kikwit. A panel of recombinant human mAbs to EBOV NP, GP, and sGP was then isolated and characterized (Maruyama, Rodriguez et al. 1999). A GP-specific antibody (KZ52) was found to strongly neutralize EBOV *in vitro*, and subsequently tested for efficacy in guinea pigs. Administration of KZ52 IP at a dose of 50mg/kg was found to confer complete, dose-dependent protection in guinea pigs when administered 1 hour before or after lethal GA-EBOV challenge despite high viremia in surviving animals, indicating that the mechanism of protection extends beyond viremia control through virus neutralization (Parren, Geisbert et al. 2002). Regrettably, KZ52 studies in NHPs fell short of expectations. Four rhesus macaques were given an IV dose of 50 mg/kg KZ52 24 hours before EBOV challenge, followed by an identical dose at 4 dpi. No protection was conferred by the passive transfer of KZ52. In addition, KZ52 was unable to control viral replication following infection despite the lack of neutralization escape virus mutants (Oswald, Geisbert et al. 2007). In another study, transfusion of whole blood harvested from 3 NHPs that had survived a lethal EBOV infection failed to protect 4 naïve rhesus macaques when administered at 0 and 3-4 days after challenge (Jahrling, Geisbert et al. 2007). The negative results from these setbacks, coupled with previously mentioned studies, which promote the specific $CD8^+$ T-cell response as the major mechanism for survival against EBOV disease, resulted in a bias in the predominant belief about the protective mechanism to EBOV towards cell-mediated immunity. As a result, the development of an antibody-based therapy against EBOV received only limited attention and modest interest levels (Qiu and Kobinger 2014).

Monoclonal antibodies specific for EBOV GP has already been developed previously by our research group. Briefly, BALB/c mice were immunized with IP

administration of 10^7 PFU of VSVΔG/EBOVGP, with three identical boosters subsequently given at 4 week intervals, and a final boost with 20 μg of EBOV VLPs 3-4 days before fusion of mouse splenocytes with SP2/0 myeloma cells (Qiu, Alimonti et al. 2011). Individual hybridomas were then obtained by limiting dilution and supernatants were screened for reactivity to GP by an indirect ELISA using EBOV VLPs as a capture antigen, or by an immunofluorescence assay (IFA) using 293T cells transfected with a plasmid expressing EBOV GP (Qiu, Alimonti et al. 2011). Eight murine mAbs (1H3, 2G4, 4G7, 5D2, 5E6, 7C9, 7G4 and 10C8) were generated using this method, and by using different GP variants and mutants as the ELISA capture antigen, the different binding locations for the mAbs were identified (Qiu, Alimonti et al. 2011). Specific epitopes for 1H3, 2G4 and 4G7 are shown below (Figure 5.1A and B), where mAb 1H3 binds to sGP, 2G4 binds to GP2, and 4G7 binds to the C-terminal portion of GP1. The GP-specific mAbs are not cross-reactive with MARV or other Ebola species, but did specifically recognize other variants of EBOV.

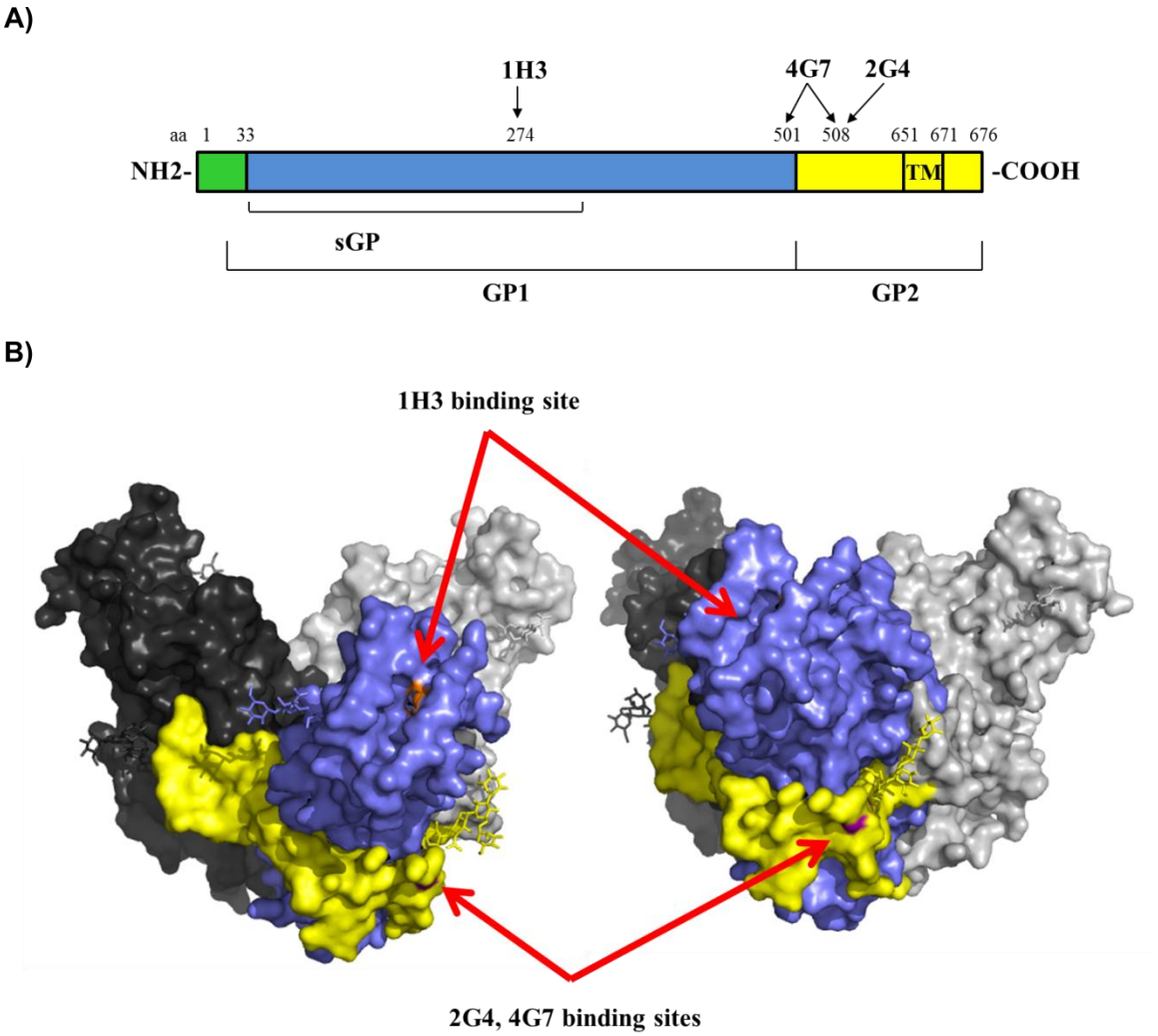

Figure 5.1. Location of binding sites by monoclonal antibodies 1H3, 2G4 and 4G7 on EBOV GP. (A) schematic view and (B) 3D view of the GP trimer.

The mAbs were then screened for protective efficacy in mice and guinea pigs against challenge with MA-EBOV and GA-EBOV, respectively. In mice, an IP injection of 100 μg 1H3, 2G4, 4G7, 5D2, 5E6, 7C9, 7G4 or 10C8 at 1 dpi is sufficient for providing at least partial protection (between 40-100%), with significant delays in the average time to death of all treated non-survivor animals (Qiu, Fernando et al. 2012). Partial protection was also observed when the same dose of mAbs was given instead at 2 dpi, and was more effective when administered as a post-exposure intervention as opposed to a prophylactic (Qiu, Fernando et al. 2012). In guinea pigs, an IP injection of 5 mg with the individual mAbs at 1 dpi was not as protective, with only 2G4 and 4G7 treatments resulting in 60% survival. However, all mAbs demonstrated a significant increase in the average time to death, with 1H3 providing the best results. On this basis, the murine 1H3, 2G4 and 4G7 (hereafter referred to as ZMAb) were combined for further testing in guinea pigs. Administration of ZMAb totaling 5mg per animal resulted in complete survival when given at 2 dpi, with partial survival observed when treated at 3 dpi (Qiu, Fernando et al. 2012).

Based on the success of this combination therapy in guinea pigs, the next step was to test the efficacy of ZMAb in the NHP animal model, which constitutes the premise of the results presented in this thesis chapter. Cynomolgus macaques (n=4 per group) were treated with three identical IV doses of 25 mg/kg ZMAb spaced three days apart, beginning at 1 (Group A) or 2 dpi (Group B) with 1000 PFU of EBOV. The dose at 25 mg/kg was chosen because the accepted human dose for clinical use is between 25 to 50 mg/kg (Qiu, Audet et al. 2012). A control NHP (n=1) was treated with an identical regiments of PBS starting at 1 dpi. In addition to survival, NHPs were assessed daily for

detectable clinical manifestations such as weight and temperature changes, as well as selected blood cell counts and blood biochemistry parameters, and viral shedding by RT-qPCR and $TCID_{50}$ on treatment and sample days (Figure 5.2). Humoural immune responses were monitored by IgM and IgG ELISAs, as well as nAb assays on treatment and sample days. Cell-mediated immune responses were monitored by IFN-γ ELISpot and FACS at 21 dpi. It was expected that administration of ZMAb will be able to confer at least partial post-exposure protection to NHPs from EBOV disease. A corresponding decrease and delayed onset of EBOV-related clinical symptoms will be observed, in addition to the induction of robust specific immune responses in survivors.

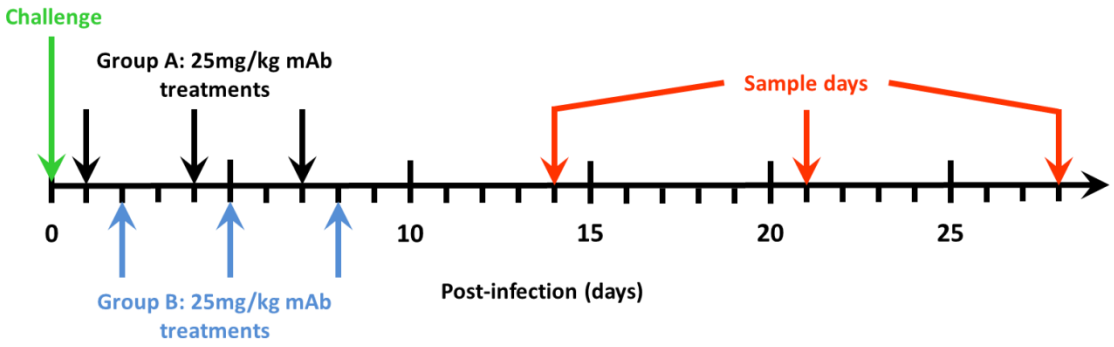

Figure 5.2. Timeline of the ZMAb treatment regimens in NHPs. Groups of four cynomolgus macaques were given three identical ZMAb treatments at the indicated times post-exposure. Major events over the course of the experiment are indicated by the arrows on the timeline.

5.2 Results

5.2.1 Survival and clinical observations

Survival was observed in both treatment groups, with a delayed time to death in all non-survivors compared to the control NHP. All animals from Group A (A1 to A4)

survived, whereas 2 of 4 Group B (B1 and B4) macaques were protected from infection. Non-surviving animals B2 and B3 were euthanized at 8 and 11 dpi, respectively, due to the severity of EBOV disease. The PBS-treated control animal (C1) was euthanized on day 5 due to similar concerns (Figure 5.3). Symptoms indicative of typical EBOV infections in NHPs were observed with all infected animals between 4-5 and 14 dpi. Increasingly severe clinical findings indicative of disease progression were spotted in moribund NHPs, in contrast to full recovery by 28 dpi in convalescent animals at the termination of the experiment. Animals treated with ZMAb beginning at 1 dpi showed less severe clinical signs as a group compared with ZMAb-treated NHPs starting at 2 dpi (Table 2). Specific clinical features in EBOV-infected NHPs include anorexia leading to weight loss (Figure 5.4A), inflammation leading to fever (Figure 5.4B), decreased activity and behavioural changes, and signs of cutaneous hemorrhage, such as petechiae and rash. These features are combined into a total clinical score, which estimates disease severity (Figure 5.4C). Other measured parameters include levels of the liver enzymes alanine aminotransferase (ALT) (Figure 5.4D) and alkaline phosphatase (ALP) (Figure 5.4E) along with levels of albumin (ALB), total bilirubin (TBIL), blood urea nitrogen (BUN), phosphate (PHOS), globulin (GLOB) and glucose (GLU), in addition to leukocytopenia/leukocytosis and thrombocytopenia/thrombocytosis (Figure 5.4F).

The hematology and blood biochemistry profiles of most surviving animals remain mostly constant throughout the experiments, with the exception of a transient rise in platelet counts between 7 and 21 dpi in all NHPs except for A1. In contrast, nonsurvivors demonstrated noticeable changes by 4-5 dpi including leukocytopenia, thrombocytopenia and elevated ALT and ALP levels, which are indicative of

hematologic and liver dysfunction due to the progression of EBOV disease (Ryabchikova, Kolesnikova et al. 1999). Clinical scores remained low for all surviving animals throughout the experiment with the exception of A4 and B4, which showed signs of EBOV disease, including reduced activity as well as lowered food and water intake leading to weight loss. However, the clinical scores for A4 and B4 dropped to zero by 28 dpi, indicating full recovery from EBOV disease.

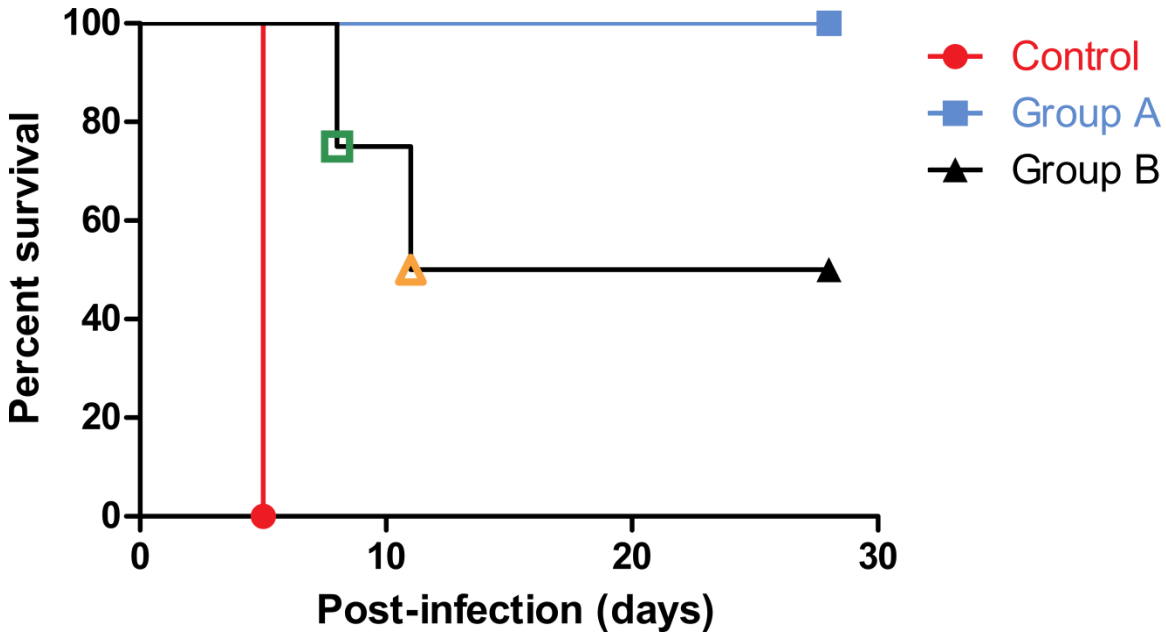

Figure 5.3. ZMAb provides post-exposure protection to EBOV-infected NHPs. Group A animals were given three 25 mg/kg doses of ZMAb starting at 1 dpi, and Group B animals were given the same treatment starting at 2 dpi. A control animal was treated with PBS starting at 1 dpi.

Table 5.1. Clinical findings of EBOV-infected NHPs from 1 to 28 dpi. Fever was defined as >1.0°C higher than baseline. Mild rash was defined as focal areas of petechiae covering <10% of the skin. Leukocytopenia and thrombocytopenia were defined as a >30% decrease in the numbers of WBCs and platelets, respectively. Leukocytosis and thrombocytosis were defined as a twofold or greater increase in numbers of WBCs and platelets above baseline, where WBC counts are greater than 11.0 x 10^3 cells/mm^3. ↑, two- to threefold increase; ↑↑, four- to fivefold increase; ↑↑↑, greater than fivefold increase; ↓, two- to threefold decrease; ↓↓, four- to fivefold decrease; ↓↓↓, greater than fivefold decrease. ALB, albumin; ALP, alkaline phosphatase; ALT, alanine aminotransferase; TBIL, total bilirubin; BUN, blood urea nitrogen; PHOS, phosphate; GLOB, globulin; GLU, glucose.

Animal ID	Treatment	Clinical findings	Outcome
A1	25mg/kg ZMAb starting at 1 dpi	Leukocytosis (7-8, 14 dpi), Thrombocytopenia (14 dpi)	Survived
A2	25mg/kg ZMAb starting at 1 dpi	Fever (4-5 dpi), Thrombocytosis (7-8, 14 dpi), GLU↑ (7-8 dpi)	Survived
A3	25mg/kg ZMAb starting at 1 dpi	Fever (7-8 dpi), Leukocytosis (7-8 dpi), Thrombocytosis (14 dpi), TBIL↑ (7-8 dpi), GLOB↑ (7-8, 14 dpi)	Survived
A4	25mg/kg ZMAb starting at 1 dpi	Fever (7-8 dpi), Leukocytopenia (4-5 dpi), Thrombocytosis (14 dpi), ALP↑ (7-8, 14 dpi), ALT↑ (14 dpi)	Survived
B1	25mg/kg ZMAb starting at 2 dpi	Fever (4-5, 7-8 dpi), Leukocytosis (7-8 dpi), Thrombocytopenia (7-8 dpi), Thrombocytosis (14 dpi), TBIL↑ (7-8 dpi), GLOB↑ (7-8, 14 dpi)	Survived
B2	25mg/kg ZMAb starting at 2 dpi	Fever (4-5, 7-8 dpi), Leukocytopenia (7-8 dpi), Mild rash (7-8 dpi), Anorexia (7-8 dpi), ALP↑ (14 dpi), ALT↑ (14 dpi), GLOB↑ (14 dpi)	Dead, 8 dpi
B3	25mg/kg ZMAb starting at 2 dpi	Fever (7-8, 11 dpi), Leukocytosis (4-5, 7-8, 11 dpi), Thrombocytopenia (7-8, 11 dpi), Anorexia (7-8, 11 dpi), ALP↑ (7-8 dpi) ↑↑↑ (11 dpi), ALT↑ (7-8 dpi) ↑↑↑ (11 dpi), TBIL↑ (7-8, 11 dpi), BUN↑ (7-8, 11 dpi), GLOB↑ (7-8, 11 dpi), GLU↑ (11 dpi)	Died, 11 dpi
B4	25mg/kg ZMAb starting at 2 dpi	Leukocytosis (14 dpi), Thrombocytopenia (7-8 dpi), Thrombocytosis (14 dpi), ALP↑ (7-8 dpi)	Survived
C1	PBS control starting at 1 dpi	Fever (4-5 dpi), Leukocytosis (4-5 dpi), Anorexia (4-5 dpi), ALP↑ (4-5 dpi), ALT↑ (4-5 dpi), BUN↑ (4-5 dpi)	Died, 5 dpi

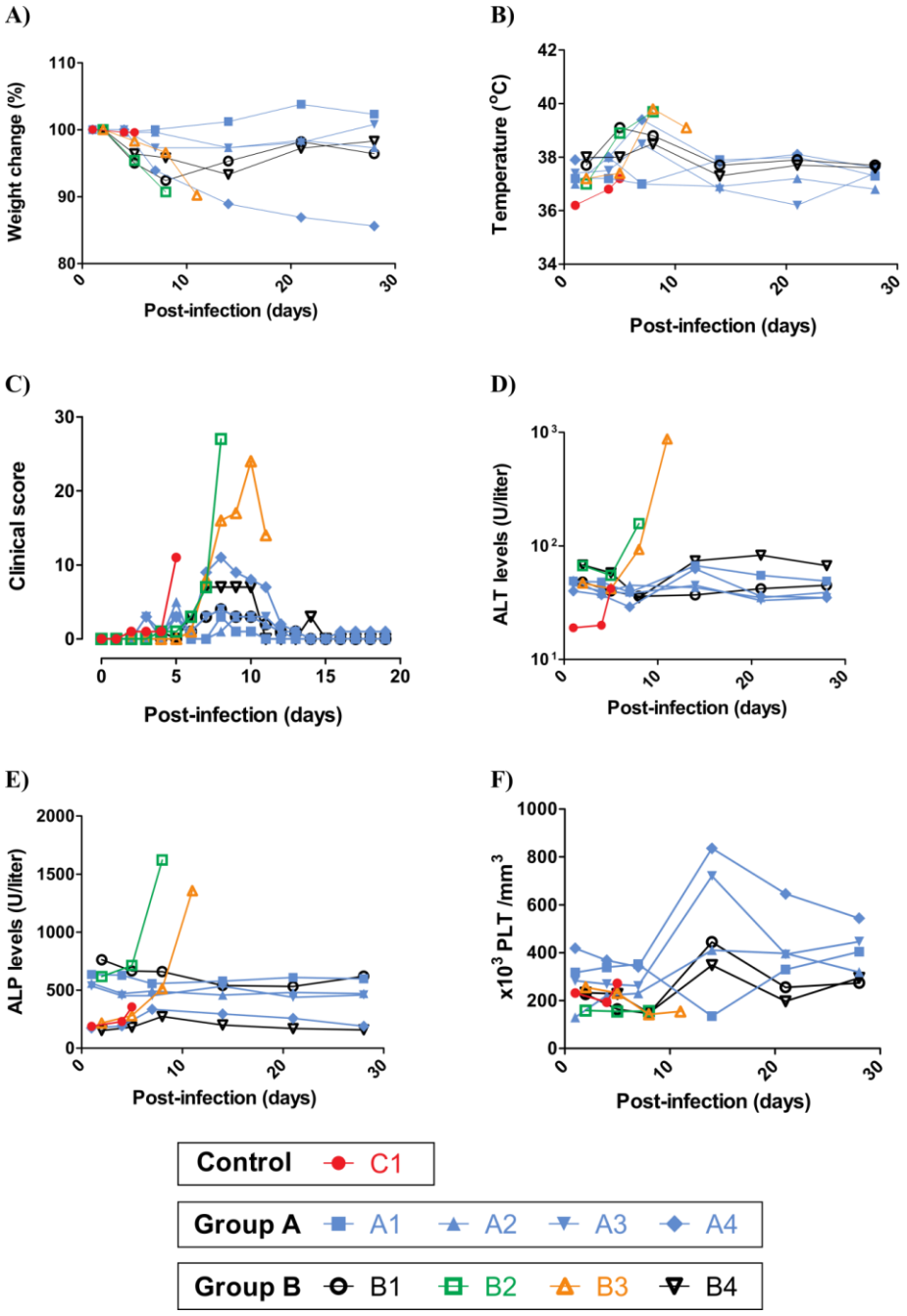

Figure 5.4. Moribund NHPs exhibit clinical symptoms consistent with that of EBOV disease. Clinical overview of NHPs after challenge, with selected parameters presented. (A) Weight change was expressed as a percentage change from baseline values taken at 1 dpi (for Group A and C NHPs) or 2 dpi (for Group B NHPs). (B) Rectal temperatures measured during sample and treatment days. (C) Clinical scores as an estimate for disease severity. Animals were evaluated daily and results up to 19 dpi were presented. Changes in selected blood biochemistry and hematological parameters were measured: (D) alanine aminotransferase (ALT), (E) alkaline phosphatase (ALP), and (F) platelet counts.

5.2.2 Viremia and escape mutations in ZMAb-treated, EBOV-infected animals

Levels of EBOV were first measured by real-time reverse transcription–polymerase chain reaction (RT-qPCR) from the blood of all NHPs. With the exception of A2, EBOV RNA was detected in all other animals (Figure 5.5A). The PBS-treated NHP C1 had explosive viral growth as determined by RT-qPCR, with levels reaching ~10^7 and ~10^8 genome equivalents (GEQ) per mL of blood by 4 and 5 dpi, respectively, which was confirmed by the presence of live virus at ~10^5 and ~10^7 $TCID_{50}$ at 4 and 5 dpi, as determined by $TCID_{50}$ (Figure 5.5B). In the Group A animals, lowered EBOV viremia was observed compared to the PBS control. RNA was detectable in animals A1, A3 and A4 at 7 dpi between ~10^3 and ~10^4 GEQ/mL of blood, but live virus was only detected in animal A1 at the same time point at ~10^2 $TCID_{50}$. Regardless, EBOV was undetectable in these animals by 14 dpi (Figures 5.5A and B). In the Group B animals, lowered EBOV viremia was also observed in survivors compared to the PBS control. RNA was detected between ~10^2 and ~10^3 GEQ/mL of blood starting at 5 dpi, peaking at 7 dpi for B1 and B4 and eventually dropping to undetectable levels by 28 dpi, whereas live virus was detected in B1 between ~10^2 and ~10^3 $TCID_{50}$ before decreasing to undetectable levels by 14 dpi (Figures 5.5A and B). For animal B2, increased viremia was detected at 8 dpi at ~10^8 GEQ/mL of blood and ~10^5 $TCID_{50}$, several logs higher than the survival animals within its treatment group suggesting that ZMAb treatment was ineffective for this animal (Figures 5.5A and B). Increased viremia was also observed in B3 at 8 dpi, with RNA detected at ~10^4 GEQ/mL of blood and live virus at ~10^3 $TCID_{50}$. Treatment with ZMAb was unable to reduce viremia for this animal, with RNA detected between ~10^4 to ~10^5 GEQ/mL of blood and live EBOV at ~10^4 $TCID_{50}$ at 11 dpi, the time of euthanasia for this animal (Figures 5.5A and B). However, B3 was terminated for humane reasons because of hind limb paralysis. Despite increased viremia as well

as hematological and blood biochemistry changes, the clinical score was improving due to a drop in fever and the resumption of eating and drinking by the animal (Figure 5.4).

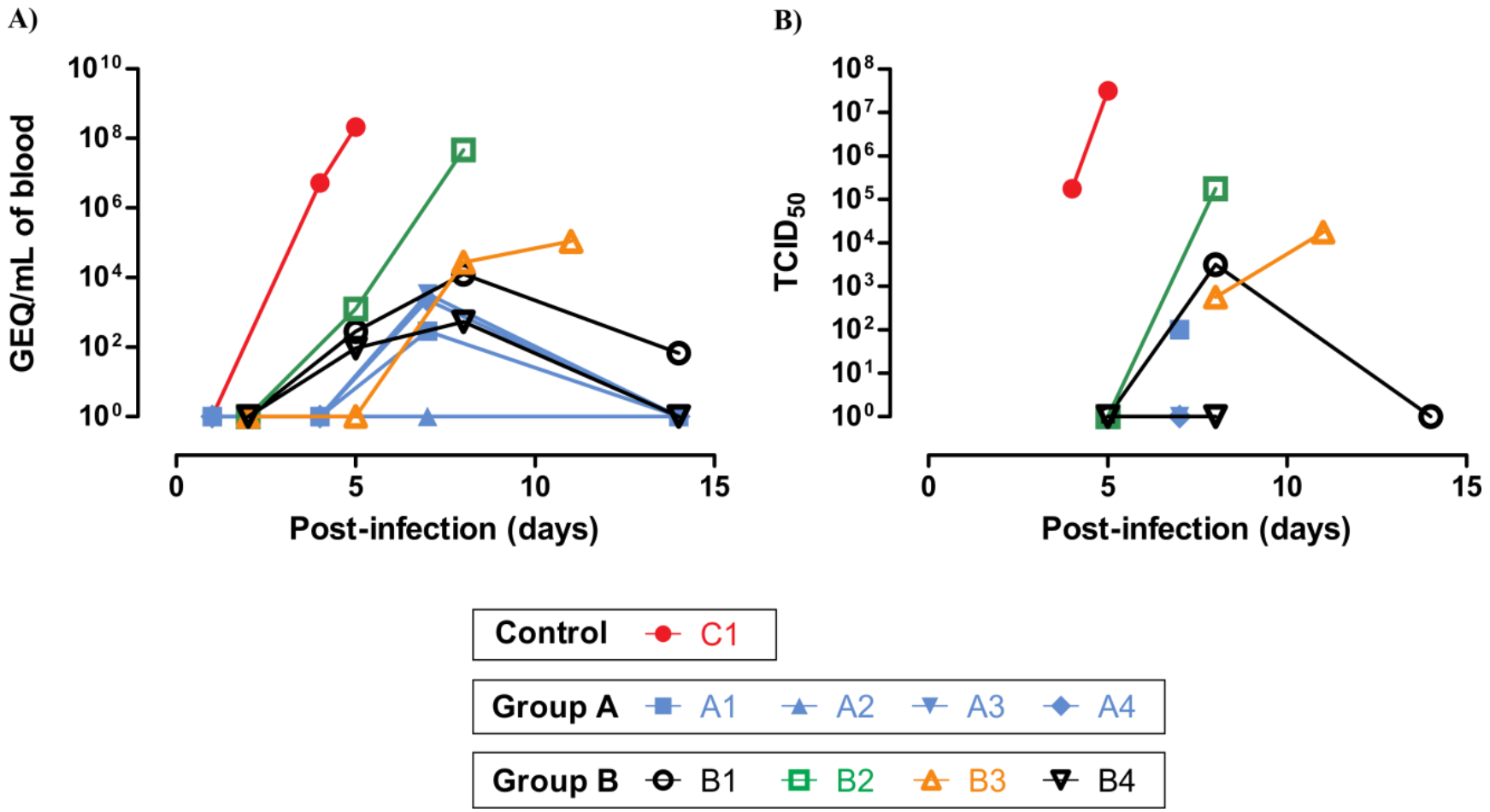

Figure 5.5. Survivor NHPs demonstrate better ability to control EBOV viremia compared to non-surviving animals. EBOV viremia of various NHPs at specified time points after challenge. Titers were either detected by (A) RT-qPCR or (B) live virus titration and were expressed as genome equivalents (GEQ) per mL of blood or $TCID_{50}$, respectively. Only samples positive by PCR were assayed for levels of live virus.

To determine whether ZMAb-treated nonsurvivors B2 and B3 succumbed to EBOV infection due to the presence of escape mutations, EBOV RNA was extracted from blood on the euthanasia dates for both animals and subjected to sequence analysis. Comparison of B2 and B3 sequences with the challenge virus sequence found that the virus isolated from B2 contained two mutations located at amino acids 275 (W275L) and 508 (Q508R) of EBOV GP (Figures 5.6A and B), which likely abolishes the efficacy of ZMAb since all three mAb components in ZMAb is directed towards these two epitopes. These mutations were not found in any other natural EBOV isolates available on GenBank. Interestingly, escape mutants were not detected in animal B3.

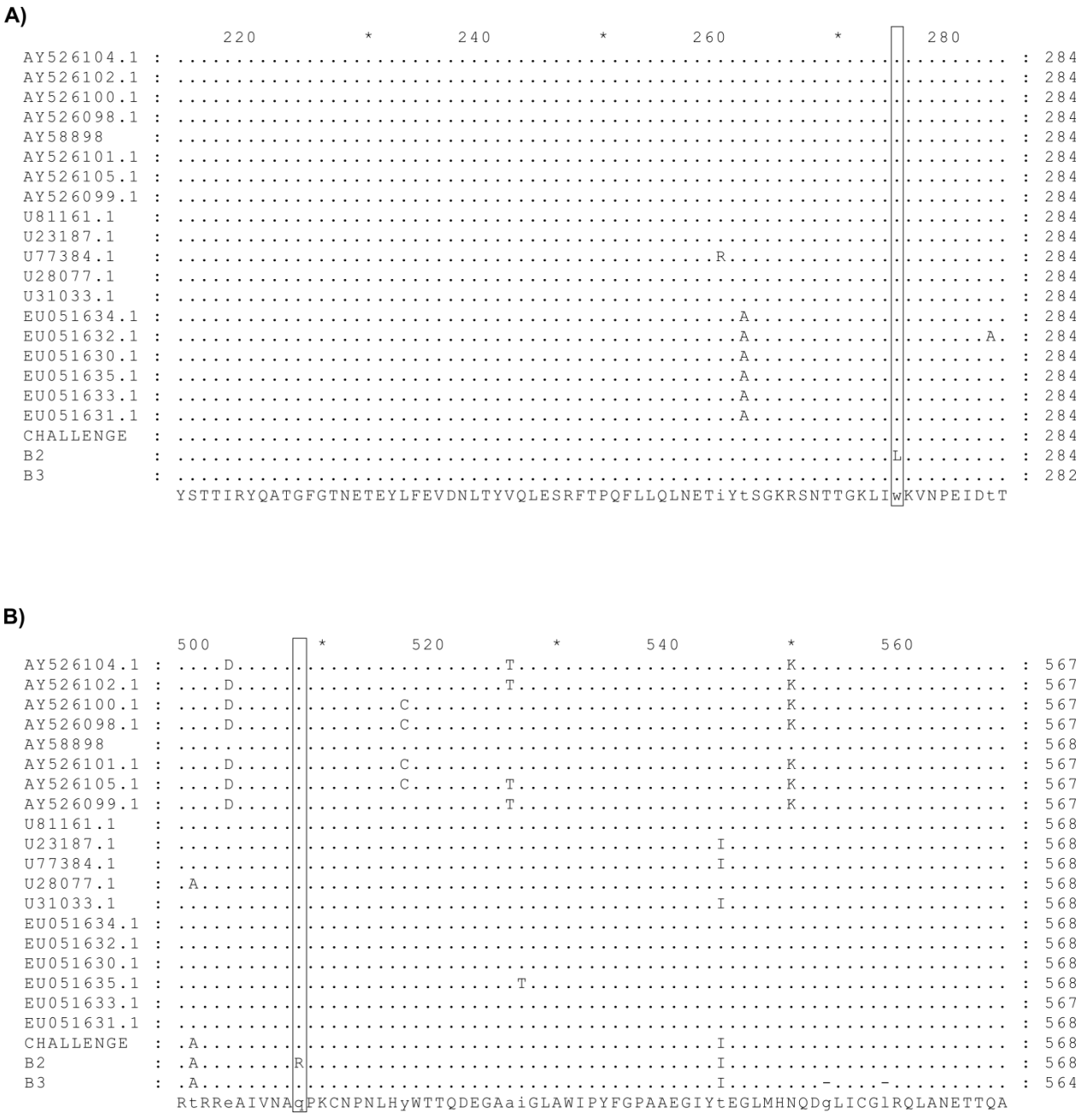

Figure 5.6. Escape mutations were detected from one of two non-surviving NHPs. Sequences isolated from animal B2 and B3 at the time of euthanasia were sequenced and compared to the challenge virus in addition to available EBOV sequences available on GenBank, aligned using the Clustal W algorithm. Alignment of amino acid sequences are shown around positions (A) 275 and (B) 508.

5.2.3 EBOV–specific B-cell responses

Immune responses were monitored after challenge to determine whether ZMAb is able to control EBOV replication long enough for the animals to mount a robust, protective immune response leading to survival. The humoural immune response was characterized by measuring total GP-specific IgM and IgG, as well as neutralizing antibody levels. Although neutralizing antibody activity is attributed to both ZMAb and endogenous antibodies produced in response to infection, IgM and IgG measurements were specifically targeted to endogenous antibody responses produced by the cynomolgus macaques, by using a secondary antibody specific for NHP IgM or IgG.

IgM specific to EBOV GP were detected early in all surviving animals between ~10^3 and ~10^5 reciprocal dilutions, starting between 5 to 7 dpi and remained at constant levels in all survivors up to 28 dpi (Figure 5.7A). B2 had IgM levels comparable to surviving NHPs at 5 and 8 dpi, whereas those for B3 were below the assay detection limit. Variable levels of GP-specific IgG were detected between 8 to 21 dpi in all surviving animals, increasing over time and peaking between ~10^3 and ~10^5 reciprocal dilutions at 28 dpi. In contrast, IgG levels were below the detection limit in animal B2, but found in B3 at comparable levels to surviving animals at 8 and 11 dpi (Figure 5.7B). IgM and IgG titers were also below the threshold of detection for C1.

Levels of neutralizing antibodies peaked at 7 dpi and were generally between 10 and 150 reciprocal dilutions for all animals in this study, with the exception of A4, which had over 400 reciprocal dilutions but returned to undetectable levels by 14 to 21 dpi (Figure 5.7C). The levels of neutralizing antibodies were higher for surviving animals over moribund NHPs (Figure 5.7C). The presence of neutralizing antibodies was not detected for animal C1. While this assay cannot distinguish the difference between the neutralizing activities of antibodies produced by NHPs

versus exogenous ZMAb, EBOV-specific neutralizing antibodies produced by the immune response should be increasing throughout the experiment. The decrease observed in neutralizing antibody titers by 14 to 21 dpi suggests that ZMAb was responsible for providing the majority of antibodies with neutralizing activity. The half-life of ZMAb in cynomolgus macaques has not yet been determined. However, it can been observed from these results that all surviving animals possess a complete IgM and IgG response in addition to elevated neutralizing antibody levels, whereas in the non-survivors B2 lacked a IgG response, B3 lacked a IgM response and both animals demonstrated lowered levels of neutralizing antibodies, suggesting that humoural immunity in these animals is not sufficiently robust for survival.

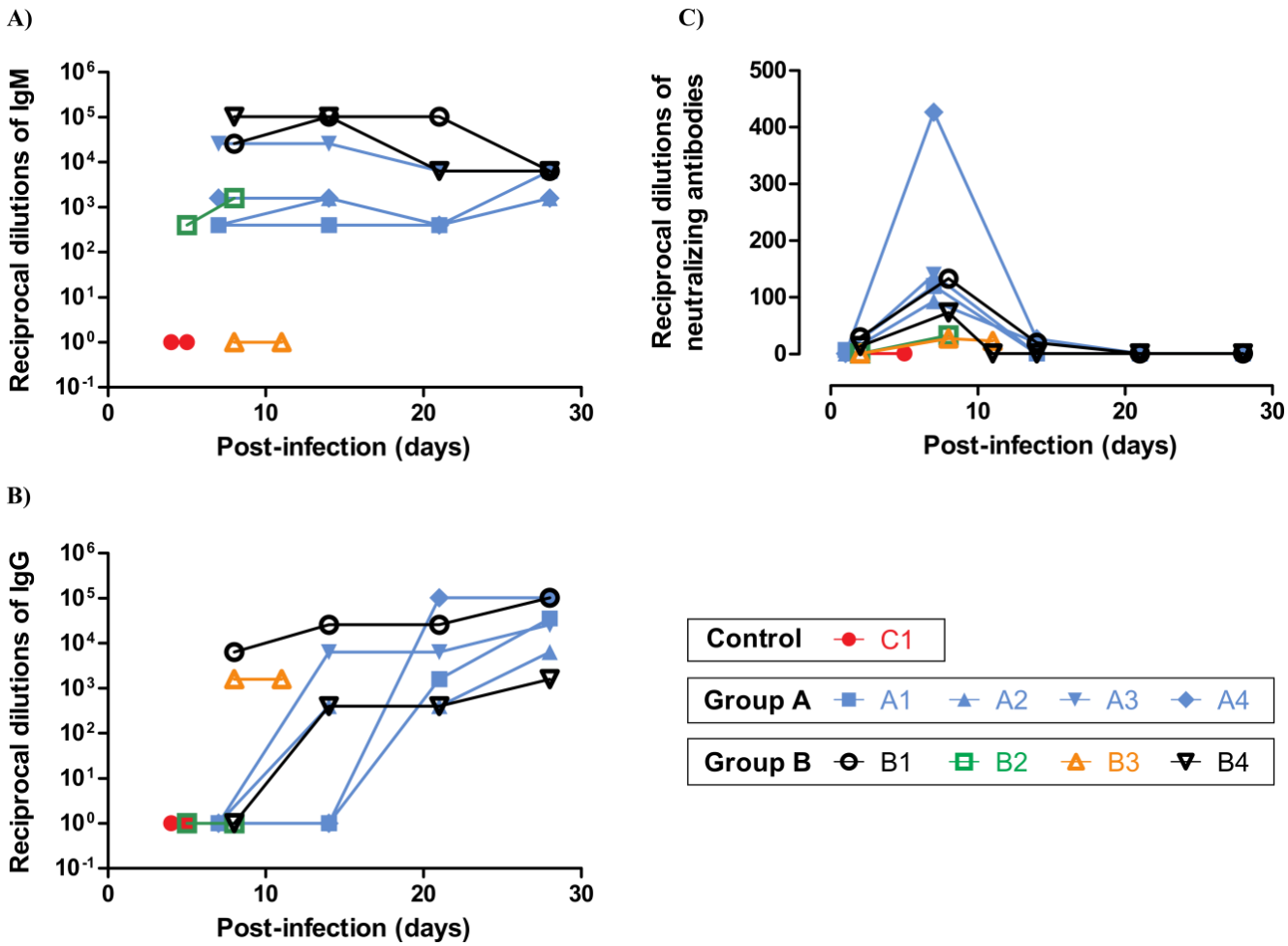

Figure 5.7. Specific IgG and IgM antibody responses were detected in all surviving NHPs. Humoural immune responses in cynomolgus macaques were measured at various times after EBOV challenge. (A) Total GP-specific IgM and (B) IgG levels as well as (C) EBOV-specific neutralizing antibodies are reported as reciprocal dilutions.

5.2.4 EBOV-specific T-cell responses

The cellular immune response was characterized by two different methods after isolation of peripheral blood mononuclear cells (PBMCs) from survivors at 21 dpi. This day was favoured over earlier time points for T-cell assays because a larger volume of blood (up to 10 mL) is required to perform these assays. Furthermore, due to lymphocyte apoptosis as a result of EBOV disease, it is often difficult to isolate a sufficient number of PBMCs early after infection, and the process of anaesthetizing these animals for a large blood draw between 10 and 14 dpi may negatively impact NHP survival. The number of GP-specific IFN-γ producing cells was first measured by IFN-γ ELISpot after stimulation of isolated PBMCs with four different peptide pools spanning the entire EBOV GP antigen. In order to determine whether the production of IFN-γ can be attributed to $CD4^+$ and $CD8^+$ T-cells, a flow cytometric intracellular cytokine staining assay was carried out.

The ELISpot assay showed that IFN-γ–secreting cells in PBMCs can be stimulated by GP peptide *in vitro* in all animals except for A4 (Figure 5.8A). PBMCs responded to stimulation with all four peptide pools in three of four Group A animals, however the predominant response was to pool 3 (amino acids 347 to 495), followed by pool 2 (amino acids 180 to 347). Group B animals responded predominantly to pools 2 and 4 (amino acids 496 to 679), with a slightly weaker response to pool 3 (Figure 5.8A). Analysis by flow cytometry revealed that different immune cell subpopulations were responsible for the synthesis of observed IFN-γ (Figure 5.8B). It was shown that the IFN-γ response in animals A1 and A2 were secreted predominantly by $CD8^+$ T-cells, whereas A3 and B1 demonstrated a greater percentage of $CD4^+$ T-cells secreting IFN-γ. $CD4^+$ and $CD8^+$ T-cells producing IFN-γ were both detected in NHP B4, whereas A4 was characterized by the absence of an IFN-γ response (Figure 5.8B). The overall $CD8^+$

mediated IFN-γ response was broad in nature, as demonstrated by PBMCs responding to all four peptide pools in all NHPs except A4. Peptide pools 3 and 4 prompted the greatest percentage of double-positive $CD8^+$ IFN-γ^+ cells (Figure 5.8C). The overall $CD4^+$ mediated IFN-γ response was also broad in nature since these cells also responded to stimulation with all four peptide pools, however none of the pools can be considered immunodominant (Figure 5.8D).

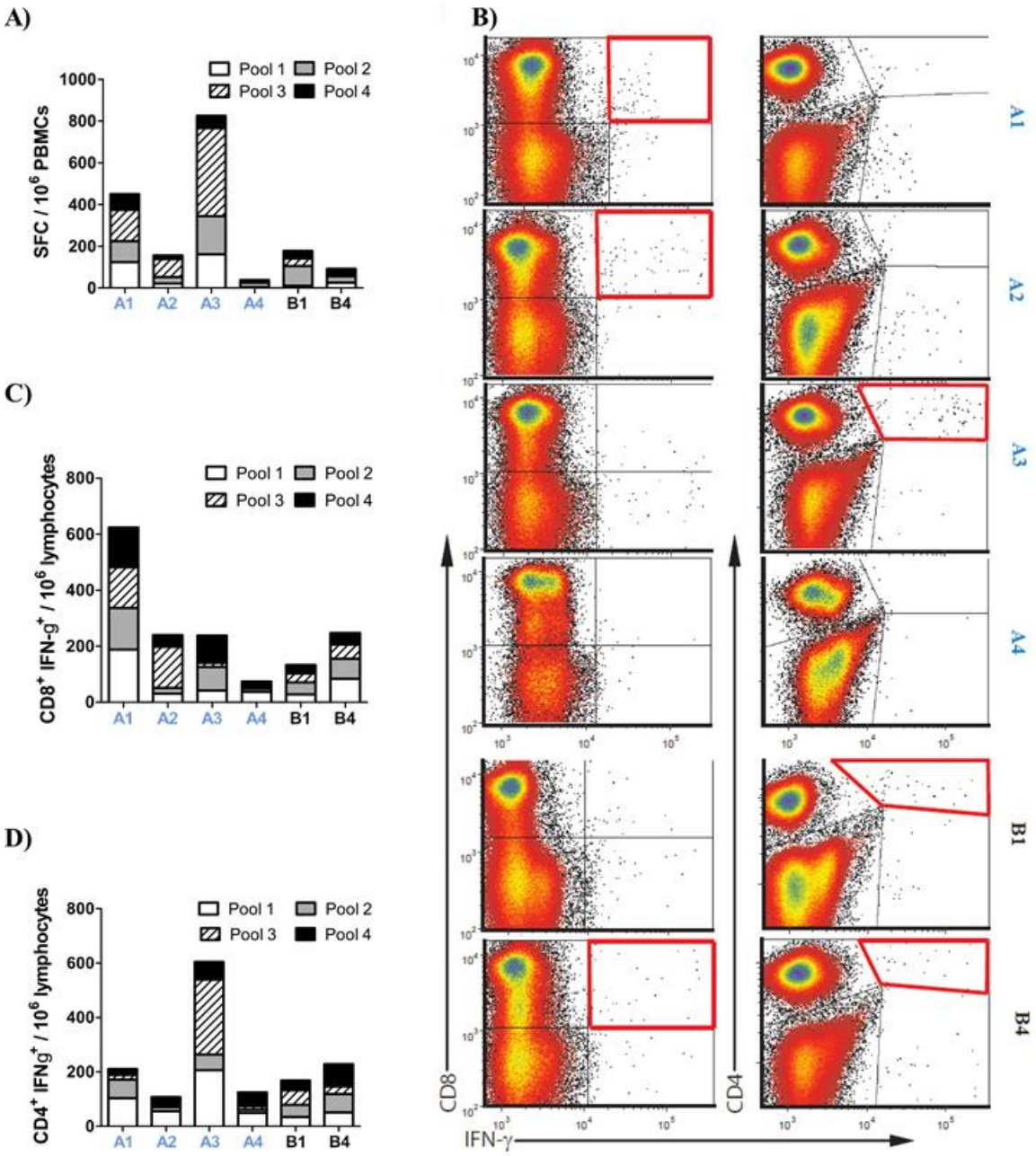

Figure 5.8. Specific T-cell responses were detected in 5 of 6 surviving NHPs. Cell-mediated immune response in cynomolgus macaques measured 21 days after EBOV challenge. PBMCs from surviving animals were isolated and stimulated to four different peptide pools of EBOV GP. (A) The number of IFN-γ secreting cells per million PBMCs as determined by ELISpot; (B) Sample density plot gated for $CD8^+$ or $CD4^+$ lymphocytes producing IFN-γ as determined by FACS after stimulation with peptide pool 3. The graphical representation of total (C) $CD8^+$ IFN-γ^+ and (D) $CD4^+$ IFN-γ^+ responses after stimulation by all four GP peptide pools as determined by FACS.

IL-2 is another important cytokine for the cell-mediated immune response during its amplification phase. It was found to be strongly induced in response to VSVΔG/EBOVGP vaccinated mice in a previous study (Qiu, Fernando et al. 2011). The percentage of $CD4^+$ and $CD8^+$ T-cells expressing IL-2, IFN-γ, or both were measured by the intracellular cytokine staining assay. It was found that the majority of IL-2 was secreted by $CD4^+$ T-cells, although a minority of $CD8^+$ $IL\text{-}2^+$ cells do exist (Figure 5.9A). In contrast, IFN-γ expression was found more equally split amongst both $CD4^+$ and $CD8^+$ cells and seems to be dependent on the animal in question (Figure 5.9B). The percentage of $CD8^+$ $IFN\text{-}\gamma^+$ and $CD4^+$ $IFN\text{-}\gamma^+$ cells also producing IL-2 was below 30% for CD8, and greater than 73% for CD4 T-cells. With the exception of A4, there is a strong GP–specific cell-mediated immune response at 21 dpi in the survivors.

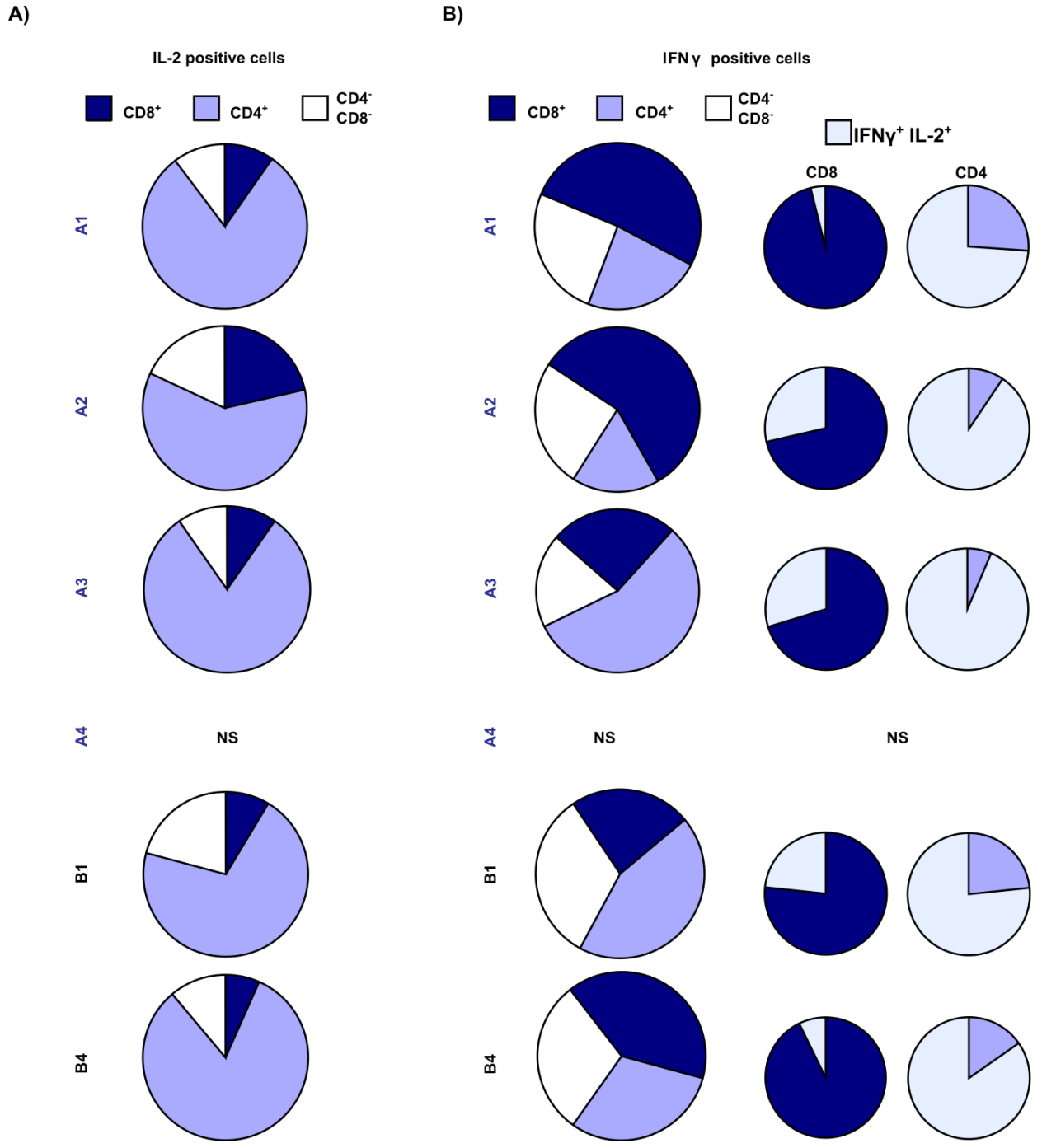

Figure 5.9. IL-2 and IFN-γ secreting T-cells were detected in 5 of 6 surviving NHPs. Characterization of IL-2 and IFN-γ producing cells after stimulation of EBOV GP peptide pools *in vitro*, 21 days after EBOV challenge. PBMCs were stimulated with all four GP peptide pools and added together. The relative distribution of (A) IL-2^+ and (B) IFN-γ^+ secreting cells is displayed for $CD4^+$, $CD8^+$ and $CD4^-$ $CD8^-$ cells. The smaller circles represent the relative proportion of IL-2^+ IFN-γ^+ (lighter shade) versus IFN-γ^+ (darker shade) secreting $CD4^+$ and $CD8^+$ T-cells.

5.3 Discussion

The results presented in this thesis chapter demonstrate that treatment with a cocktail comprised of three murine-derived neutralizing mAbs specific for EBOV GP can provide 100% or 50% protection when given at 1 or 2 dpi, respectively. The treated survivors had lowered virus loads and milder clinical symptoms compared to moribund NHPs. Furthermore, surviving animals had hematology and blood biochemistry parameters that were largely within the normal range, highlighting the effectiveness of ZMAb in preventing morbidity, a desired feature of any candidate therapeutic intervention. Surviving animals given ZMAb were able to mount a detectable GP–specific humoral and/or cell-mediated immune response, and most likely the treatment was able to sufficiently delay and reduce EBOV replication in order for the host immune response to develop.

A previous attempt at developing a treatment protocol with the mAb KZ52 (Oswald, Geisbert et al. 2007) against EBOV infection had failed to save macaques lethally infected with EBOV. Several factors may have played a role in this failure. First, the KZ52 study used rhesus macaques, whereas the ZMAb study used cynomolgus macaques, which raise the possibility of interspecies differences having an impact on survival. However, when comparing the efficacy of ZMAb and KZ52 within an identical guinea pig model, ZMAb was more efficacious than KZ52. ZMAb treatment is able to provide complete protection when given as late as 2 dpi, compared with 1 hour after challenge for KZ52. Furthermore, the onset of disease in control cynomolgus macaques infected with EBOV is fairly rapid compared to control rhesus macaques (Bente, Gren et al. 2009). Therefore, cynomolgus macaques succumb to disease earlier than their rhesus counterparts, making successful intervention against EBOV disease a more difficult task in cynomolgus macaques. Notably, the KZ52 study used a dose of 50 mg/kg, compared to ZMAb,

which used 8.3 mg/kg of each mAb per dose, or 25 mg/kg in total. The combination of these factors suggests that the ZMAb is likely more efficacious than KZ52, and improved protection may be possible in rhesus macaques when delivered as late as 2 dpi. Second, the mAbs comprising ZMAb and KZ52 are of different isotypes. ZMAb antibodies are mouse IgG2a,κ and IgG2b,κ isotypes, whereas KZ52 is human IgG1. While mouse isotypes can bind human Fc receptors, there may be a difference in the half-life between ZMAb and KZ52 in the NHP animal model. The half-life of KZ52 was revealed to be 7 days (Parren, Geisbert et al. 2002), whereas the ZMAb half-life is currently unknown. Further studies are needed to determine whether there are any functional differences between the two antibody treatment protocols. Finally, ZMAb is composed of three distinct antibodies, which recognize three different areas of GP, whereas KZ52 only recognizes one epitope. Therefore, the increased efficacy may have been observed due to less competition for available GP epitopes.

While mAbs constitute a practical option that could potentially be used in future outbreaks and especially in case of accidental laboratory exposures, this approach also has its own limitations. While extremely effective at targeting specific epitopes, mutations of those target regions will at least reduce and likely abolish treatment efficacy, as observed with animal B2 in this study. In this event, new GP-specific antibodies will need to be generated, which adds to the time and cost compared with other post-exposure treatment options. To minimize the risk of escape mutants, several efficacious mAb combinations should be developed and tested as alternate options, and outbreak viruses need to be closely monitored to detect mutations as soon as possible. Another issue at hand is serum sickness; it will be important to determine the highest levels of mAbs that can be safely administered to patients without compromising efficacy.

The results presented in this thesis chapter highlight the use of antibodies to control EBOV replication in NHPs resulting in survival, and demonstrate that antibodies alone are required and sufficient for protection against EBOV infection. Furthermore, this study supports the idea that antibodies are a mechanistic correlate of protection against EBOV disease, and can be used to predict as well as confer protection to recipients in the event of EBOV exposure. This study failed to correlate the T-cell response with clinical outcome, as animal A4 survived infection despite the lack of specific cellular responses. However, A4 did have a strong antibody response, which reinforces the hypothesis that antibodies can be used as a reliable marker of protection. Indeed, amongst the non-surviving NHPs (B2 and B3), an incomplete antibody response was observed as noted by the absence of at least one antibody isotype (IgM or IgG). These results also contradict the findings from an earlier report, which showed that the depletion of $CD8^+$ T-cells of Ad5-GP vaccinated NHPs before challenge reduced survival rates (Sullivan, Hensley et al. 2011), however it should be mentioned that in the non-surviving animals from that study also had poor $CD4^+$ T-cell activation levels before the depletion, suggesting an impaired Th2 immune response. Interestingly, the sole survivor NHP from the $CD8^+$ T-cell depleted group demonstrated the highest levels of $CD4^+$ T-cell responses (Sullivan, Hensley et al. 2011). Furthermore, the depletion antibody used in that study (cM-T807) is known to also deplete natural killer cells *in vivo* (Gaufin, Ribeiro et al. 2010) (Van Rompay, Blackwood et al. 2006), which may impact the efficacy of GP-specific antibodies if their mechanism of action is dependent on antibody-dependent cellular cytotoxicity.

The successful treatment of NHPs by mAb therapy was substantiated by the findings of two other research groups, which were also able to demonstrate protection from EBOV disease using mAbs. In the first study, rhesus macaques were treated using a mixture of two human-

mouse chimeric mAbs (ch133 and ch226) that demonstrated strong neutralizing activity *in vitro* against EBOV. NHPs (n=3) were administered three IV doses of 50 mg mAb mixture per animal at 24 hours before challenge, as well as 1 and 3 dpi. One of three NHPs survived challenge with no clinical symptoms and reduced viremia, and a significant decrease of circulating mAb levels was observed in the two non-survivors with a concomitant increase in viral load (Marzi, Yoshida et al. 2012).

In the second study, the researchers administered a cocktail of three anti-EBOV human-mouse chimeric (c) or humanized (h) mAbs (c13C6, h13F6, and c6D8, called MB-003) to rhesus macaques. The chimeric mAbs were initially raised in mice immunized with VEEV-GP, and then produced in large amounts in the tobacco plant, *Nicotiana benthamiana*. The rationale behind mAb production in plants is twofold. The first is that plant-derived proteins can be inexpensively produced on an industrial scale, which is important for antibody therapies as the high cost of production is currently the main limiting factor in their progression from bench to bedside. The second is that plants can be engineered to produce antibodies lacking a core fucose on the glycan attached to the antibody Fc region, thereby promoting improved binding to the host FcγRIII receptor and increased antibody activity and potency (Castilho, Bohorova et al. 2011) (Zeitlin, Pettitt et al. 2011). NHPs (n=3) were given an IV dose of 50 mg/kg plant-derived MB-003 beginning at 1 or 2 dpi, with three additional, identical doses spaced 2-3 days apart per treatment. This approach protected two of three EBOV infected animals in both the 1 and 2 dpi treatment groups. Surviving animals experienced little to no viremia and had few clinical symptoms (Olinger, Pettitt et al. 2012). A follow-up study investigated the efficacy of MB-003 treatment in rhesus macaques after two clinical triggers: a positive RT-qPCR result, and a fever of greater than 1.5°C above the baseline temperature taken just before EBOV challenge.

Administration of 50 mg/kg MB-003 typically began by day 5 after the challenge, with follow-up doses at approximately 7 and 10 days after challenge, and resulted in the protection of 43% (3 of 7) of the animals (Pettitt, Zeitlin et al. 2013).

The successful post-exposure treatment of NHPs with mAbs is a significant breakthrough in the field of therapeutics against filovirus infections. Since there are no prophylactic options available for clinical use, there is a pressing need for effective post-exposure therapy, which promotes survival in patients exposed to EBOV. A 100% survival rate when initiating treatment as late as 1 dpi represents at least a 24-fold improvement over current experimental therapies, which are only fully efficacious if initiated within 30 to 60 minutes of exposure. However, as outbreak patients typically demonstrate symptoms of infection several days after exposure, strategies that enhance the efficacy of mAb-based and expand the therapeutic window should be explored to translate these promising findings closer towards practical use in the clinic.

CHAPTER VI: FINAL DISCUSSION, THOUGHTS AND PERSPECTIVES

6.1 Significance of research

The developments presented in this thesis have significantly impacted the field of EBOV research in several ways. Prior to 2012, the immune responses that correlate with protection from EBOV disease were still poorly defined. The general consensus, including the initial opinion of our research group, was biased towards cellular immunity as the predictive indicator of protection. This was mainly due to the failure of protection after treatment with antibody KZ52 in NHPs, as well as the depletion study, which implicated the $CD8^+$ T-cell response in survival of Ad5-GP vaccinated NHPs. However, the results of Chapter III and IV have strongly contradicted this trend, showing that protection can indeed be predicted with EBOV GP-specific IgG levels with statistical significance ($p<0.0001$). This observation is true regardless of different vaccination platforms (Ad5 or VSV), timing of challenge (28 days after vaccination or 30 minutes before treatment), or choice of animal model (mouse, guinea pigs or NHPs). Since the results were in part established over 96 outbred NHPs, these findings are likely to hold true when translated to a larger, genetically diverse population, such as humans. The results from this research can be applied when measuring the quality of commercially produced GP-specific mAbs, as well as providing a reliable measure of protection to existing and past clinical trials for EBOV vaccines, both of which can now be evaluated quickly and efficiently with a simple ELISA assay (Saijo, Niikura et al. 2006) without the need for *in vivo* studies.

Furthermore, no FDA-approved prophylactics or post-exposure treatments exist for filovirus infections, therefore current procedures for dealing with suspected or

confirmed EBOV cases are based around disrupting virus transmission in the form of quarantine and barrier protection (Raabea and Borcherta 2012) and palliative care (Borchert, Mutyaba et al. 2011). Supportive care strategies were never evaluated for clinical efficacy and therefore not evidence-based (Clark, Jahrling et al. 2012). The swiftness and aggressiveness of filovirus pathogenesis, coupled with the morbidity of disease, has posed many unique challenges to the development of an effective post-exposure therapy, in which protection has only been achieved in NHPs if the countermeasure was administered within minutes of infection. The results from Chapter V describe a candidate treatment, which provides for now the best efficacy for post-exposure treatment of EBOV in NHPs. More importantly, the results demonstrate that infectious diseases can be controlled by antibody therapy and confer protection even after exposure, therefore confirming that GP-specific IgG antibodies are a mechanistic correlate of protection. Now that a highly effective experimental treatment for EBOV is available, the same template strategy can be used towards infections with lower-profile filovirus species, thus providing a concrete solution to the public health and biosecurity sectors against one of the most feared human pathogens. The use of mAb therapy against infectious diseases has enjoyed a renaissance since these mAb studies were published. Indeed, several monoclonal antibodies have been found to be effective against several high-impact viruses, including human immunodeficiency virus (Barouch, Whitney et al. 2013) (Shingai, Nishimura et al. 2013) as well as Nipah and Hendra viruses (Bossart, Geisbert et al. 2011) in NHPs, in addition to Chikungunya virus in a mouse model of infection (Goh, Hobson-Peters et al. 2013).

6.2 Future directions

6.2.1 Enhancement of current mAb treatments

There are several strategies to improve the protective efficacy of mAb treatments. In order to determine the combination of mAbs that confer the best protection at the lowest doses, a collaborative effort has been initiated with the research group that produced MB-003, where ZMAb are being produced as chimeric human-mouse antibodies in the tobacco plant. In addition to improving efficacy, concerns regarding serum sickness and the large costs of antibody production can also be addressed simultaneously. The individual mAbs from ZMAb and MB-003 are currently being tested separately or in combination in guinea pigs, in which the best two mAb cocktails will be verified for improved therapeutic efficacy in NHPs.

It is very unlikely that immune responses can be induced more rapidly than the systemic administration of the critical immune component directly into the patient. Therefore, mAbs should also be integrated and tested with other strategies to determine whether the beneficial effects of a combined treatment are superior to those from a single candidate treatment. One such strategy is the use of an Ad5-based expressing IFN-α (Ad5-IFN-α), which has been previously investigated as a general antiviral and has been effective against several viral pathogens, including Yellow Fever virus (Julander, Ennis et al. 2011) and Punta Toro virus (Gowen, Ennis et al. 2012), as well as the Severe Acute Respiratory Syndrome virus (Kumaki, Ennis et al. 2011) and Pinchindé virus (Gowen, Ennis et al. 2011). Furthermore, a previous study comparing different strategies that modulate the innate immune response to boost the effectiveness of EBOV vaccines showed that Ad5-IFN-α was the superior adjuvant in terms of survival. This was due to

its ability to replenish the deficient Type I IFN stemming from EBOV infection and enhance vaccine-induced adaptive immune responses (Richardson, Wong et al. 2011), likely through the promotion of bystander DC maturation (Hensley, Giles-Davis et al. 2005).

The combination of Ad5-IFN-α and ZMAb (adjuvanted ZMAb) was first screened for enhanced efficacy in guinea pigs challenged with GA-EBOV. When given at 3 and 4 dpi, animals treated IM with adjuvanted ZMAb resulted in 100% and 50% survival, respectively. This is superior to treatment with 10 mg ZMAb alone, which resulted in 33% survival when given at 3 dpi. The addition of Ad5-lacZ in place of Ad5-IFN-α to 10 mg ZMAb did not improve survival rates, but did extend the mean time to death of non-surviving guinea pigs. If Ad5-IFN-α was administered separately as a general antiviral beginning at 1 and 2 dpi, then the treatment window for ZMAb could be delayed until 7 or 5 dpi, respectively before the loss of complete protection (Qiu, Wong et al. 2013). A follow-up study in NHPs (n=4 per treatment group) showed that adjuvanted ZMAb treatment resulted in improved protection rates compared with ZMAb alone. When adjuvanted ZMAb was administered beginning at 3 dpi with two subsequent 50 mg/kg ZMAb doses at 3 day intervals, the resulting survival rates were 75% and 100% in cynomolgus and rhesus macaques, respectively. If Ad5-IFN-α was given first at 1 dpi, then ZMAb treatment beginning at 4 dpi resulted in 50% survival in cynomolgus macaques (Qiu, Wong et al. 2013). Importantly, this treatment regimen is effective even after a positive diagnosis of EBOV viremia by RT-qPCR in addition to observable clinical signs, suggesting that adjuvanted ZMAb is a very strong candidate for

the delayed treatment of EBOV infections. The current progress made by mAb-based therapies against EBOV is summarized below (Table 6.1).

Table 6.1. Summary of monoclonal antibody-based treatments in NHPs against EBOV infection.

Treatment	Time of first intervention after exposure	Dose	Number of doses (days of treatment)	Survival (%)	Clinical trials?	Reference
MB-003	24 hours	50 mg/kg, IV	4 (1, 5, 8, and 10)	2/3 (67%)	No	(Olinger, Pettitt et al. 2012)
	48 hours	50 mg/kg, IV	4 (2, 6, 8, and 10)	2/3 (67%)		
	103-120 hours	50 mg/kg, IV	3 (every 72 hours)	3/7 (43%)		(Pettitt, Zeitlin et al. 2013)
ZMAb (± Ad5-IFN-α)	24 hours	25 mg/kg, IV	3 (every 72 hours)	4/4 (100%)	No	(Qiu, Audet et al. 2012)
	48 hours	25 mg/kg, IV	3 (every 72 hours)	2/4 (50%)		
	72 hours, cynomolgus macaques	50 mg/kg IV, with 1 x 10^9 PFU Ad5-IFN-α, IM	3 (every 72 hours)	3/4 (75%)		(Qiu, Wong et al. 2013)
	72 hours, rhesus macaques	50 mg/kg IV, with 1 x 10^9 PFU Ad5-IFN-α, IM	3 (every 72 hours)	4/4 (100%)		
	24 hours (Ad5-IFN-α) and 96 hours (ZMAb)	50 mg/kg IV, with 1 x 10^9 PFU Ad5-IFN-α, IM	3 (every 72 hours)	2/4 (50%)		

6.2.2 Mechanisms of antibody action

From a basic research perspective, the mechanisms of action need to be elucidated for these EBOV-specific antibodies, because understanding the processes behind antibody-mediated protection may provide a guideline to generate and evaluate more potent mAbs. As mentioned previously, virus neutralization does not appear to contribute significantly to protection (Wong, Richardson et al. 2012), despite the control of viremia playing a major role in the success of these ZMAb. Therefore other antibody-mediated mechanisms must be involved in protection, with several possibilities including antibody dependent cellular cytotoxicity, complement-dependent cytotoxicity, and neonatal Fragment crystallizable receptor-mediated cross-presentation. These mechanisms are not mutually exclusive, but determining their relative importance to antibody efficacy and hence survival will yield further insight to the specific mechanisms in which MB-003 and ZMAb help protect against EBOV disease. Another possible mechanism of protection could be the inhibition of viral egress from infected host cells. This has been observed with specific antibodies against MARV, where non-neutralizing antibodies that do not inhibit entry of virus into host cells act instead to reduce the extracellular release of virus particles *in vitro* (Kajihara, Marzi et al. 2012). Another study has suggested that the EBOV sGP acts as a decoy antigen to deplete the host of sGP-reacting IgG, in addition to subverting the host humoural immune response to produce antibodies that cross-react with sGP (Mohan, Li et al. 2012), thereby propagating the cycle in which sGP is able to deplete the host of all GP-specific antibodies that are important for survival. In ZMAb, it is known that 1H3 binds specifically to the sGP region, and therefore it is possible that the presence of large amounts of exogenous 1H3 administered after EBOV exposure may have prevented sGP from subverting the host humoural immune response, while leaving 2G4 and 4G7 to combat EBOV replication through other

mechanisms. Interestingly the MB-003 cocktail also contains a sGP-binding antibody (c13C6) (Wilson, Hevey et al. 2000), but ch133, ch226 and KZ52 do not recognize sGP (Takada, Feldmann et al. 2003) (Lee, Fusco et al. 2008), despite ch226 recognizing three different sites that are shared between sGP and GP. It is believed that the tertiary epitopes are either altered or obscured during sGP oligomerization (Takada, Feldmann et al. 2003). Nevertheless, it will be interesting to investigate whether combining ch133 and ch226, or KZ52 with a sGP-specific antibody will improve therapeutic efficacy in NHPs.

6.2.3 Long-term immune responses in humans

The development of a short-term solution to EBOV infections was a priority in the design of vaccines and therapeutics, therefore long-term, persistent memory immune responses that can be used to predict survival had been comparatively overlooked as a result. Now that a reliable short-term measure of protection from EBOV is available along with a treatment that consistently protects against post-exposure EBOV infections, the focus should be switched to the development of vaccines, which will confer long-lasting immunity to recipients. A reliable marker of protection indicating the need for a vaccine boost is also required.

A study was recently conducted into characterizing sustained immune responses in 6 vaccinated survivor NHPs, 9 weeks after EBOV infection. Four of six animals survived the subsequent re-challenge with EBOV. GP-specific IgG antibody levels were again found to correlate with survival, in which non-surviving animals had at least a 10-fold decrease of IgG titers that were measured in serum harvested at the time of re-challenge. The absence of memory $CD4^+$ $IFN\gamma^+$ EBOV GP-specific T-cells in the two non-survivors, coupled with decreased circulating IgG levels, indicates that these two animals developed a non-protective memory

response after initial infection and as a result succumbed to reinfection 9 weeks after original challenge (Qiu, Audet et al. 2013).

Sustained immune responses were characterized from the available samples of human survivors during several earlier outbreaks of EBOV. A study consisting of 14 survivors after the 1995 Kikwit outbreak found that specific IgG antibodies were still detectable in surviving patients when sampled 2 years after symptom onset (Ksiazek, Rollin et al. 1999), and two survivors from the 1976 Yambuku outbreak also had persistent IgG responses when sampled 10 years after infection (Ksiazek, West et al. 1999). However, another study showed that while survivors aggregated from three separate EBOV outbreaks in Gabon from 1996 and 2001 had detectable levels of IgG when sampled in 2007; there was an apparent decline in EBOV-specific IgG levels from five of nine survivors between 1996 and 2007 (Wauquier, Becquart et al. 2009), which may be indicative of their susceptibility to EBOV reinfection.

For infections with SUDV, whole blood from 6 survivors of the 2000 Gulu outbreak were sampled 12 years after infection and examined for antibody responses and cytokine expression after stimulation. In addition to the up-regulation of pro-inflammatory cytokines, a robust SUDV- and GP-specific IgG responses was also observed, even though these antibodies were neutralizing in only 4 of the survivors (Sobarzo, Ochayon et al. 2013). The prevalence of SUDV-specific IgG antibodies amongst the survivors declined over time. During the original outbreak, 61% of survivors (33 individuals/54 total) initially tested positive for SUDV-specific antibodies, but when re-tested after 6 months, 2 years and 10 years, the seroprevalence was 73% (29/40), 66% (32/48), and 41% (13/32), respectively (Sobarzo, Groseth et al. 2013). More studies are needed to determine whether these observed sustained humoural and cell-mediated immune responses will be sufficient for protection from disease in case of potential re-exposure.

The template strategy described in Chapters III and IV of this thesis can also be applied to test for immune responses that are predictive of long-term survival in rodents and NHPs, in order to facilitate the development of a vaccine able to induce sustained protective immune responses against EBOV.

6.3 Final thoughts

The immediate aim should be to move an optimized EBOV GP-specific mAb cocktail towards licensure. While neither ZMAb nor MB-003 have completed Phase I testing for safety and immunogenicity in humans, mAbs are a known clinical quantity and are often fast-tracked towards clinical approval. Palivizumab, which is used to prevent Respiratory Syncytial Virus infections, took only three years between the filing of an investigational new drug (IND) application to licensure (Sobarzo, Groseth et al. 2013; FDA.gov 2014). Furthermore, monoclonal antibodies have traditionally enjoyed marked success in the clinic (Waldmann 2003) (Reichert, Rosensweig et al. 2005) and ~350 mAbs are currently in clinical trials (Reichert 2013). Its other advantages include low rates of adverse reactions, the capacity to confer rapid and specific immunity in all populations, including the young, the elderly and the immunocompromised, and if necessary, the ability to provide higher-than-natural levels of immune responses compared to vaccinations (UPMChealthsecurity.org 2013).

Monoclonal antibodies are currently the most promising of the available experimental post-exposure options against filovirus infections, as evidenced by the consistently higher rates of survival in lethally challenged NHPs despite a delayed initiation of treatment. The success of mAb-based therapy for EBOV marks a significant advancement in the medical intervention of filovirus infections, and heralds a novel approach in the treatment of infectious diseases. Since

ZMAb and MB-003 mAbs are not likely to be cross-protective against other antigenically distinct filoviruses, another priority is to develop and test mAbs raised against other pathogenic filoviruses, in particular MARV, SUDV and BDBV. It would also be interesting to screen for common epitopes and sequences amongst the filovirus species and determine if cross-protective antibodies can be generated.

From a practical perspective, it will be important to determine whether protective mAbs developed against newly discovered filoviruses can simply be added to an existing antibody cocktail without interfering with the existing efficacy. Since filoviruses are endemic mainly in developing and third-world countries, it is important for antibody production costs to be lowered to reasonable levels such that the stockpiling of these treatments for emergency purposes will not become an economic burden. The most cost-effective method would be to employ existing antibody production plants, which were built by contract manufacturing organizations (CMO) to produce clinically approved mAbs for the treatment of other human conditions, such as cancer. Under idealized conditions, CMOs can produce a desired mAb at a unit cost as low as US$60/gram inclusive of material costs, production, testing and release, without the need for any substantial capital investment (Kelley 2009). Therefore at concentrations of 50 mg/kg, one full course of mAb treatment will cost a total of US$540 for a 60 kg human. Based on recent developments, there is cause for optimism that mAb-based therapy against filovirus infections will become available for emergency use within the next 2 years and commercially within 5 to 10 years, and that by then filovirus outbreaks will no longer be a public health concern.

LITERATURE CITED

Allela, L., O. Boury, et al. (2005). "Ebola virus antibody prevalence in dogs and human risk." Emerging infectious diseases **11**(3): 385-390.

Anonymous (1978a). "Ebola haemorrhagic fever in Zaire, 1976. Report of an International Commission." Bulletin of the World Health Organization **56**(2): 271-293.

Anonymous (1978b). "Ebola haemorrhagic fever in Sudan, 1976. Report of a WHO/International Study Team." Bulletin of the World Health Organization **56**(2): 247-270.

Anonymous (1990). "Update: filovirus infection in animal handlers." MMWR. Morbidity and mortality weekly report **39**(13): 221.

Anonymous (2009). "Outbreak news. Ebola Reston in pigs and humans, Philippines." Releve epidemiologique hebdomadaire / Section d'hygiene du Secretariat de la Societe des Nations = Weekly epidemiological record / Health Section of the Secretariat of the League of Nations **84**(7): 49-50.

Barouch, D. H., J. B. Whitney, et al. (2013). "Therapeutic efficacy of potent neutralizing HIV-1-specific monoclonal antibodies in SHIV-infected rhesus monkeys." Nature **503**(7475): 224-228.

Barrette, R. W., S. A. Metwally, et al. (2009). "Discovery of swine as a host for the Reston ebolavirus." Science **325**(5937): 204-206.

Basler, C. F., A. Mikulasova, et al. (2003). "The Ebola virus VP35 protein inhibits activation of interferon regulatory factor 3." Journal of virology **77**(14): 7945-7956.

Bausch, D. G., J. S. Towner, et al. (2007). "Assessment of the risk of Ebola virus transmission from bodily fluids and fomites." The Journal of infectious diseases **196 Suppl 2**: S142-147.

Bavari, S., C. M. Bosio, et al. (2002). "Lipid raft microdomains: a gateway for compartmentalized trafficking of Ebola and Marburg viruses." The Journal of experimental medicine **195**(5): 593-602.

Beniac, D. R., P. L. Melito, et al. (2012). "The organisation of Ebola virus reveals a capacity for extensive, modular polyploidy." PloS one **7**(1): e29608.

Bente, D., J. Gren, et al. (2009). "Disease modeling for Ebola and Marburg viruses." Disease models & mechanisms **2**(1-2): 12-17.

Bharat, T. A., T. Noda, et al. (2012). "Structural dissection of Ebola virus and its assembly determinants using cryo-electron tomography." Proceedings of the National Academy of Sciences of the United States of America **109**(11): 4275-4280.

Blaney, J. E., A. Marzi, et al. (2013). "Antibody quality and protection from lethal Ebola virus challenge in nonhuman primates immunized with rabies virus based bivalent vaccine." PLoS pathogens **9**(5): e1003389.

Borchert, M., I. Mutyaba, et al. (2011). "Ebola haemorrhagic fever outbreak in Masindi District, Uganda: outbreak description and lessons learned." BMC infectious diseases **11**: 357.

Bosio, C. M., M. J. Aman, et al. (2003). "Ebola and Marburg viruses replicate in monocyte-derived dendritic cells without inducing the production of cytokines and full maturation." The Journal of infectious diseases **188**(11): 1630-1638.

Bossart, K. N., T. W. Geisbert, et al. (2011). "A neutralizing human monoclonal antibody protects african green monkeys from hendra virus challenge." Science translational medicine **3**(105): 105ra103.

Bradfute, S. B., D. R. Braun, et al. (2007). "Lymphocyte death in a mouse model of Ebola virus infection." The Journal of infectious diseases **196 Suppl 2**: S296-304.

Bradfute, S. B., K. L. Warfield, et al. (2008). "Functional CD8+ T cell responses in lethal Ebola virus infection." Journal of immunology **180**(6): 4058-4066.

Bray, M. (2001). "The role of the Type I interferon response in the resistance of mice to filovirus infection." The Journal of general virology **82**(Pt 6): 1365-1373.

Bray, M., K. Davis, et al. (1998). "A mouse model for evaluation of prophylaxis and therapy of Ebola hemorrhagic fever." The Journal of infectious diseases **178**(3): 651-661.

Bray, M., K. Davis, et al. (1999). "A mouse model for evaluation of prophylaxis and therapy of Ebola hemorrhagic fever." The Journal of infectious diseases **179 Suppl 1**: S248-258.

Bray, M. and T. W. Geisbert (2005). "Ebola virus: the role of macrophages and dendritic cells in the pathogenesis of Ebola hemorrhagic fever." The international journal of biochemistry & cell biology **37**(8): 1560-1566.

Brewer, J. M., M. Conacher, et al. (1999). "Aluminium hydroxide adjuvant initiates strong antigen-specific Th2 responses in the absence of IL-4- or IL-13-mediated signaling." Journal of immunology **163**(12): 6448-6454.

Brunetti-Pierri, N., D. J. Palmer, et al. (2004). "Acute toxicity after high-dose systemic injection of helper-dependent adenoviral vectors into nonhuman primates." Human gene therapy **15**(1): 35-46.

Buchbinder, S. P., D. V. Mehrotra, et al. (2008). "Efficacy assessment of a cell-mediated immunity HIV-1 vaccine (the Step Study): a double-blind, randomised, placebo-controlled, test-of-concept trial." Lancet **372**(9653): 1881-1893.

Bukreyev, A., P. E. Rollin, et al. (2007). "Successful topical respiratory tract immunization of primates against Ebola virus." Journal of virology **81**(12): 6379-6388.

Cardenas, W. B., Y. M. Loo, et al. (2006). "Ebola virus VP35 protein binds double-stranded RNA and inhibits alpha/beta interferon production induced by RIG-I signaling." Journal of virology **80**(11): 5168-5178.

Carette, J. E., M. Raaben, et al. (2011). "Ebola virus entry requires the cholesterol transporter Niemann-Pick C1." Nature **477**(7364): 340-343.

Castilho, A., N. Bohorova, et al. (2011). "Rapid high yield production of different glycoforms of Ebola virus monoclonal antibody." PloS one **6**(10): e26040.

Chang, T. H., T. Kubota, et al. (2009). "Ebola Zaire virus blocks type I interferon production by exploiting the host SUMO modification machinery." PLoS pathogens **5**(6): e1000493.

Chirmule, N., K. Propert, et al. (1999). "Immune responses to adenovirus and adeno-associated virus in humans." Gene therapy **6**(9): 1574-1583.

Clark, D. V., P. B. Jahrling, et al. (2012). "Clinical management of filovirus-infected patients." Viruses **4**(9): 1668-1686.

Clark, E. A. and J. A. Ledbetter (1994). "How B and T cells talk to each other." Nature **367**(6462): 425-428.

ClinicalTrials.gov. (2014a). "Safety, Tolerability and Pharmacokinetic First in Human (FIH) Study of Intravenous (IV) TKM-100201 Infusion." from http://clinicaltrials.gov/ct2/show/NCT01518881.

ClinicalTrials.gov. (2014b). "Safety Study of Single Administration Post-Exposure Prophylaxis Treatment for Ebola Virus." from http://clinicaltrials.gov/ct2/show/NCT01353027.

ClinicalTrials.gov. (2014c). "Dose-Escalation Study of CG0070 for Bladder Cancer After BCG (Bacillus Calmette-Guerin) Failure." from http://www.clinicaltrials.gov/ct2/show/NCT00109655.

ClinicalTrials.gov. (2014d). "Safety Study on AdCD40L Gene Therapy for Bladder Cancer." from http://www.clinicaltrials.gov/ct2/show/NCT00891748.

ClinicalTrials.gov. (2014e). "Phase I/IIa AdCD40L Immunogene Therapy for Malignant Melanoma." from http://www.clinicaltrials.gov/ct2/show/NCT01455259.

ClinicalTrials.gov. (2014f). "Combined Cytotoxic and Immune-Stimulatory Therapy for Glioma." from http://www.clinicaltrials.gov/ct2/show/NCT01811992.

ClinicalTrials.gov. (2014g). "Efficacy and Safety of Ad5FGF-4 for Myocardial Ischemia in Patients With Stable Angina Due to Coronary Artery Disease (ASPIRE)." from http://www.clinicaltrials.gov/ct2/show/NCT01550614.

ClinicalTrials.gov. (2014h). "Investigation of V520 in an HIV Vaccine Proof-of-Concept Study (V520-023)." from http://www.clinicaltrials.gov/ct2/show/results/NCT00095576.

Cohen, J. (2004). "Containing the threat--don't forget Ebola." PLoS medicine **1**(3): e59.

Connolly, B. M., K. E. Steele, et al. (1999). "Pathogenesis of experimental Ebola virus infection in guinea pigs." The Journal of infectious diseases **179 Suppl 1**: S203-217.

Cook, J. D. and J. E. Lee (2013). "The secret life of viral entry glycoproteins: moonlighting in immune evasion." PLoS pathogens **9**(5): e1003258.

Cote, M., J. Misasi, et al. (2011). "Small molecule inhibitors reveal Niemann-Pick C1 is essential for Ebola virus infection." Nature **477**(7364): 344-348.

Croyle, M. A., A. Patel, et al. (2008). "Nasal delivery of an adenovirus-based vaccine bypasses pre-existing immunity to the vaccine carrier and improves the immune response in mice." PloS one **3**(10): e3548.

Dolnik, O., V. Volchkova, et al. (2004). "Ectodomain shedding of the glycoprotein GP of Ebola virus." The EMBO journal **23**(10): 2175-2184.

Dye, J. M., A. S. Herbert, et al. (2012). "Postexposure antibody prophylaxis protects nonhuman primates from filovirus disease." Proceedings of the National Academy of Sciences of the United States of America **109**(13): 5034-5039.

Ebihara, H., A. Takada, et al. (2006). "Molecular determinants of Ebola virus virulence in mice." PLoS pathogens **2**(7): e73.

Ebihara, H., M. Zivcec, et al. (2013). "A Syrian golden hamster model recapitulating ebola hemorrhagic fever." The Journal of infectious diseases **207**(2): 306-318.

Eming, S. A., T. Krieg, et al. (2007). "Inflammation in wound repair: molecular and cellular mechanisms." The Journal of investigative dermatology **127**(3): 514-525.

FDA.gov. (2014). "Palivizumab Clinical Review." from http://www.fda.gov/downloads/Drugs/DevelopmentApprovalProcess/HowDrugsareDevelopedandApproved/ApprovalApplications/TherapeuticBiologicApplications/ucm113384.pdf.

Feldmann, H., H. Bugany, et al. (1996). "Filovirus-induced endothelial leakage triggered by infected monocytes/macrophages." Journal of virology **70**(4): 2208-2214.

Feldmann, H., S. M. Jones, et al. (2007). "Effective post-exposure treatment of Ebola infection." PLoS pathogens **3**(1): e2.

Feldmann, H. and M. P. Kiley (1999). "Classification, structure, and replication of filoviruses." Current topics in microbiology and immunology **235**: 1-21.

Feldmann, H. and H. D. Klenk (1996). "Marburg and Ebola viruses." Advances in virus research **47**: 1-52.

Feldmann, H., A. Sanchez, et al. (2013). Filoviridae: Marburg and Ebola viruses. Philadelphia, PA, USA, Lippincott Williams and Wilkins.

Ferron, F., S. Longhi, et al. (2002). "Viral RNA-polymerases -- a predicted 2'-O-ribose methyltransferase domain shared by all Mononegavirales." Trends in biochemical sciences **27**(5): 222-224.

Fisher-Hoch, S. P., G. S. Platt, et al. (1983). "Haematological and biochemical monitoring of Ebola infection in rhesus monkeys: implications for patient management." Lancet **2**(8358): 1055-1058.

Formenty, P., C. Hatz, et al. (1999). "Human infection due to Ebola virus, subtype Cote d'Ivoire: clinical and biologic presentation." The Journal of infectious diseases **179 Suppl 1**: S48-53.

Francica, J. R., A. Varela-Rohena, et al. (2010). "Steric shielding of surface epitopes and impaired immune recognition induced by the ebola virus glycoprotein." PLoS pathogens **6**(9): e1001098.

Ftika, L. and H. C. Maltezou (2013). "Viral haemorrhagic fevers in healthcare settings." The Journal of hospital infection **83**(3): 185-192.

Gabitzsch, E. S., Y. Xu, et al. (2011). "Induction and comparison of SIV immunity in Ad5 naive and Ad5 immune non-human primates using an Ad5 [E1-, E2b-] based vaccine." Vaccine **29**(45): 8101-8107.

Garbutt, M., R. Liebscher, et al. (2004). "Properties of replication-competent vesicular stomatitis virus vectors expressing glycoproteins of filoviruses and arenaviruses." Journal of virology **78**(10): 5458-5465.

Gaufin, T., R. M. Ribeiro, et al. (2010). "Experimental depletion of CD8+ cells in acutely SIVagm-infected African Green Monkeys results in increased viral replication." Retrovirology **7**: 42.

Geisbert, T. W., M. Bailey, et al. (2010). "Vector choice determines immunogenicity and potency of genetic vaccines against Angola Marburg virus in nonhuman primates." Journal of virology **84**(19): 10386-10394.

Geisbert, T. W. and L. E. Hensley (2004). "Ebola virus: new insights into disease aetiopathology and possible therapeutic interventions." Expert reviews in molecular medicine **6**(20): 1-24.

Geisbert, T. W., L. E. Hensley, et al. (2003). "Treatment of Ebola virus infection with a recombinant inhibitor of factor VIIa/tissue factor: a study in rhesus monkeys." Lancet **362**(9400): 1953-1958.

Geisbert, T. W., L. E. Hensley, et al. (2003). "Pathogenesis of Ebola hemorrhagic fever in cynomolgus macaques: evidence that dendritic cells are early and sustained targets of infection." The American journal of pathology **163**(6): 2347-2370.

Geisbert, T. W., A. C. Lee, et al. (2010). "Postexposure protection of non-human primates against a lethal Ebola virus challenge with RNA interference: a proof-of-concept study." Lancet **375**(9729): 1896-1905.

Geisbert, T. W., H. A. Young, et al. (2003). "Mechanisms underlying coagulation abnormalities in ebola hemorrhagic fever: overexpression of tissue factor in primate monocytes/macrophages is a key event." The Journal of infectious diseases **188**(11): 1618-1629.

Goh, L. Y., J. Hobson-Peters, et al. (2013). "Neutralizing monoclonal antibodies to the E2 protein of chikungunya virus protects against disease in a mouse model." Clinical immunology **149**(3): 487-497.

Gowen, B. B., J. Ennis, et al. (2011). "Use of recombinant adenovirus vectored consensus IFN-alpha to avert severe arenavirus infection." PloS one **6**(10): e26072.

Gowen, B. B., J. Ennis, et al. (2012). "Extended protection against phlebovirus infection conferred by recombinant adenovirus expressing consensus interferon (DEF201)." Antimicrobial agents and chemotherapy **56**(8): 4168-4174.

Gray, G. E., M. Allen, et al. (2011). "Safety and efficacy of the HVTN 503/Phambili study of a clade-B-based HIV-1 vaccine in South Africa: a double-blind, randomised, placebo-controlled test-of-concept phase 2b study." The Lancet infectious diseases **11**(7): 507-515.

Grolla, A., S. M. Jones, et al. (2011). "The use of a mobile laboratory unit in support of patient management and epidemiological surveillance during the 2005 Marburg Outbreak in Angola." PLoS neglected tropical diseases **5**(5): e1183.

Groseth, A., J. E. Charton, et al. (2009). "The Ebola virus ribonucleoprotein complex: a novel VP30-L interaction identified." Virus research **140**(1-2): 8-14.

Groseth, A., H. Feldmann, et al. (2007). "The ecology of Ebola virus." Trends in microbiology **15**(9): 408-416.

Groseth, A., A. Marzi, et al. (2012). "The Ebola virus glycoprotein contributes to but is not sufficient for virulence in vivo." PLoS pathogens **8**(8): e1002847.

Groseth, A., U. Stroher, et al. (2002). "Molecular characterization of an isolate from the 1989/90 epizootic of Ebola virus Reston among macaques imported into the United States." Virus research **87**(2): 155-163.

Guimard, Y., M. A. Bwaka, et al. (1999). "Organization of patient care during the Ebola hemorrhagic fever epidemic in Kikwit, Democratic Republic of the Congo, 1995." The Journal of infectious diseases **179 Suppl 1**: S268-273.

Gupta, M., S. Mahanty, et al. (2001). "Passive transfer of antibodies protects immunocompetent and imunodeficient mice against lethal Ebola virus infection without complete inhibition of viral replication." Journal of virology **75**(10): 4649-4654.

Gupta, M., S. Mahanty, et al. (2004). "Persistent infection with ebola virus under conditions of partial immunity." Journal of virology **78**(2): 958-967.

Haasnoot, J., W. de Vries, et al. (2007). "The Ebola virus VP35 protein is a suppressor of RNA silencing." PLoS pathogens **3**(6): e86.

Hartlieb, B., T. Muziol, et al. (2007). "Crystal structure of the C-terminal domain of Ebola virus VP30 reveals a role in transcription and nucleocapsid association." Proceedings of the National Academy of Sciences of the United States of America **104**(2): 624-629.

Hayman, D. T., M. Yu, et al. (2012). "Ebola virus antibodies in fruit bats, Ghana, West Africa." Emerging infectious diseases **18**(7): 1207-1209.

Hensley, L. E., E. L. Stevens, et al. (2007). "Recombinant human activated protein C for the postexposure treatment of Ebola hemorrhagic fever." The Journal of infectious diseases **196 Suppl 2**: S390-399.

Hensley, L. E., H. A. Young, et al. (2002). "Proinflammatory response during Ebola virus infection of primate models: possible involvement of the tumor necrosis factor receptor superfamily." Immunology letters **80**(3): 169-179.

Hensley, S. E., W. Giles-Davis, et al. (2005). "Dendritic cell maturation, but not CD8+ T cell induction, is dependent on type I IFN signaling during vaccination with adenovirus vectors." Journal of immunology **175**(9): 6032-6041.

Hoenen, T., A. Groseth, et al. (2006). "Infection of naive target cells with virus-like particles: implications for the function of ebola virus VP24." Journal of virology **80**(14): 7260-7264.

Hoenen, T., S. Jung, et al. (2010). "Both matrix proteins of Ebola virus contribute to the regulation of viral genome replication and transcription." Virology **403**(1): 56-66.

Hood, C. L., J. Abraham, et al. (2010). "Biochemical and structural characterization of cathepsin L-processed Ebola virus glycoprotein: implications for viral entry and immunogenicity." Journal of virology **84**(6): 2972-2982.

Huang, Y., L. Xu, et al. (2002). "The assembly of Ebola virus nucleocapsid requires virion-associated proteins 35 and 24 and posttranslational modification of nucleoprotein." Molecular cell **10**(2): 307-316.

Ikegami, T., M. Saijo, et al. (2003). "Immunoglobulin G enzyme-linked immunosorbent assay using truncated nucleoproteins of Reston Ebola virus." Epidemiology and infection **130**(3): 533-539.

Jahrling, P. B., J. B. Geisbert, et al. (2007). "Ebola hemorrhagic fever: evaluation of passive immunotherapy in nonhuman primates." The Journal of infectious diseases **196 Suppl 2**: S400-403.

Jahrling, P. B., T. W. Geisbert, et al. (1990). "Preliminary report: isolation of Ebola virus from monkeys imported to USA." Lancet **335**(8688): 502-505.

Jahrling, P. B., T. W. Geisbert, et al. (1999). "Evaluation of immune globulin and recombinant interferon-alpha2b for treatment of experimental Ebola virus infections." The Journal of infectious diseases **179 Suppl 1**: S224-234.

Janeway, C. A., P. Travers, et al. (2001). Immunobiology: The Immune System in Health and Disease: 5th edition. New York, Garland Science.

Jasenosky, L. D., G. Neumann, et al. (2001). "Ebola virus VP40-induced particle formation and association with the lipid bilayer." Journal of virology **75**(11): 5205-5214.

Jin, H., Z. Yan, et al. (2010). "The VP35 protein of Ebola virus impairs dendritic cell maturation induced by virus and lipopolysaccharide." The Journal of general virology **91**(Pt 2): 352-361.

John, S. P., T. Wang, et al. (2007). "Ebola virus VP30 is an RNA binding protein." Journal of virology **81**(17): 8967-8976.

Johnson, E., N. Jaax, et al. (1995). "Lethal experimental infections of rhesus monkeys by aerosolized Ebola virus." International journal of experimental pathology **76**(4): 227-236.

Jones, S. M., H. Feldmann, et al. (2005). "Live attenuated recombinant vaccine protects nonhuman primates against Ebola and Marburg viruses." Nature medicine **11**(7): 786-790.

Julander, J. G., J. Ennis, et al. (2011). "Treatment of yellow fever virus with an adenovirus-vectored interferon, DEF201, in a hamster model." Antimicrobial agents and chemotherapy **55**(5): 2067-2073.

Kajihara, M., A. Marzi, et al. (2012). "Inhibition of Marburg virus budding by nonneutralizing antibodies to the envelope glycoprotein." Journal of virology **86**(24): 13467-13474.

Kapsenberg, M. L. (2003). "Dendritic-cell control of pathogen-driven T-cell polarization." Nature reviews. Immunology **3**(12): 984-993.

Kash, J. C., E. Muhlberger, et al. (2006). "Global suppression of the host antiviral response by Ebola- and Marburgviruses: increased antagonism of the type I interferon response is associated with enhanced virulence." Journal of virology **80**(6): 3009-3020.

Kaur, S., T. Kaur, et al. (2008). "Effect of dose and route of inoculation on the generation of CD4+ Th1/Th2 type of immune response in murine visceral leishmaniasis." Parasitology research **103**(6): 1413-1419.

Kelley, B. (2009). "Industrialization of mAb production technology: the bioprocessing industry at a crossroads." mAbs **1**(5): 443-452.

Kimberlin, C. R., Z. A. Bornholdt, et al. (2010). "Ebolavirus VP35 uses a bimodal strategy to bind dsRNA for innate immune suppression." Proceedings of the National Academy of Sciences of the United States of America **107**(1): 314-319.

Kobinger, G. P., A. Leung, et al. (2011). "Replication, pathogenicity, shedding, and transmission of Zaire ebolavirus in pigs." The Journal of infectious diseases **204**(2): 200-208.

Koob, G., M. J. Hicks, et al. (2011). "Anti-cocaine vaccine based on coupling a cocaine analog to a disrupted adenovirus." CNS & neurological disorders drug targets **10**(8): 899-904.

Kracker, S. and A. Radbruch (2004). "Immunoglobulin class switching: in vitro induction and analysis." Methods in molecular biology **271**: 149-159.

Krasnianskii, B. P., V. V. Mikhailov, et al. (1995). "[Preparation of hyperimmune horse serum against Ebola virus]." Voprosy virusologii **40**(3): 138-140.

Ksiazek, T. G., P. E. Rollin, et al. (1992). "Enzyme immunosorbent assay for Ebola virus antigens in tissues of infected primates." Journal of clinical microbiology **30**(4): 947-950.

Ksiazek, T. G., P. E. Rollin, et al. (1999). "Clinical virology of Ebola hemorrhagic fever (EHF): virus, virus antigen, and IgG and IgM antibody findings among EHF patients in Kikwit, Democratic Republic of the Congo, 1995." The Journal of infectious diseases **179 Suppl 1**: S177-187.

Ksiazek, T. G., C. P. West, et al. (1999). "ELISA for the detection of antibodies to Ebola viruses." The Journal of infectious diseases **179 Suppl 1**: S192-198.

Kuhl, A. and S. Pohlmann (2012). "How Ebola virus counters the interferon system." Zoonoses and public health **59 Suppl 2**: 116-131.

Kuhn, J. H., S. Becker, et al. (2010). "Proposal for a revised taxonomy of the family Filoviridae: classification, names of taxa and viruses, and virus abbreviations." Archives of virology **155**(12): 2083-2103.

Kumaki, Y., J. Ennis, et al. (2011). "Single-dose intranasal administration with mDEF201 (adenovirus vectored mouse interferon-alpha) confers protection from mortality in a lethal SARS-CoV BALB/c mouse model." Antiviral research **89**(1): 75-82.

Kurono, Y., M. Yamamoto, et al. (1999). "Nasal immunization induces Haemophilus influenzae-specific Th1 and Th2 responses with mucosal IgA and systemic IgG antibodies for protective immunity." The Journal of infectious diseases **180**(1): 122-132.

Lawson, N. D., E. A. Stillman, et al. (1995). "Recombinant vesicular stomatitis viruses from DNA." Proceedings of the National Academy of Sciences of the United States of America **92**(10): 4477-4481.

Ledgerwood, J. E., P. Costner, et al. (2010). "A replication defective recombinant Ad5 vaccine expressing Ebola virus GP is safe and immunogenic in healthy adults." Vaccine **29**(2): 304-313.

Lee, A., G. Agnelli, et al. (2001). "Dose-response study of recombinant factor VIIa/tissue factor inhibitor recombinant nematode anticoagulant protein c2 in prevention of postoperative venous thromboembolism in patients undergoing total knee replacement." Circulation **104**(1): 74-78.

Lee, J. E., M. L. Fusco, et al. (2008). "Structure of the Ebola virus glycoprotein bound to an antibody from a human survivor." Nature **454**(7201): 177-182.

Lehrman, S. (1999). "Virus treatment questioned after gene therapy death." Nature **401**(6753): 517-518.

Leroy, E. M., A. Epelboin, et al. (2009). "Human Ebola outbreak resulting from direct exposure to fruit bats in Luebo, Democratic Republic of Congo, 2007." Vector borne and zoonotic diseases **9**(6): 723-728.

Leroy, E. M., J. P. Gonzalez, et al. (2011). "Ebola and Marburg haemorrhagic fever viruses: major scientific advances, but a relatively minor public health threat for Africa." Clinical microbiology and infection : the official publication of the European Society of Clinical Microbiology and Infectious Diseases **17**(7): 964-976.

Leroy, E. M., B. Kumulungui, et al. (2005). "Fruit bats as reservoirs of Ebola virus." Nature **438**(7068): 575-576.

Leung, D. W., K. C. Prins, et al. (2010). "Structural basis for dsRNA recognition and interferon antagonism by Ebola VP35." Nature structural & molecular biology **17**(2): 165-172.

Mahanty, S., K. Hutchinson, et al. (2003). "Cutting edge: impairment of dendritic cells and adaptive immunity by Ebola and Lassa viruses." Journal of immunology **170**(6): 2797-2801.

Martin, J. E., N. J. Sullivan, et al. (2006). "A DNA vaccine for Ebola virus is safe and immunogenic in a phase I clinical trial." Clinical and vaccine immunology : CVI **13**(11): 1267-1277.

Martini, G. A. and R. Siegert (1971). Marburg Virus Disease. New York, NY, USA, Springer.

Maruyama, T., L. L. Rodriguez, et al. (1999). "Ebola virus can be effectively neutralized by antibody produced in natural human infection." Journal of virology **73**(7): 6024-6030.

Marzi, A., F. Engelmann, et al. (2013). "Antibodies are necessary for rVSV/ZEBOV-GP-mediated protection against lethal Ebola virus challenge in nonhuman primates." Proceedings of the National Academy of Sciences of the United States of America **110**(5): 1893-1898.

Marzi, A., R. Yoshida, et al. (2012). "Protective efficacy of neutralizing monoclonal antibodies in a nonhuman primate model of Ebola hemorrhagic fever." PloS one **7**(4): e36192.

Mehedi, M., D. Falzarano, et al. (2011). "A new Ebola virus nonstructural glycoprotein expressed through RNA editing." Journal of virology **85**(11): 5406-5414.

Miller, E. H., G. Obernosterer, et al. (2012). "Ebola virus entry requires the host-programmed recognition of an intracellular receptor." The EMBO journal **31**(8): 1947-1960.

Miranda, M. E., M. E. White, et al. (1991). "Seroepidemiological study of filovirus related to Ebola in the Philippines." Lancet **337**(8738): 425-426.

Miranda, M. E., Y. Yoshikawa, et al. (2002). "Chronological and spatial analysis of the 1996 Ebola Reston virus outbreak in a monkey breeding facility in the Philippines." Experimental animals / Japanese Association for Laboratory Animal Science **51**(2): 173-179.

Modrof, J., E. Muhlberger, et al. (2002). "Phosphorylation of VP30 impairs ebola virus transcription." The Journal of biological chemistry **277**(36): 33099-33104.

Mohan, G. S., W. Li, et al. (2012). "Antigenic subversion: a novel mechanism of host immune evasion by Ebola virus." PLoS pathogens **8**(12): e1003065.

Moons, A. H., R. J. Peters, et al. (2003). "Recombinant nematode anticoagulant protein c2, an inhibitor of the tissue factor/factor VIIa complex, in patients undergoing elective coronary angioplasty." Journal of the American College of Cardiology **41**(12): 2147-2153.

Moons, A. H., R. J. Peters, et al. (2002). "Recombinant nematode anticoagulant protein c2, a novel inhibitor of tissue factor-factor VIIa activity, abrogates endotoxin-induced coagulation in chimpanzees." Thrombosis and haemostasis **88**(4): 627-631.

Mosca, F., E. Tritto, et al. (2008). "Molecular and cellular signatures of human vaccine adjuvants." Proceedings of the National Academy of Sciences of the United States of America **105**(30): 10501-10506.

Mosmann, T. R., H. Cherwinski, et al. (1986). "Two types of murine helper T cell clone. I. Definition according to profiles of lymphokine activities and secreted proteins." Journal of immunology **136**(7): 2348-2357.

Muhlberger, E. (2007). "Filovirus replication and transcription." Future virology **2**(2): 205-215.

Muhlberger, E., S. Trommer, et al. (1996). "Termini of all mRNA species of Marburg virus: sequence and secondary structure." Virology **223**(2): 376-380.

Muhlberger, E., M. Weik, et al. (1999). "Comparison of the transcription and replication strategies of marburg virus and Ebola virus by using artificial replication systems." Journal of virology **73**(3): 2333-2342.

Mupapa, K., M. Massamba, et al. (1999). "Treatment of Ebola hemorrhagic fever with blood transfusions from convalescent patients. International Scientific and Technical Committee." The Journal of infectious diseases **179 Suppl 1**: S18-23.

Nakayama, E. and M. Saijo (2013). "Animal models for Ebola and Marburg virus infections." Frontiers in microbiology **4**: 267.

Nakayama, E., A. Yokoyama, et al. (2010). "Enzyme-linked immunosorbent assay for detection of filovirus species-specific antibodies." Clinical and vaccine immunology : CVI **17**(11): 1723-1728.

Nakayama, E., A. Yokoyama, et al. (2010). "Enzyme-linked immunosorbent assay for the detection of filovirus species-specific antibodies." Clinical and vaccine immunology : CVI.

Nanbo, A., M. Imai, et al. (2010). "Ebolavirus is internalized into host cells via macropinocytosis in a viral glycoprotein-dependent manner." PLoS pathogens **6**(9): e1001121.

Ndayimirije, N. and M. K. Kindhauser (2005). "Marburg hemorrhagic fever in Angola--fighting fear and a lethal pathogen." The New England journal of medicine **352**(21): 2155-2157.

Negredo, A., G. Palacios, et al. (2011). "Discovery of an ebolavirus-like filovirus in europe." PLoS pathogens **7**(10): e1002304.

Nidom, C. A., E. Nakayama, et al. (2012). "Serological evidence of Ebola virus infection in Indonesian orangutans." PloS one **7**(7): e40740.

Nkoghe, D., P. Formenty, et al. (2004). "[Practical guidelines for the management of Ebola infected patients in the field]." Medecine tropicale : revue du Corps de sante colonial **64**(2): 199-204.

Nkoghe, D., E. M. Leroy, et al. (2012). "Cutaneous manifestations of filovirus infections." International journal of dermatology **51**(9): 1037-1043.

Nkoghe, D., C. Padilla, et al. (2011). "Risk factors for Zaire ebolavirus--specific IgG in rural Gabonese populations." The Journal of infectious diseases **204 Suppl 3**: S768-775.

Noda, T., H. Ebihara, et al. (2006). "Assembly and budding of Ebolavirus." PLoS pathogens **2**(9): e99.

Noyori, O., K. Matsuno, et al. (2013). "Differential potential for envelope glycoprotein-mediated steric shielding of host cell surface proteins among filoviruses." Virology **446**(1-2): 152-161.

Olinger, G. G., Jr., J. Pettitt, et al. (2012). "Delayed treatment of Ebola virus infection with plant-derived monoclonal antibodies provides protection in rhesus macaques." Proceedings of the National Academy of Sciences of the United States of America **109**(44): 18030-18035.

Olival, K. J., A. Islam, et al. (2013). "Ebola virus antibodies in fruit bats, bangladesh." Emerging infectious diseases **19**(2): 270-273.

Oswald, W. B., T. W. Geisbert, et al. (2007). "Neutralizing antibody fails to impact the course of Ebola virus infection in monkeys." PLoS pathogens **3**(1): e9.

Ou, W., J. Delisle, et al. (2012). "Induction of ebolavirus cross-species immunity using retrovirus-like particles bearing the Ebola virus glycoprotein lacking the mucin-like domain." Virology journal **9**: 32.

Palucka, K. and J. Banchereau (1999). "Dendritic cells: a link between innate and adaptive immunity." Journal of clinical immunology **19**(1): 12-25.

Parren, P. W., T. W. Geisbert, et al. (2002). "Pre- and postexposure prophylaxis of Ebola virus infection in an animal model by passive transfer of a neutralizing human antibody." Journal of virology **76**(12): 6408-6412.

Patel, A., S. Tikoo, et al. (2010). "A porcine adenovirus with low human seroprevalence is a promising alternative vaccine vector to human adenovirus 5 in an H5N1 virus disease model." PloS one **5**(12): e15301.

Peterson, A. T., J. T. Bauer, et al. (2004). "Ecologic and geographic distribution of filovirus disease." Emerging infectious diseases **10**(1): 40-47.

Pettitt, J., L. Zeitlin, et al. (2013). "Therapeutic intervention of Ebola virus infection in rhesus macaques with the MB-003 monoclonal antibody cocktail." Science translational medicine **5**(199): 199ra113.

Plotkin, S. A. (2008). "Vaccines: correlates of vaccine-induced immunity." Clinical infectious diseases : an official publication of the Infectious Diseases Society of America **47**(3): 401-409.

Plotkin, S. A. (2010). "Correlates of protection induced by vaccination." Clinical and vaccine immunology : CVI **17**(7): 1055-1065.

Plotkin, S. A. and P. B. Gilbert (2012). "Nomenclature for immune correlates of protection after vaccination." Clinical infectious diseases : an official publication of the Infectious Diseases Society of America **54**(11): 1615-1617.

Pushko, P., M. Bray, et al. (2000). "Recombinant RNA replicons derived from attenuated Venezuelan equine encephalitis virus protect guinea pigs and mice from Ebola hemorrhagic fever virus." Vaccine **19**(1): 142-153.

Qiu, X., J. B. Alimonti, et al. (2011). "Characterization of Zaire ebolavirus glycoprotein-specific monoclonal antibodies." Clinical immunology **141**(2): 218-227.

Qiu, X., J. Audet, et al. (2013). "Sustained protection against Ebola virus infection following treatment of infected nonhuman primates with ZMAb." Scientific reports **3**: 3365.

Qiu, X., J. Audet, et al. (2012). "Successful treatment of ebola virus-infected cynomolgus macaques with monoclonal antibodies." Science translational medicine **4**(138): 138ra181.

Qiu, X., L. Fernando, et al. (2011). "Protective immunodominant *Zaire Ebolavirus* glycoprotein epitope in mice." Journal of bioterrorism & biodefense **S1**: 006.

Qiu, X., L. Fernando, et al. (2012). "Ebola GP-specific monoclonal antibodies protect mice and guinea pigs from lethal Ebola virus infection." PLoS neglected tropical diseases **6**(3): e1575.

Qiu, X. and G. P. Kobinger (2014). "Antibody therapy for Ebola: is the tide turning around?" Human vaccines & immunotherapeutics **10**(4).

Qiu, X., G. Wong, et al. (2013). "mAbs and Ad-Vectored IFN-alpha therapy rescue ebola-infected nonhuman primates when administered after the detection of viremia and symptoms." Science translational medicine **5**(207): 207ra143.

Qiu, X., G. Wong, et al. (2013). "Monoclonal antibodies combined with adenovirus-vectored interferon significantly extend the treatment window in Ebola virus-infected guinea pigs." Journal of virology **87**(13): 7754-7757.

Raabea, V. N. and M. Borcherta (2012). "Infection control during filoviral hemorrhagic Fever outbreaks." Journal of global infectious diseases **4**(1): 69-74.

Reed, L. J. and H. Muench (1938). "A simple method of estimating fifty per cent endpoints." American journal of hygiene **27**: 493-497.

Reichert, J. M. (2013). "Which are the antibodies to watch in 2013?" mAbs **5**(1): 1-4.

Reichert, J. M., C. J. Rosensweig, et al. (2005). "Monoclonal antibody successes in the clinic." Nature biotechnology **23**(9): 1073-1078.

Reid, S. P., L. W. Leung, et al. (2006). "Ebola virus VP24 binds karyopherin alpha1 and blocks STAT1 nuclear accumulation." Journal of virology **80**(11): 5156-5167.

Reid, S. P., C. Valmas, et al. (2007). "Ebola virus VP24 proteins inhibit the interaction of NPI-1 subfamily karyopherin alpha proteins with activated STAT1." Journal of virology **81**(24): 13469-13477.

Richardson, J. S., M. C. Abou, et al. (2011). "Impact of systemic or mucosal immunity to adenovirus on Ad-based Ebola virus vaccine efficacy in guinea pigs." The Journal of infectious diseases **204 Suppl 3**: S1032-1042.

Richardson, J. S., J. D. Dekker, et al. (2010). "Recent advances in Ebolavirus vaccine development." Human vaccines **6**(6): 439-449.

Richardson, J. S., G. Wong, et al. (2011). "Evaluation of Different Strategies for Post-Exposure Treatment of Ebola Virus Infection in Rodents." Journal of bioterrorism & biodefense **S1:007**(S1).

Richardson, J. S., M. K. Yao, et al. (2009). "Enhanced protection against Ebola virus mediated by an improved adenovirus-based vaccine." PloS one **4**(4): e5308.

Robertson, M. J. (2002). "Role of chemokines in the biology of natural killer cells." Journal of leukocyte biology **71**(2): 173-183.

Roddy, P., D. Weatherill, et al. (2007). "The Medecins Sans Frontieres intervention in the Marburg hemorrhagic fever epidemic, Uige, Angola, 2005. II. lessons learned in the community." The Journal of infectious diseases **196 Suppl 2**: S162-167.

Rodriguez, L. L., A. De Roo, et al. (1999). "Persistence and genetic stability of Ebola virus during the outbreak in Kikwit, Democratic Republic of the Congo, 1995." The Journal of infectious diseases **179 Suppl 1**: S170-176.

Roels, T. H., A. S. Bloom, et al. (1999). "Ebola hemorrhagic fever, Kikwit, Democratic Republic of the Congo, 1995: risk factors for patients without a reported exposure." The Journal of infectious diseases **179 Suppl 1**: S92-97.

Rowe, A. K., J. Bertolli, et al. (1999). "Clinical, virologic, and immunologic follow-up of convalescent Ebola hemorrhagic fever patients and their household contacts, Kikwit, Democratic Republic of the Congo. Commission de Lutte contre les Epidemies a Kikwit." The Journal of infectious diseases **179 Suppl 1**: S28-35.

Ryabchikova, E., L. Kolesnikova, et al. (1996). "Ebola virus infection in guinea pigs: presumable role of granulomatous inflammation in pathogenesis." Archives of virology **141**(5): 909-921.

Ryabchikova, E. I., L. V. Kolesnikova, et al. (1999). "An analysis of features of pathogenesis in two animal models of Ebola virus infection." The Journal of infectious diseases **179 Suppl 1**: S199-202.

Saeed, M. F., A. A. Kolokoltsov, et al. (2010). "Cellular entry of ebola virus involves uptake by a macropinocytosis-like mechanism and subsequent trafficking through early and late endosomes." PLoS pathogens **6**(9): e1001110.

Saijo, M., M. Niikura, et al. (2006). "Laboratory diagnostic systems for Ebola and Marburg hemorrhagic fevers developed with recombinant proteins." Clinical and vaccine immunology : CVI **13**(4): 444-451.

Saijo, M., M. Niikura, et al. (2001). "Enzyme-linked immunosorbent assays for detection of antibodies to Ebola and Marburg viruses using recombinant nucleoproteins." Journal of clinical microbiology **39**(1): 1-7.

Sanchez, A. (2007). "Analysis of filovirus entry into vero e6 cells, using inhibitors of endocytosis, endosomal acidification, structural integrity, and cathepsin (B and L) activity." The Journal of infectious diseases **196 Suppl 2**: S251-258.

Sanchez, A. and M. P. Kiley (1987). "Identification and analysis of Ebola virus messenger RNA." Virology **157**(2): 414-420.

Sanchez, A., M. P. Kiley, et al. (1993). "Sequence analysis of the Ebola virus genome: organization, genetic elements, and comparison with the genome of Marburg virus." Virus research **29**(3): 215-240.

Sanchez, A., S. G. Trappier, et al. (1996). "The virion glycoproteins of Ebola viruses are encoded in two reading frames and are expressed through transcriptional editing." Proceedings of the National Academy of Sciences of the United States of America **93**(8): 3602-3607.

Schumann, M., T. Gantke, et al. (2009). "Ebola virus VP35 antagonizes PKR activity through its C-terminal interferon inhibitory domain." Journal of virology **83**(17): 8993-8997.

Scott, P. (1991). "IFN-gamma modulates the early development of Th1 and Th2 responses in a murine model of cutaneous leishmaniasis." Journal of immunology **147**(9): 3149-3155.

Segal, A. W. (2005). "How neutrophils kill microbes." Annual review of immunology **23**: 197-223.

Shingai, M., Y. Nishimura, et al. (2013). "Antibody-mediated immunotherapy of macaques chronically infected with SHIV suppresses viraemia." Nature **503**(7475): 277-280.

Smyth, M. J., Y. Hayakawa, et al. (2002). "New aspects of natural-killer-cell surveillance and therapy of cancer." Nature reviews. Cancer **2**(11): 850-861.

Sobarzo, A., A. Groseth, et al. (2013). "Profile and persistence of the virus-specific neutralizing humoral immune response in human survivors of Sudan ebolavirus (Gulu)." The Journal of infectious diseases **208**(2): 299-309.

Sobarzo, A., D. E. Ochayon, et al. (2013). "Persistent immune responses after Ebola virus infection." The New England journal of medicine **369**(5): 492-493.

Stroher, U., E. West, et al. (2001). "Infection and activation of monocytes by Marburg and Ebola viruses." Journal of virology **75**(22): 11025-11033.

Strong, J. E., G. Wong, et al. (2008). "Stimulation of Ebola virus production from persistent infection through activation of the Ras/MAPK pathway." Proceedings of the National Academy of Sciences of the United States of America **105**(46): 17982-17987.

Sullivan, N. J., T. W. Geisbert, et al. (2003). "Accelerated vaccination for Ebola virus haemorrhagic fever in non-human primates." Nature **424**(6949): 681-684.

Sullivan, N. J., L. Hensley, et al. (2011). "CD8+ cellular immunity mediates rAd5 vaccine protection against Ebola virus infection of nonhuman primates." Nature medicine **17**(9): 1128-1131.

Sullivan, N. J., Martin, J.E., Graham, B.S., Nabel, G.J. (2009). "Correlates of protective immunity for Ebola vaccines: implications for regulatory approval by the animal rule." Nat. Rev. Microbiol. **7**(5): 393-400.

Sullivan, N. J., A. Sanchez, et al. (2000). "Development of a preventive vaccine for Ebola virus infection in primates." Nature **408**(6812): 605-609.

Suomalainen, M. (2002). "Lipid rafts and assembly of enveloped viruses." Traffic **3**(10): 705-709.

Swain, S. L., A. D. Weinberg, et al. (1990). "IL-4 directs the development of Th2-like helper effectors." Journal of immunology **145**(11): 3796-3806.

Swanepoel, R., P. A. Leman, et al. (1996). "Experimental inoculation of plants and animals with Ebola virus." Emerging infectious diseases **2**(4): 321-325.

Takada, A., H. Feldmann, et al. (2003). "Identification of protective epitopes on ebola virus glycoprotein at the single amino acid level by using recombinant vesicular stomatitis viruses." Journal of virology **77**(2): 1069-1074.

Takada, A., C. Robison, et al. (1997). "A system for functional analysis of Ebola virus glycoprotein." Proceedings of the National Academy of Sciences of the United States of America **94**(26): 14764-14769.

Taniguchi, S., S. Watanabe, et al. (2011). "Reston Ebolavirus antibodies in bats, the Philippines." Emerging infectious diseases **17**(8): 1559-1560.

Towner, J. S., B. R. Amman, et al. (2009). "Isolation of genetically diverse Marburg viruses from Egyptian fruit bats." PLoS pathogens **5**(7): e1000536.

Towner, J. S., P. E. Rollin, et al. (2004). "Rapid diagnosis of Ebola hemorrhagic fever by reverse transcription-PCR in an outbreak setting and assessment of patient viral load as a predictor of outcome." Journal of virology **78**(8): 4330-4341.

Towner, J. S., T. K. Sealy, et al. (2008). "Newly discovered ebola virus associated with hemorrhagic fever outbreak in Uganda." PLoS pathogens **4**(11): e1000212.

Twenhafel, N. A., M. E. Mattix, et al. (2013). "Pathology of experimental aerosol zaire ebolavirus infection in rhesus macaques." Veterinary pathology **50**(3): 514-529.

UPMChealthsecurity.org (2013). Next-Generation Monoclonal Antibodies: Challenges and Opportunities, UPMC Center for Biosecurity.

Van Rompay, K. K., E. J. Blackwood, et al. (2006). "Role of CD8+ cells in controlling replication of nonpathogenic Simian Immunodeficiency Virus SIVmac1A11." Virology journal **3**: 22.

Vlasuk, G. P., A. Bradbury, et al. (2003). "Pharmacokinetics and anticoagulant properties of the factor VIIa-tissue factor inhibitor recombinant Nematode Anticoagulant Protein c2 following subcutaneous administration in man. Dependence on the stoichiometric binding to circulating factor X." Thrombosis and haemostasis **90**(5): 803-812.

Volchkov, V. E., S. Becker, et al. (1995). "GP mRNA of Ebola virus is edited by the Ebola virus polymerase and by T7 and vaccinia virus polymerases." Virology **214**(2): 421-430.

Volchkov, V. E., A. A. Chepurnov, et al. (2000). "Molecular characterization of guinea pig-adapted variants of Ebola virus." Virology **277**(1): 147-155.

Volchkov, V. E., V. A. Volchkova, et al. (1999). "Characterization of the L gene and 5' trailer region of Ebola virus." The Journal of general virology **80 (Pt 2)**: 355-362.

Volchkova, V. A., H. D. Klenk, et al. (1999). "Delta-peptide is the carboxy-terminal cleavage fragment of the nonstructural small glycoprotein sGP of Ebola virus." Virology **265**(1): 164-171.

Wahl-Jensen, V., S. K. Kurz, et al. (2005). "Role of Ebola virus secreted glycoproteins and virus-like particles in activation of human macrophages." Journal of virology **79**(4): 2413-2419.

Waldmann, T. A. (2003). "Immunotherapy: past, present and future." Nature medicine **9**(3): 269-277.

Warfield, K. L., D. L. Swenson, et al. (2007). "Ebola virus-like particle-based vaccine protects nonhuman primates against lethal Ebola virus challenge." The Journal of infectious diseases **196 Suppl 2**: S430-437.

Warren, T. K., A. C. Shurtleff, et al. (2012). "Advanced morpholino oligomers: a novel approach to antiviral therapy." Antiviral research **94**(1): 80-88.

Warren, T. K., K. L. Warfield, et al. (2010). "Advanced antisense therapies for postexposure protection against lethal filovirus infections." Nature medicine **16**(9): 991-994.

Watanabe, S., T. Noda, et al. (2006). "Functional mapping of the nucleoprotein of Ebola virus." Journal of virology **80**(8): 3743-3751.

Watanabe, S., A. Takada, et al. (2000). "Functional importance of the coiled-coil of the Ebola virus glycoprotein." Journal of virology **74**(21): 10194-10201.

Wauquier, N., P. Becquart, et al. (2009). "Immunoglobulin G in Ebola outbreak survivors, Gabon." Emerging infectious diseases **15**(7): 1136-1137.

Wauquier, N., P. Becquart, et al. (2010). "Human fatal zaire ebola virus infection is associated with an aberrant innate immunity and with massive lymphocyte apoptosis." PLoS neglected tropical diseases **4**(10).

Weingartl, H. M., C. Embury-Hyatt, et al. (2012). "Transmission of Ebola virus from pigs to non-human primates." Scientific reports **2**: 811.

Whelan, S. P., J. N. Barr, et al. (2004). "Transcription and replication of nonsegmented negative-strand RNA viruses." Current topics in microbiology and immunology **283**: 61-119.

Wilson, J. A. and M. K. Hart (2001). "Protection from Ebola virus mediated by cytotoxic T lymphocytes specific for the viral nucleoprotein." Journal of virology **75**(6): 2660-2664.

Wilson, J. A., M. Hevey, et al. (2000). "Epitopes involved in antibody-mediated protection from Ebola virus." Science **287**(5458): 1664-1666.

Wong, G., J. S. Richardson, et al. (2012). "Immune parameters correlate with protection against ebola virus infection in rodents and nonhuman primates." Science translational medicine **4**(158): 158ra146.

Wu, J. Q., N. D. Barabe, et al. (2007). "Pre- and post-exposure protection against Western equine encephalitis virus after single inoculation with adenovirus vector expressing interferon alpha." Virology **369**(1): 206-213.

Xu, L., A. Sanchez, et al. (1998). "Immunization for Ebola virus infection." Nature medicine **4**(1): 37-42.

Yang, Z., R. Delgado, et al. (1998). "Distinct cellular interactions of secreted and transmembrane Ebola virus glycoproteins." Science **279**(5353): 1034-1037.

Yuan, J., Y. Zhang, et al. (2012). "Serological evidence of ebolavirus infection in bats, China." Virology journal **9**: 236.

Zaki, S. R. and C. S. Goldsmith (1999). "Pathologic features of filovirus infections in humans." Current topics in microbiology and immunology **235**: 97-116.

Zampieri, C. A., N. J. Sullivan, et al. (2007). "Immunopathology of highly virulent pathogens: insights from Ebola virus." Nature immunology **8**(11): 1159-1164.

Zeitlin, L., J. Pettitt, et al. (2011). "Enhanced potency of a fucose-free monoclonal antibody being developed as an Ebola virus immunoprotectant." Proceedings of the National Academy of Sciences of the United States of America **108**(51): 20690-20694.

Zivcec, M., D. Safronetz, et al. (2011). "Validation of assays to monitor immune responses in the Syrian golden hamster (Mesocricetus auratus)." Journal of immunological methods **368**(1-2): 24-35.